W-Pos104

MODIFICATION OF SINGLE ACh-CHANNEL CURRENTS BY THE PARALYTIC AGENT 2,4-DITHIOBIURET. J.M. Spitsbergen and W.D. Atchison Department of Pharmacology and Toxicology and Neuroscience Program, Michigan State University, E. Lansing, MI 48824.

2,4-dithiobiuret (DTB) is a substituted thiourea derivative with moderate reducing properties. Treatment of rats with small daily doses of DTB leads to the development of a delayed onset neuromuscular weakness after approximately 1 week of treatment. Previous voltage-clamp experiments have demonstrated a shortening of the decay time constant for miniature end-plate currents (MEPCs) in muscles taken from DTB-treated rats during the onset of muscle weakness. The purpose of the present experiments was to determine whether the open time for ACh-channels in muscle cells are altered following exposure to DTB. Single ACh-channel currents were recorded in outside-out, cell-free patches from differentiated myotubes formed from the G8 mouse myoblast cell line. Although channels with several conductance levels were detected, the majority of channels had a slope conductance of 37 pS and a mean open time of 1.47 msec. Addition of 10 to 100 μM DTB to the extracellular medium caused a decrease in the mean channel open time to less than 0.5 msec. Moreover, channel events recorded in DTB-free buffer, from cells grown for 5 to 7 days in medium containing 10 μM DTB, had a mean open time of 1.07 msec compared to 1.47 msec in control cells. Thus, both acute and chronic exposure of cultured muscle cells to DTB alters the mean open time of ACh-channels in a manner consistent with effects observed on MEPC decay time constants at intact neuromuscular preparations taken from rats treated with DTB.

Supported by NIH grant NS20683 and a BRSG grant from the College of Veterinary Medicine at MSU. WDA was supported by Research Career Development Award 1-K04-ES00178. JMS was supported by Neuroscience Training Grant NS07279.

W-Pos105

COMPARISON OF CHARACTERISTICS OF NEURONAL TYPE AND END-PLATE TYPE NICOTINIC RECEPTORS IN CULTURED CELLS

Marga Oortgiesen, Regina G.D.M. van Kleef and Henk P.M. Vijverberg: Research Institute of Toxicology, University of Utrecht, P.O. Box 80.167, 3508 TD Utrecht, The Netherlands

In electrophysiological experiments cell lines of the clones N1E-115 and BC3H1 have been used to study fundamental properties of neuronal type and endplate type nicotinic receptors, respectively. In both cell types rapid superfusion of voltage clamped cells with acetylcholine results in a transient inward current, which can be blocked by d-tubocurarine and not by atropine. The two types of nicotinic receptors can be distinguished on their sensitivity to snake toxins. The neuronal type nicotinic receptor in N1E-115 cells is insensitive to α-BuTX and can be blocked by nanomolar concentrations of kappa-BuTX. For the endplate type nicotinic receptor in BC3H1 cells a reversed sensitivity to these toxins is observed.

Table 1 presents the results of concentration-effect curves for receptor activation and receptor desensitization.

Table 1

	activation		desentization	
	EC50 (uM)	n_H	IC50 (uM)	n_H
N1E-115[1]	55	0.8	1.1	0.6
BC3H1	8.5	0.8	0.35	1.6

The endplate type nicotinic receptor is more sensitive to acetylcholine than the neuronal type nicotinic receptor. In addition, the time course of desensitization is much faster in BC3H1 cells than in N1E-115 cells. Although the general mechanism of receptor and ion channel functioning are similar, the distinct slope factors of the concentration-effect curves for receptor desensitization suggest a difference in the coupling between receptor and ion channels.

[1] M. Oortgiesen et al. (1989), Neuroscience, 31, 169-179

W-Pos106

ADULT EXTRAOCULAR AND INTERCOSTAL MUSCLE EXPRESS THE γ SUBUNIT OF FETAL AChR. HJ Kaminski,R Fenstermaker, RL Ruff. Depts of Neurology & Neurosurgery, Cleveland Vets Affairs Med Ctr & Case Western Reserve University, Cleveland, Ohio 44106.

Previously, transcription of the γ subunit of mammalian AChR has been found only during fetal and perinatal periods. Using the polymerase chain reaction (PCR) to amplify cDNA derived from adult bovine extraocular (EOM) and intercostal muscle, we have found transcripts encoding the γ subunit. Under identical amplification conditions adult liver was not found to express α, γ, or ϵ transcripts, and fetal muscle did not express ϵ subunit. Therefore, "illegitimate" transcription is an unlikely explanation for our results. Qualitative comparisons of the levels of expression among the 3 subunits indicate that extraocular muscle expresses γ at higher levels than intercostal muscle. Quantitative PCR is in progress to confirm this observation. Our findings suggest that the γ subunit of AChR may be expressed in adult muscle. In EOM, there may be fetal-type AChRs present on the postsynaptic membrane of multiterminal fibers, as was found on snake tonic fibers (Dione, J Physiol 1989; Ruff & Spiegel, Am J Physiol in press). The fetal-type AChR on multiterminal fibers may partially explain antigenic differences between EOM and other skeletal muscles (Kaminski et al, Neurology in press).

(Supported by Department of Veterans Affairs Associate Investigator Award (HJK), Merit Reviewed funding to RLR and RAGS funding to RF; also NIH Grant NS 26661)

W-Pos107

CHOLESTEROL ENRICHMENT DECREASES THE CONDUCTANCE OF NICOTINIC ACETYLCHOLINE RECEPTOR CHANNELS IN TISSUE CULTURED CHICK MUSCLE. **J. A. Lasalde & C. Zuazaga. Inst. of Neurobiol., U. of Puerto Rico Med. Sci. Campus, San Juan, PR 00901**

Acetylcholine receptor (AChR) channel function in reconstituted membranes has been found to be controlled by the lipids surrounding this receptor-channel complex. To understand the role of lipids in determining AChR channel function in cell membranes, patch clamp and fluorescence anisotropy studies have been performed using embryonic chick pectoral muscles cultured in both normal and cholesterol-enriched media. In cell-attached recordings from cells grown in normal media (2.4 μM cholesterol), only one type of AChR channel, with a conductance of ca. 50 pS, was observed. Recordings from cells grown 2-3 days in cholesterol-enriched media (29 μM cholesterol), revealed the presence of two types of ACh-activated channels. The conductance and open time of one type matched those of the control AChR channel. The other had reduced conductance (ca. 35 pS) and open time; it was activated by low (0.6 μM) and high (6 μM) concentrations of ACh, and was slightly more permeable to Cs^+ than to Na^+. Reversal potentials of both types of channels were essentially the same (ca. 0 mV). Fluorescence polarization measurements indicate that the microviscosity of the plasma membrane lipid bilayer in cells grown in cholesterol-enriched media was about 2-fold higher than that of control cells. Fluorescence lifetimes were determined by the phase-modulation method. For control cells, fluorescence decay occured with a single exponential time constant; two time constants were apparent in cells grown in cholesterol-enriched media, suggesting that the fluorophore is located in two different microenvironments. These results suggest that cholesterol is incorporated into the muscle cell membrane forming distinct lipid domains and that AChR channels within these domains have reduced conductance and mean open time. (Supported by NIH grant NS07464 and MARC-GM 13089).

W-Pos108

CHARACTERIZATION OF HIGH AFFINITY NICOTINE RECEPTORS ON CULTURED CORTICAL NEURONS FROM RAT BRAIN.
E.N. Fluhler, P.M. Lippiello, K.G. Fernandes. RJR Tobacco Co., Winston-Salem, NC 27102

Our laboratory previously described the properties of nicotinic receptors in neuronal membrane preparations from primary cultures of fetal rat cortex (JPET 246:409-416 (1988)). In the present study, we have further characterized the binding properties, locations, and functional properties of these sites on intact cells. The binding properties of receptors on cultured cortical neurons are similar to those determined for high affinity receptors in adult rat brain preparations (K_d = 2.5 nM). The pharmacological specificity of nicotinic receptors on these neurons also parallels that found in adult tissue, with nicotinic agonists (e.g. cytisine and DMPP) being significantly more potent competitive inhibitors of nicotine binding than antagonists (e.g. decamethonium). The locations of the sites were determined using anti-idiotypic antibodies against nicotine. These antibodies represent structural analogs of nicotine and have been shown to recognize neuronal nicotinic receptors (Bjercke and Langone, BBRC 162:1085-1092 (1989)). We found that two of these antibodies, 422F11 and 420G11, competitively inhibit more than 80% of the high affinity [^{3}H]-nicotine binding at concentrations as low as 100 nM. Using indirect immunofluorescence techniques, nicotine receptors were identified on cell bodies, dendritic processes, and the distal portions of axons. We also have begun to study the functional properties of these receptors using the ion-specific fluorescent probe fura-2 to measure ligand-evoked intracellular calcium changes. Nicotine (100-1000nM) caused significant increases (40-100nM) in intracellular calcium in 10% of the neurons tested. The ability of the classical nicotine antagonist, decamethonium, to attenuate these calcium increases is consistent with the involvement of nicotine receptor activation in the response. Our results suggest that nicotine binding sites located on cultured cortical neurons are functional nicotinic cholinergic receptors, many of which may be located post-synaptically.

W-Pos109

MOLECULAR MODELLING OF THE NICOTINIC ACETYLCHOLINE RECEPTOR-LIPID INTERFACE AND MOLECULAR DYNAMICS OF ION CHANNEL FORMING TRANSMEMBRANE SEGMENTS V. B. Cockroft, D. J. Osguthorpe, G. G. Lunt and F. J. Barrantes*. Molecular Graphics Unit, University of Bath, Bath BA2 7AY, U. K., and * Instituto de Investigaciones Bioquimicas, 8000 Bahia Blanca, Argentina.

It is of considerable interest to learn about two interfaces formed by the transmembrane portions of the nicotinic acetylcholine receptor (nAChR), the paradigm rapid ligand-gated ion channel: i) that corresponding to the intramembranous portions interacting with the bilayer lipid and ii) that formed by the polypeptide chains forming the lining of the ion channel proper. High-temperature (800K) molecular dynamics was performed on the M1 to M3 region of the *Torpedo* alpha subunit in order to define a structural template model. A 20 picosecond trajectory was computed using a starting structure with residue positions 209-236, 244-265 and 275-299 in a helical conformation (phi -60, psi -40), and the intervening linker regions in an extended conformation (phi -120, psi 120). Within the first 10 ps of the dynamic trajectory the three helical segments folded into an antiparallel bundle. Several features of the final model are consistent with experimental data which indicate that a partly hydrophilic surface of the M2 segment contributes to the wall of the ion-channel. A static model of the packing of phospholipids in the immediate perimeter of the pentameric receptor, i.e. the annular lipid, has also been produced. Correlations can be established between the structural packing of phospholipid molecules in the annulus and the composition and dynamic properties of these lipids revealed by spectroscopic techniques on *Torpedo* AChR membranes (reviewed in Barrantes, *Crit. Rev. Biochem. Mol. Biol.* 24:437-478, 1989).

* *Supported by John Simon Guggenheim Memorial Foundation, Volkswagen Stiftung and Fundacion Antorchas.*

W-Pos110

INWARD RECTIFICATION OF NICOTINIC CURRENTS IN PC12 CELLS: REDUCED INTERNAL DIVALENT CATION CONCENTRATIONS REVEAL A DIVERGENCE BETWEEN SINGLE CHANNEL AND WHOLE-CELL CURRENTS.
C.K. Ifune and J.H. Steinbach, Dept. of Anesthesiology, Washington Univ. Sch. of Med., St. Louis, MO 63110

The current-voltage (I-V) relationship for macroscopic ACh-elicited currents in PC12 cells displays inward rectification. When the intracellular Mg++ concentration is over 1 mM, the voltage dependence of the whole-cell current can be satisfactorily explained by the voltage dependence of the channel burst duration and the inward rectification of the single channel current. The rectification of the single channel current is dependent on intracellular and extracellular concentrations of free Mg++ and removing Mg++ from the internal solution linearizes the single channel I-V relationship. However, removing Mg++ from the intracellular solution does not linearize the whole-cell I-V relationship.

We examined the properties of the whole-cell current rectification in the absence of intracellular Mg++. The I-V relationship for the instantaneous whole-cell current following voltage jumps was inwardly rectifying in contrast to the linear single channel I-V in excised patches. In addition, comparing whole-cell inward currents at -80 mV after voltage jumps from various positive potentials suggested that the channel probability of being open (Popen) relative to Popen at -80 mV is about 2-fold lower than expected from measurements of Popen of single channels in outside-out patches.

From these observations we conclude that properties of single channels in excised patches do not agree with those determined indirectly from whole-cell currents when divalent cation concentrations are low. The remaining rectification of the whole-cell current in the absence of intracellular inorganic divalent cations may be due to block resulting from an agent that is lost when the patch is excised. (Supported by NIH RO1NS22356 and PHS 2732 HLO 7275-11.)

W-Pos111

RELATIONSHIP OF THE SOLUTION STRUCTURE OF A CHOLINERGIC AGONIST TO ITS FUNCTIONAL ACTIVITY AT THE NICOTINIC ACETYLCHOLINE RECEPTOR. Kathleen A. McGroddy, Alison A. Carter, & R.E. Oswald. Dept. Pharmacology, Cornell Univ., Ithaca, NY.

The activation of a ligand gated ion channel, such as the nicotinic acetylcholine receptor (nAChR), by an agonist is a complex series of events involving the binding of the small molecule and structural changes of the receptor/ion channel. The binding interaction is in turn dependent upon the structure and dynamics of the agonist both in solution and in the binding site. We have synthesized two classes of structurally similar cholinergic ligands based on the parent compounds shown below. Patch clamp studies of the nAChR (BC_3H1 cells) have shown that both sets of compounds are agonists but the more flexible TED compounds are two to three orders of magnitude less potent that the rigid PIP compounds. In addition systematic variations in function appear within each set of compounds. Similar differences in affinity were observed using the inhibition of [^{125}I]αbungarotoxin binding and the stimulation of [^{3}H]phencyclidine binding to *Torpedo* nAChR.

The structural and dynamic variations of these compounds have been compared both experimentally and theoretically through the use of one- and two-dimensional NMR experiments and molecular modeling techniques. Both theoretical and experimental studies indicate that the TED compounds exist in a stable solution structure that differs significantly from the rigid PIP structure and which can account at least in part for the difference in affinities observed in the functional studies.

These studies indicate that the solution structure and dynamics of a compound can make an important contribution to the binding affinity of a ligand to its receptor.

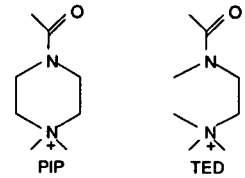

W-Pos112

DETERMINATION OF THE OPENING RATE OF ACETYLCHOLINE RECEPTOR CHANNELS BY RAPID PERFUSION OF AGONIST.

Y. Liu and J.P. Dilger, Departments of Physics and Anesthesiology, SUNY, Stony Brook, NY 11794-8480.

The nicotinic acetylcholine (ACh) receptor is responsible for rapid conversion of chemical signals to electrical signals at the neuromuscular junction. Since the receptor and its ion channel are components of a single transmembrane protein, the time between ACh binding and channel opening can be minimized. Just how quickly does the channel open? Rapid (100-400 μs) applications of 0.1-10 mM ACh were made to outside-out, multi-channel membrane patches from BC3H-1 cells, while the onset of current flow through the channels was measured. Experiments were performed at 11°C; currents were filtered at 10-30 kHz and sampled at 3 μs/point. Onset time was steeply dependent upon ACh concentration when channel activation was limited by binding of ACh (0.1-1 mM). For measurements at +50 mV, the onset time reached a plateau near 80 μs above 5 mM ACh as channel opening became rate-limiting. Thus, we calculate the opening rate (β) without reference to specific channel activation schemes. At –50 mV, onset time was always shorter and continued to decrease at high ACh concentrations. This effect arises from rapid, voltage-dependent block of channels by ACh combined with a finite solution exchange time. To determine opening rate at –50 mV, it was necessary to calculate the kinetic parameters of block from steady-state current and noise analyses, assume a sequential model of channel activation/block and numerically simulate current responses to rapid perfusion of ACh. At –50 mV, the equilibrium blocking constant is 6.4 mM and the dissociation rate constant is 140/ms. Using these values, we find β=15/ms and determine the solution exchange time for each patch. In contrast to the channel closing rate, the opening rate is relatively insensitive to voltage.

(Supported by grant GM42095 from the N.I.H.)

W-Pos113

A METHOD FOR ANALYSING THE CONCENTRATION DEPENDENCE OF ION CHANNEL KINETICS IN CELL-ATTACHED PATCHES.

Anthony Auerbach, Dept. Biophysics, SUNY, Buffalo, NY 14214

In order to study the kinetics of cholinergic channels as a function of the concentration of ACh in cell-attached patches we have combined a backfilled pipette technique with interval likelihood analysis. Pipettes with tips filled with normal saline are backfilled with drug-containing solution; ligand diffuses to the tip and channel currents change accordingly. The problems are how to determine the concentration of ligand as a function of time, and how to analyse the nonstationary channel kinetics.

We have quantified the [ACh] vs time in three ways. The diffusion of blockers (e.g. QX-222) produces a decrease in the open time that scales linearly with concentration (below left, upper panel). The diffusion of Na (tips filled with 30 mM Na saline, backfilled with normal saline) produces an increase in the current amplitude that scales as a nonlinear but quantifiable function of [Na]. AChR kinetics (the effective opening rate β'; see below right) scales linearly with [ACh] over a certain range and can serve as an index of [ACh]. With all methods, after a delay of several minutes the ligand concentration increases exponentially and, assuming a conical geometry, the diffusional time constant can be used to compute the concentration of ligand over all times (left, lower panel). We have used the interval likelihood approach of Horn and Lange to analyse the nonstationary currents. For each burst, the concentration of ACh is determined from the absolute time of occurrence of the burst, and the transition rate matrix is appropriately scaled before the likelihood is calculated. Scaling on an interval -by-interval basis is possible but unnecessary as bursts are short (<sec) compared to diffusional time constants (minutes).

With this method a single kinetic scheme can be fit over a wide range of agonist values (e.g., 10-100 μm ACh). This not only greatly speeds and contrains the fit, but also minimizes variability in rate estimates that arise from patch-to-patch heterogeneity in channel kinetics.

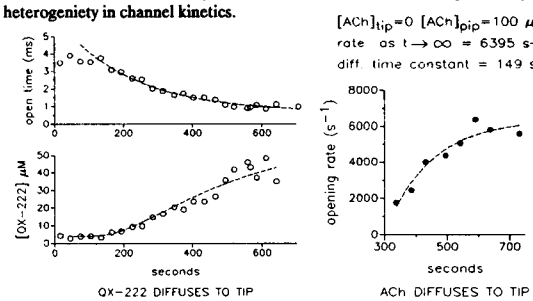

W-Pos114

ATTENUATED TOTAL REFLECTANCE FTIR STUDIES OF THE CONFORMATIONAL CHANGES ASSOCIATED WITH DESENSITIZATION OF THE NICOTINIC ACETYLCHOLINE RECEPTOR.

John E. Baenziger+*, Keith W. Miller+*, and Kenneth J. Rothschild*. +Depertment of Biological Chemistry and Molecular Pharmacology, Harvard Medical School, and *Department of Physics and Program in Cellular Biophysics, Boston University, Boston, MA.

We have developed a system for investigating the conformational changes associated with the desensitization of the nicotinic Acetylcholine Receptor (nAChR) using Fourier Transform Infrared (FTIR) *difference* spectroscopy. This involves drying the nAChR membranes in a thin film on a germanium internal reflection crystal, fixing the films to the germanium surface, and acquiring FTIR spectra in the presence and absence of cholinergic agonists by the attenuated total reflectance technique. We examined the functionality of the nAChR films using the fluorescent probe, ethidium bromide. In the absence of nAChR membranes, ethidium emits fluorescence with a maximum intensity at 615 nm. In the presence of nAChR membranes, ethidium binds non-specifically to the lipid bilayer and with very low affinity to the nAChR, but upon addition of a cholinergic ligand such as carbamylcholamine (CARB), binds with high affinity and specificity to a site on the desensitized receptor. The emission maximum then shifts to 595 nm and an increase in fluorescence intensity is observed. Fluoresence emission spectra of ethidium acquired in the presence of nAChR films showed the expected intensity increase and shift in the emission maximum upon addition of CARB thus establishing that the fixation process yields films of active nAChR. Furthermore, the spectral changes were prevented by preincubation of the film with the competitive antagonist, α-bungarotoxin. The CARB is washed from the nAChR films by exchanging the surrounding buffer which allows the nAChR films to be cycled between the resting and desensitized state. FTIR difference spectroscopy shows that the films adhere to the germanium crystal surface even after exchanging the bathing solution. FTIR *difference* measurements acquired in the presence and absence of CARB reveal information about the conformational changes associated with receptor desensitization.

W-Pos115

DEVELOPMENT AND PHARMACOLOGICAL PROPERTIES OF THE NICOTINIC ACETYLCHOLINE RECEPTOR ION CHANNELS (nAChR) OF RAT HIPPOCAMPAL NEURONS.

M. Alkondon & E.X. Albuquerque. Dept. Pharm. Exp. Ther., Univ. Maryland Sch. Med., Baltimore, MD 21201.

The developmental and pharmacological profiles of neuronal nAChR were studied using tissue cultured fetal (17 days gestation) rat hippocampal neurons. Ionic currents were measured by means of whole-cell patch-clamp technique. Selected agonists and antagonists were applied to the neurons through a 'U'-tube rapid delivery system. Acetylcholine (ACh) and (+)anatoxin (AnTX) (Mol. Pharmacol. 29:250, 1986), two nAChR agonists, elicited inward currents in neurons clamped near their resting membrane potentials. AnTX was nearly 10 to 20 times more potent than ACh in inducing these currents. The currents activated by both agonists displayed inward rectification; a linear I-V relationship was seen between -100 and -10 mV, the reversal potential being ≈0 mV. The currents induced by both agonists showed a desensitization pattern during prolonged agonist application which was completely reversible. Up to 7 days in culture, nAChR currents were either undetectable (<10 pA peak) or very small (<50 pA peak), however, larger currents (200 to 2000 pA peak) were recorded at 14 or more days. The currents produced by AnTX were reversibly blocked by d-tubocurarine, dihydro-ß-erythroidine and (±)mecamylamine, but they were unaffected by NMDA antagonists, $MgCl_2$ and APV, and the quisqualate antagonist DNQX. The $GABA_A$ receptor antagonist bicuculline had a marginal inhibitory effect. Atropine and tetrodotoxin did not block the responses to AnTX. VX, an irreversible cholinesterase inhibitor, potentiated the responses to ACh but not AnTX and caused an increase in the frequency of spontaneous miniature synaptic currents possibly by affecting the presynaptic nerve terminals. The failure to observe single channel currents at the soma of the neurons in most of the trials indicate that the nAChR are located at the axodendritic regions. The observed properties of nAChR of the hippocampal neurons resemble that reported in PC12 pheochromocytoma cells (P.N.A.S. 87: 4794, 1990) and in sympathetic ganglion (J. Physiol. 427: 625, 1990).

Support: US Army Med. Res. & Devel. Comm. Contract DAMD17-88-C-8119 & USPHS Grant NS25296.

W-Pos116

TETRAHYDROAMINOACRIDINE (THA), 9-AMINOACRIDINE (9-AA) AND QUISQUALATE (QUIS) SELECTIVELY DEPRESS THE SLOW COMPONENT OF QUIS-ACTIVATED CURRENTS. A.C.S. Costa and E.X. Albuquerque. Dept. Pharm. Exp. Ther., UMAB, Sch. Med., Baltimore, MD 21201 & Lab. Mol. Pharm. II, IBCCF, UFRJ, RJ, 21944, Brazil.

The actions of THA and 9-AA were studied on QUIS-activated currents recorded from rat hippocampal neurons (cultured for 2-4 wks) using the technique of whole-cell patch-clamp. QUIS and either THA or 9-AA were applied as concentration pulses via a 'U'-tube. QUIS (≥5 μM) activated triphasic currents. The 1st current component was a high amplitude transient which saturated at ≈500 μM; the 2nd, "slow" component, was a lower amplitude current which saturated at ≈1 μM and at ≥5 μM QUIS started to decrease in amplitude. The 3rd component started to develop by the end of the agonist removal and its amplitude was dependent on the concentration of QUIS applied. The first two current components resembled those described by Tang *et al.* (Science 243:1474, 1989), and may represent two different populations of receptors. The 3rd had a time course similar to the "post-stimulation component" we have observed in association with many channel blockers of both NMDA and peripheral nicotinic receptors (Costa and Albuquerque, Soc. Neurosci. Abs. 16:1017, 1990), and also the agonists NMDA and ACh when used at concentrations above the saturation level. THA (0.5-2.5 mM) and 9-AA (0.25-1 mM) caused only a slight depression on the 1st current component. These agents significantly depressed the 2nd current component and increased the amplitude of the 3rd component in a concentration-dependent and voltage-independent fashion. The depression of the 2nd component could represent a transition to a "semi-absorbent" non-conducting state, while the development of the 3rd could reflect reversion of this transition made observable by the relatively fast (50-100 msec) removal time of the superfusion system. Because of the similarities between the actions of THA, 9-AA and QUIS itself, we propose that QUIS is also able to produce transitions to long-lived non-conducting states. THA and 9-AA may act by accelerating transition toward the same state(s) or by creating an alternative non-conducting state(s). THA and 9-AA may help to clarify the mechanism by which QUIS "blocks" QUIS-activated currents. Support: USPHS Grant NS-25296.

W-Pos117

CHEMICAL REDUCTION INCREASES Ca^{2+} FLUX THROUGH THE NMDA CHANNEL WITHOUT CHANGING THE Ca^{2+}/Na^{+} PERMEABILITY RATIO.

Linda A. Wong, Nikolaus J. Sucher and Stuart A. Lipton, Dept. of Neurology, The Children's Hospital, and Program in Neuroscience, Harvard Medical School, Boston, MA 02115.

Chemical reduction increases NMDA-evoked currents in mammalian central neurons *(Aizenman, Lipton & Loring, Neuron 1989;2:1257)*. It is not known, however, which functional parts of the NMDA receptor complex are involved. A functionally important feature of the NMDA-gated ionophore is its higher permeability for Ca^{2+} ions compared to Na^{+} ($P_{[Ca]}>P_{[Na]}$). Therefore, we studied the effect of chemical reduction on NMDA receptor-mediated Ca^{2+} flux in cultured rat retinal ganglion cells (RGCs) and cortical neurons. Using fura-2 fluorescence imaging, we found that in low $[Mg^{2+}]_o$, NMDA (200 μM) reversibly increased $[Ca^{2+}]_i$ from 59 ± 5 nM (n = 18) to 421 ± 70 nM in ~80% of the RGCs tested. This rise in $[Ca^{2+}]_i$ was blocked by the NMDA antagonists APV (200 μM) or $[Mg^{2+}]_o$ (1 mM). After exposure to the reducing agent dithiothreitol (DTT; 2 mM), the NMDA-induced rise in $[Ca^{2+}]_i$ was increased 164 ± 22%. In addition, NMDA-evoked whole-cell currents were recorded in cortical neurons before and after reduction with DTT. Prior to DTT application, at a holding potential of –60 mV, NMDA induced inward currents of –762.33 ± 211.54 pA (n = 3) in nominally Ca^{2+}-free external solution and –953.80 ± 223.87 pA (n = 4) with 30 mM $[Ca^{2+}]_o$. The current evoked by NMDA reversed in polarity at 3.8 ± 0.58 mV in the absence of Ca^{2+}, and at 17.2 ± 2.3 mV with 30 mM external Ca^{2+}. These values correspond to a whole-cell slope conductance of 11.98 ± 3.38 nS and 12.63 ± 3.11 nS, respectively. Addition of DTT to the bath for 2-5 minutes led to an increase in the whole-cell conductance of 168.9 ± 25.3% and 185.0 ± 27.4%, respectively. Applying the Goldman-Hodgkin-Katz equation with ionic concentrations, the permeability of NMDA channels was calculated to be 7.10 ± 1.30 fold greater for Ca^{2+} ions compared to monovalent cations ($P_{[Ca]}/P_{[Na]}$). Chemical reduction with DTT did not significantly alter this permeability ratio (7.91 ± 0.94). Thus, reduction with DTT increased current flow without altering the ionic permeabilities of the NMDA-activated channel. This indicates that reduction probably does not alter the structure of the interior of the channel pore itself.

W-Pos118

WITHDRAWN

W-Pos119

SYNAPTIC CO-LOCALIZATION OF NMDA AND non-NMDA RECEPTORS IN SPINAL MOTONEURONS

Bernhard U. Keller*, Aharony Lev-Tov+ and Arthur Konnerth*

*Max Planck Institut für biophys. Chemie, D-3400 Göttingen, Germany, + Hebrew University Medical School, Jerusalem 91010, Israel.

Excitatory synaptic transmission was investigated by applying the patch-clamp technique to visually identified α motorneurones in thin slices of rat spinal cord. Excitatory postsynaptic currents (EPSCs) were elicited by stimulation of intraspinal presynaptic fibers. EPSCs could be separated pharmacologically into N-methyl-D-aspartate (NMDA) and non-NMDA receptor mediated components. At -60 mV, the EPSC was dominated by the non-NMDA component which was characterized by a fast rise time of 0.7 ± 0.4 ms and a decay time constant of 3.7 ± 1.4 ms (n = 7; 22° C). The much slower NMDA mediated EPSC component could be detected only at holding potentials more positive than -50mV. Graded stimulation of intraspinal fibers showed that the NMDA and non-NMDA receptors were activated by excitatory transmitter released from the same set of presynaptic fibers. The close resemblance between the multimodal distributions of the single fiber NMDA and non-NMDA EPSCs under various conditions indicate that NMDA and non-NMDA receptors are postsynaptically co-localized.

W-Pos120

DOPAMINE UP-MODULATES A GLUTAMATE GATED CURRENT IN ON-BIPOLAR CELLS OF THE TIGER SALAMANDER RETINA. *Greg Maguire and Frank Werblin.* Department of Molecular & Cell Biology, Division of Neurobiology, University of California at Berkeley, Berkeley, CA 94720.

Previous studies have shown that a glutamate gated current in OFF-bipolar cells is up-modulated by dopamine through a D1 receptor/cAMP-PK pathway (Maguire and Werblin, ARVO Abstracts, 31:535, 1990). Here we show that a glutamate gated current in ON-bipolar cells is also up-modulated by dopamine.

Whole cell patch recordings were made of retinal bipolar cells either in the slice or in isolation to record the currents elicited by the pressure ejection of glutamate onto the dendrites of ON-bipolar cells. ON-bipolar cells were identified by their characteristic morphology,

using Lucifer yellow filling through the recording pipette, and their voltage and transmitter gated currents.

Glutamate elicited : 1) A conductance decrease with a reversal potential near 0 mV, and 2) A conductance increase with a reversal potential near -70 mV, potassium probably the permeant ion. The current which reverses near 0 mV was unaffected by the bath application of 20 uM dopamine, whereas the current reversing near -70 mV was greatly enhanced by 20 uM dopamine.

The up-modulation of the current reversing at -70 mV was blocked by the D1 receptor specific antagonist, SCH23390, suggesting that the modulation was mediated by a D1 receptor. Bath application of CPTcAMP, a membrane permeable analogue of cAMP, also led to an enhancement of the glutamate gated current suggesting that the D1 receptor may act through a cAMP pathway to up-modulate the current.

If the current that reverses at 0 mV is associated with rod inputs and the current that reverses at -70 mV is associated with cone inputs as has been suggested by Nawy and Copenhagen (Nature 325:56, 1987), then dopamine could serve to regulate the ratio of rod/cone inputs to ON-bipolar cells.

W-Pos121

DIRECT MEASUREMENT OF NEUROTRANSMITTER ACTIVATION OF CELLULAR METABOLISM IN CULTURED HIPPOCAMPAL NEURONS. K.M. Raley-Susman*, K.M. Kercso†, J.W. Parce†, J.C. Owicki†, and R.M. Sapolsky*. *Dept. of Biological Sciences, Stanford Univ., Stanford, CA 94305 and †Molecular Devices Corp., Menlo Park, CA 94025

Activation of at least one subtype of glutamate receptor has been linked to a variety of pathological states leading to neuronal necrosis, including ischemia and epilepsy. The mechanism whereby overexcitation of these receptors produces damage is unknown but one theory purports that, when cellular energy supplies are drained, the cells' energy-dependent ion extruding mechanisms cannot cope with increased Na^+ and Ca^{++} influx. The resulting ion imbalances initiate a cascade of neurotoxic biochemical events. Glucocorticoids exacerbate such neuronal damage by decreasing glucose uptake into neurons, thereby presumably imposing an energy drain that impairs the neurons' ability to cope with subsequent metabolic challenges (Neuroendo. 43:386(1986); Science 229:1397 (1987)). While much indirect evidence supports the hypothesis that glucocorticoids impair energy metabolism and thus make the cells more susceptible to excitotoxicity, no studies have directly monitored cellular metabolic rates in response to neurotransmitter overexcitation or glucocorticoid treatment. We address these issues by using a microphysiometer containing a silicon-based pH sensor to make real-time measurements of the acidification rate of the external medium bathing mixed hippocampal cultures. The acidification rate due to the extrusion of metabolic acids such as lactate and CO_2 has been shown to be a sensitive index of overall cellular metabolic rate (Science 246:243(1989)). We present evidence that activation of the kainate receptor subtype in rat hippocampal neurons increases metabolic rate in a dose-dependent, receptor-specific manner. Treatment with corticosterone 24 hr prior to the experiment does not affect the dose response or the receptor specificity of kainate; however, at high, "toxic" doses of kainate, the magnitude of the metabolic response is less with the corticosterone treatment. We further investigate the neurotoxic effects of brief exposure to doses of kainate that produce maximal stimulation of metabolism and results suggest that the microphysiometer is a sensitive method for monitoring ongoing metabolic responses to neurotransmitter and hormone activation, as well as neurotoxicity. Supported in part by DARPA and CRDEC, ARO contract DAAL03-86-C-0009 to MDC. KMR-S is an American Heart Association Postdoctoral Fellow, Santa Barbara Chapter.

W-Pos122

5-HT_3 RECEPTOR-CHANNELS IN RAT SUPERIOR CERVICAL GANGLION CELLS. Jian Yang, Alistair Mathie & Bertil Hille (Intro. by David C. Teller), Department of Physiology and Biophysics, University of Washington, Seattle, WA 98195.

Serotonin (10 μM) applied by puff pipette to rat SCG cells held at negative potentials with whole-cell voltage-clamp activates a fast inward current that is blocked by 5-HT_3 receptor-specific antagonists ICS 205-930 and MDL 72222 (<10 nM). The current reverses at -4.7 mV and shows inward rectification that develops in < 1 ms on stepping the voltage. Continued application of 10 μM 5-HT induces voltage-dependent desensitization of the response. At -70 mV the time course of desensitization can be fitted by two exponentials with time constants $\tau_f = 0.57 \pm 0.16$ s (mean±s.d., n=23) and $\tau_s = 6.0 \pm 1.4$ s (n=22). The relative amplitude of the two components (I_f/I_s) is 4.6±2.7 (n=23). At -10 mV the two time constants are similar to those at -70 mV ($\tau_f = 0.50 \pm 0.24$ s and $\tau_s = 4.5 \pm 1.3$ s, n=7), however, the relative amplitude is only 0.93±0.29 (n=7), so more of the receptors desensitize with the slow time constant at depolarized potentials.

The single-channel current estimated from fluctuation analysis of the whole-cell currents induced by bath application of 0.5-0.8 μM of 5-HT is 0.18±0.08 pA (n=9) at -74 mV, giving a chord conductance of 2.6 pS. With single-channel recording in outside-out patches, however, we identify a channel with a larger chord conductance of 11.1±0.9 pS (-74 mV, n=10) that is activated by 5-HT and blocked by ICS 205-930 and MDL 72222. The relative permeability (P_X/P_{Na}) of the channel determined from reversal potentials is: K 1.24, Cs 0.93, Tris 0.19 and glucosamine 0.06. These values are similar to those found by Yang (J. Gen. Physiol. in press) for 5-HT_3 receptors in N18 cells, which suggests that the channels in the two cell types have similar open pore size. However the receptor in SCG cells is impermeable to Cl and only half as permeable to Ca ($P_{Ca}/P_{Na} = 0.55$) as in N18 cells. This, together with the larger single-channel conductance in SCG cells suggests differences in the channel pore structure between the two cell types.

Supported by NIH grant NS08174, Fogarty International Fellowship FO5 TWO4457 (AM) and the McKnight Foundation.

W-Pos123

RELATIONSHIP BETWEEN EVOKED CHANGES IN INTRACELLULAR CALCIUM AND RELEASE AT NERVE ENDINGS. E. Stuenkel and J. J. Nordmann, Dept. of Physiology, Univ. of Michigan, Ann Arbor MI 48109 and Centre de Neurochimie du CNRS, 67084 Strasbourg Cedex, France. (Intro. by D. C. Dawson).

The reliance of neurohormone/neurotransmitter release on the free $[Ca^{2+}]_i$ in the nerve terminal suggests that the kinetics of release should be related to the kinetics of Ca^{2+} entry, rise in $[Ca^{2+}]_i$ and in the reactions which control restoration of Ca^{2+} to prestimulatory levels. Kinetic analysis of release induced with either maintained electrical stimulation or K^+-depolarization, however, shows that release rapidly inactivates. Our understanding of the inactivation process has been partially limited by the inability to directly and quantitatively analyze changes in $[Ca^{2+}]_i$ at single nerve endings. Using axon terminals isolated from the neurohypophysis of the rat, changes in $[Ca^{2+}]_i$ in individual endings in response to depolarizing stimuli were directly quantitated by dual wavelength microspectrofluorometry of cytoplasmic fura-2. Arginine vasopressin release was quantified with high temporal resolution from populations of isolated endings using a fast flow technique and RIA of collected fractions. Elevation of K^+_o leads to a dose-dependent, rapid, dihydropyridine- (DHP) sensitive increase in $[Ca^{2+}]_i$ that is sustained for the duration of the depolarizing stimulus. Succeptibility of the sustained Ca^{2+} increase to DHP or removal of Ca^{2+}_o demonstrates the sustained increase results from continued influx via "L-type" Ca^{2+} channels. Although Ca^{2+} influx is sustained, $[Ca^{2+}]_i$ rapidly reaches a steady state (influx = restorative mechanisms). Vasopressin release to a similar sustained depolarization results in a transient release response (t 1/2 = 7 sec) that corresponds to the rising phase of the $[Ca^{2+}]_i$ increase. Subsequent to inactivation of vasopressin release to an initial depolarizing stimulus an additional step depolarization produces a further increase in $[Ca^{2+}]_i$ and a resurgent transient increase in release. Inactivation of release therefore does not result from a decay of Ca^{2+}influx, depletion of releasable granules or saturation of available release sites. In addition repetitive, brief depolarizing stimuli result in $[Ca^{2+}]_i$ and release responses which donot show habituation (desensitization).

W-Pos124

SODIUM-DEPENDENT CALCIUM EFFLUX IN ADRENAL CHROMAFFIN CELLS FOLLOWING EXOCYTOSIS: POSSIBLE ROLE OF SECRETORY VESICLE MEMBRANE.

Chung-Ren Jan and Allan S. Schneider
Dept.Pharm.& Tox., Albany Medical Coll., Albany, NY 12208

The relative contributions of various processes in regulating cell calcium during and following exocytotic secretion are presently unresolved. Such calcium regulatory processes will in turn influence the magnitude and duration of hormone and neurotransmitter release. Na-dependent calcium efflux across the secretory vesicle membrane, following its incorporation into the plasma membrane, may play a significant role in calcium efflux and the decay of cytosolic calcium transients following stimulation of secretion. We have measured an enhanced ^{45}Ca efflux from cultured bovine adrenal chromaffin cells following cell stimulation with high K (75mM) depolarizing medium. Such stimulation causes calcium uptake via volatage gated calcium channels and secretion of catecholamines. Na deprivation during depolarizing stimulation with 75 mM K, blocked the enhanced calcium efflux, indicating a Na-dependent calcium efflux process. Na deprivation did not inhibit ^{45}Ca uptake or secretion. Suppression of exocytotic incorporation of secretory vesicle membrane into the plasma membrane with hypertonic medium (600-700 mOsm) also inhibited the high K-stimulated ^{45}Ca efflux in Na-containing medium, but did not inhibit stimulated calcium uptake. The inhibition of stimulated-^{45}Ca efflux by hypertonic media was roughly proportional to the inhibition of stimulated secretion. The combined results suggest that Na-dependent calcium efflux across secretory vesicle membranes following their incorporation into the plasma membrane during exocytosis, may play a significant role in regulating the decay of cytosolic calcium in nerve terminals and hormone secreting cells. (Supported in part by grants from the NIH-DK39220 and the American Heart Association, NY State Affiliate-90-49G)

W-Pos125

EXPRESSION AND CHARACTERIZATION OF A UNIQUE K^+ CHANNEL ISOLATED FROM THE RAT CARDIOVASCULAR SYSTEM.

T. Ann Blair, Steven L. Roberds*, Michael M. Tamkun* and Robert P. Hartshorne, Dept. of Pharmacology, Oregon Health Sciences University, Portland, OR 97201 and *Dept. of Physiology, Vanderbilt School of Medicine, Nashville, TN 37232.

K^+ channels are targets for antiarrhythmic and antihypertensive agents. We have isolated a K^+ channel cDNA (RK5) that encodes a 493 amino acid protein that is 70% homologous to the *Drosophila Shal* K^+ channel from a rat heart library. Functional characterization of the RK5 channel was performed utilizing the *Xenopus laevis* expression system and whole cell voltage clamp analysis. RNA transcribed from the RK5 clone induced the expression of voltage dependent, outward currents that activated in response to depolarizations greater than -30 mV and displayed an outwardly rectified I-V curve. Activation of the current followed a slow time course which required 80 ms to fully activate the channel during a voltage step to 50 mV. The activation rate decreased for smaller depolarizations. Inactivation of these currents was very slow, with current magnitude decreasing less than 20% during 2.5 s voltage steps to 50 mV. Ion substitution experiments indicated that the reversal potential of the outward currents depends on the external potassium concentration, as expected for a K^+-selective channel. The RK5 K^+ channel was blocked by external application of TEA with a K_i of ≈3 mM while 5 mM 4-AP and 50 nM Toxin I from Black Mamba (DPI) blocked only a small portion of the current. The slow activation kinetics, the lack of inactivation, and the pharmacology of this channel all indicate that RK5 codes for a classical delayed rectifier type K^+ channel.

W-Pos126

DIFFERENCES IN MACROSCOPIC AND UNITARY PROPERTIES OF TWO CLONED K CHANNELS, RMK2 AND RCK1: STRUCTURAL IMPLICATIONS

E. R. Liman, G. Koren, H. Matsubara, and P. Hess. *Dept. Physiology, Harvard Medical School, Boston, MA 02115.*

In order to define regions of functional importance in the primary sequence of mammalian K channels, two K channels with high amino acid homology (72%), RCK1 and RMK2 (isolated from rat muscle but identical to KV1), were expressed in Xenopus oocytes and their macroscopic and single channel properties compared. Oocytes injected with cRNA to RMK2 expressed delayed rectifier K currents that were similar in steepness of activation and K selectivity to currents expressed in oocytes injected with RCK1 cRNA. The RMK2 and RCK1 currents differed, however, in midpoint of activation (RMK2 is shifted 15-20 mV in the depolarizing direction), and in TEA sensitivity (k_d > 100 mM for RMK2, 0.35 mM for RCK1). Single channel recording revealed even more striking differences. RMK2 channels have half the conductance of RCK1 channels, and openings are flickery (shown below for a step depolarization to 0 mV). The flickery behavior of the RMK2 channels was not visibly different over a range of potentials, and, therefore, may be due to an intrinsic voltage independent opening process. To localize these properties, a chimeric channel was constructed, with the amino terminus of RCK1 (including the S1 and S2 regions) and the carboxy terminus of RMK2. The chimeric channel resembled RMK2 in all aspects examined, including sensitivity to TEA, voltage dependence of activation, single channel conductance and flickeriness of single channel openings (see below). This indicates that these properties are likely to be determined by differences in the carboxy (S3 and onward) half of the channel. Additional chimeras and site-directed mutants are currently being generated to more precisely identify functionally important regions of these molecules.

W-Pos127

AMINO ACIDS IN THE S5-S6 LOOP OF K_V3 AFFECT HIGH AFFINITY CHARYBDOTOXIN BLOCKADE.

Carlos Oliva, Richard Wiedmann, Zhong-Ru Gan, Kimberly Folander, Carl Bennett, Richard Swanson, Jeffrey S. Smith. Departments of Pharmacology and Biological Chemistry, Merck Sharp & Dohme Research Laboratories, West Point, PA 19486.

Charybdotoxin (Chtx), a polypeptide isolated from the venom of the scorpion *Leiurus quinquestriatus hebraeus*, has been demonstrated to block calcium activated K^+ channels with subnanomolar affinity. As demonstrated in the accompanying poster (Oliva et al.), pure (or synthetic) Chtx also blocks a cloned, mammalian delayed rectifier (K_v3) with high affinity (IC_{50} = 1 nM) but is relatively ineffective on *Shaker* K^+ channels (IC_{50} = ~300 nM). Chtx is a highly basic polypeptide and is thought to block K_{Ca} channels by direct physical occlusion of the pore. Charged residues surrounding the mouth of the channel electrostatically affect the strength of the blockade. To test this mechanism in the cloned delayed rectifier, we have mutated the (putative extracellular) region of K_v3 between the S5 and S6 hydrophobic domains by substitution with the corresponding *Shaker* sequence. The two proteins differ by 10 of the 37 amino acids in this domain, resulting in a net charge difference (K_v3 being more negative that *Shaker*). Bulk substitutions of the K_v3 domain by *Shaker* sequences alter the phenotype of Chtx block of K_v3 to one more like that of *Shaker*,ie., a reduction in the affinity of Chtx blockade. Our data are consistent with models of charged amino acids in the extracellular loops exerting electrostatic effects on the binding of Chtx to the channel and suggest that the S5-S6 loop is in close proximity to the mouth of channel. Point mutations at each of the 10 differing amino acids in this region are now being analyzed to test these models further.

W-Pos128

CHARYBDOTOXIN IS NOT A HIGH AFFINITY BLOCKER OF SHAKER K^+ CHANNELS EXPRESSED IN *XENOPUS* OOCYTES.

Carlos Oliva, Kimberly Folander, Jeffrey S. Smith. Department of Pharmacology, Merck Sharp and Dohme Research Laboratories, West Point, PA 19486.

Charybdotoxin (Chtx) is a polypeptide with K^+ channel blocking activity isolated from the venom of *Leiurus quinquestriatus hebraeus*. The purification and primary amino acid sequence of Chtx have been published (Gimenez-Gallego *et al., Proc.Natl.Acad.Sci.,USA*, 85,3329-3333;1988). Chtx is a highly basic peptide made up of 37 amino acid residues and contains three disulfide bonds. High affinity Chtx blockade of skeletal muscle calcium activated K^+ channels was originally reported by Miller *et al.,Nature(Lond.)*, 313,316-318;1985. More recently, McKinnon *et al.,Neuron*, 1,997-1002,(1988) reported that Chtx also blocks Shaker K^+ channels expressed in *Xenopus* oocytes with an IC_{50} of 4.2 nM. We find that Chtx prepared according to Gimenez-Gallego et al. or synthetic Chtx prepared at Merck show similar high affinity blocking activity against calcium activated K^+ channels in bilayers (39 and 65 picomolar K_D for native and synthetic Chtx, respectively) yet neither peptide is a good blocker of Shaker K^+ channels in oocytes. IC_{50} values for both synthetic or native toxins are 330 nM for blockade of Shaker K^+ currents. We propose that contaminants in some Chtx preparations may be responsible for the high affinity blockade of Shaker K^+ channels.

W-Pos129

EXPRESSION OF AN INWARDLY RECTIFYING K+ CHANNEL FROM RBL-2H3 CELLS IN *XENOPUS* OOCYTES

Deborah L. Lewis, Robert S. Aronstam, and Stephen R. Ikeda, *Department of Pharmacology and Toxicology, Medical College of Georgia, Augusta, GA 30912-2300*

RNA was isolated from rat basophilic leukemia cells (RBL-2H3) which have an inwardly rectifying K^+ channel. Injection of 50 ng of polyA+ mRNA into *Xenopus* oocytes resulted in the expression of an inward K^+ current after 5 days *in vitro*. The inward current was activated at hyperpolarized potentials, rectified at potentials positive to the reversal potential and was blocked by 1 mM barium. The figure shows the barium-sensitive currents obtained by subtraction. The two microelectrode voltage clamp technique was used to record currents. The oocytes were bathed in 91.2 mM KCl, 20 mM $MgCl_2$, 10 mM Hepes, pH 7.4 (NaOH), 230 mOsm.

Supported by grants from the Pharmaceutical Manufacturers Association Foundation, the American Heart Association Georgia Affiliate, and NIH NS 28894.

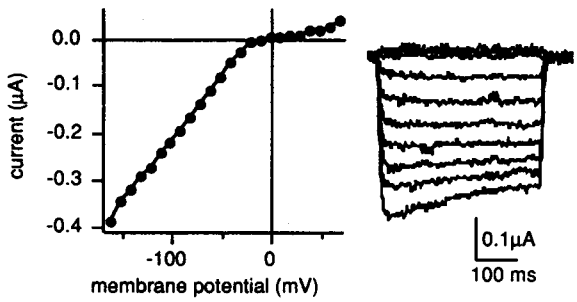

W-Pos130

DIVERSITY AND MOLECULAR EVOLUTION OF VOLTAGE-GATED POTASSIUM CHANNELS

*Michael Strong, *Grischa Chandy, *K. George Chandy and +George A. Gutman (Intro. by Russell Jacobs). *Departments of Physiology and Biophysics, and +Microbiology and Molecular Genetics, University of California Irvine, Irvine CA 92717.

Nucleotide and amino acid sequence similarities between the many voltage-gated potassium channel genes described in recent years suggest the existence of an ancient gene superfamily. In order to understand the evolutionary relationships between and within the putative potassium channel families, we have aligned both nucleotide and amino acid sequences of insect, amphibian and mammalian genes, and are using various methods for generating phylogenetic trees. Analysis of amino acid sequence alignments by the parsimony approach has shown that *Shal* and *Shab* share a common ancestor different from the ancestral gene that gave rise to *Shaker* and *Shaw*. The mammalian *Shaw*-related genes form a monophyletic group within the *Shaw* lineage. Parsimony analysis of nucleotide sequences of *Shaker*-related genes also shows the vertebrate genes to be monophyletic, with six different genes (represented by their Xenopus, mouse, rat and/or human homologues) progressively diverging from a main lineage. This second variety of tree, even more than the first described, shows substantial differences in the branch lengths leading to different modern sequences, indicating the absence of an absolute molecular clock operating in the divergence of these genes.

This work was supported by grants from the USPHS (AI24783 and AI21366), the Juvenile Diabetes Foundation International (#188209), and from Pfizer Inc.

W-Pos131

HETEROMULTIMERIC K^+ CHANNELS PRODUCED BY CO-EXPRESSION OF 2 HUMAN K^+ CHANNEL GENES.

T. E. Lee, R. E. Hice, L. H. Philipson, and D. J. Nelson. Dept. of Medicine, Univ. of Chicago, Chicago, IL 60615.

We have examined the appearance of heteromultimeric K^+ channels following co-injection of 2 human Shaker-type K^+ channel cRNAs into *Xenopus* oocytes. Our human K^+ channel clones, hPCN1 and hPCN2, are homologous to the rat brain K^+ channels kv1 (Swanson, *et al.*, *Neuron* 4:929, 1990) and RCK4 (Stühmer, *et al.*, *EMBO* 8:3235, 1989), respectively. Sequences were obtained by screening a human insulinoma cDNA library (hPCN1) and a human fetal skeletal muscle cDNA library (hPCN2). Predicted amino acid sequence identity between hPCN1 and hPCN2 is 55% (Philipson, *et al.*, *PNAS*, In press). Threshold for activation of hPCN1 current in *Xenopus* oocytes is -25 mV and outward currents elicited during depolarizing steps inactivate slowly with time. Threshold for hPCN2 current activation in oocytes is -55 mV and inactivation is largely complete by 200 msec. hPCN1 currents are reduced by approximately 3% while hPCN2 currents are completely blocked at holding potentials of -40 mV. Currents in co-injected oocytes (2.2 ng hPCN1: 0.13 ng hPCN2) differed kinetically from currents in oocytes injected with a single cRNA species, and co-injected oocytes did not appear to express homomultimeric channels. No transient outward current was observed during depolarizations to -55 to -45 mV, and no delayed outward currents were observed during depolarizing steps from a holding potential of -40 mV. Transient currents in co-injected oocytes exhibited an intermediate threshold for activation (ca. -40 mV) and a substantial transient current component remained at a holding potential of -40 mV. The novel properties of the currents in co-injected oocytes indicate that the co-assembly of variant polypeptides leads to the formation of channels with distinct characteristics. Supported by NIH RO1 GM36823.

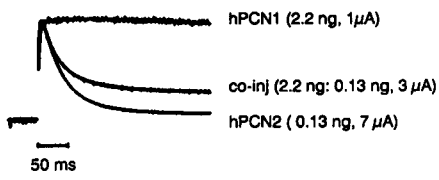

W-Pos132

MOLECULAR CLONING OF A RAT BRAIN K+ CHANNEL FAMILY WITH HOMOLOGY TO SHAW.

Christopher J. Luneau, Jeffrey Smith, Jacinta B. Williams (Intro. by David Williams), Dept of Pharmacology, Merck, Sharp and Dohme Research Laboratories, West Point, PA.

A family of K+ channel clones has been isolated from an adult rat brain library by using an oligonucleotide probe based on K_V4, a rat brain Shaw homolog which displays delayed rectifier kinetics (Luneau,et al, 1990), and by PCR of rat brain cDNA. One of these, $K_V5.1$, spans 2.6 kb and has a full length ORF which could encode a polypeptide of 638 amino acids (M_r =70,190). An oligonucleotide probe based on the sequence of the C-terminus of $K_V5.1$ hybridizes to mRNA species of 7.5 and 6.5 kb. Two additional members of this family, $K_V5.2$ and $K_V5.3$, are 5'-truncated clones which start at H1 and H6 respectively and extend through the 3'ends below their putative termination codons. These clones and another homolog, RKSHIIIA (McCormack,et al,1990), exhibit complete identity throughout their sequence before diverging completely at the same amino acid at their C-termini. K_V4 has recently been demonstrated to exist as a product of alternative splicing of a single gene which encodes both K_V4 and NGK2 (Luneau,et al,1990;Yokoyama,et al,1989). Genomic blots utilizing a probe based on the core region of this new family of clones reveal a single band in the restriction digests, implying that one gene encodes all four of the K_V5 family transcripts and that they are alternative splicing products similar to the KV4/NGK2 gene.

W-Pos133

THE I_{sK} GENE IS EXPRESSED IN HUMAN HEART

Richard Swanson, Kimberly Folander, Joanne Antanavage, and Jeffrey Smith Department of Pharmacology, Merck Sharp and Dohme Research Labs, West Point, PA 19486

Samples of human cardiac tissue were obtained from both atria (isolated during coronary artery bypass grafting and immediately frozen) and ventricle (removed at autopsy ~10 hours post mortem). RNA was prepared from both tissues and transcription of the I_{sK} gene was demonstrated in each by PCR analysis. Cloning and sequencing of the PCR products established that both the Ser^{38} and Gly^{38} alleles of the I_{sK} gene are expressed in the human heart. The expression of the I^{sK} gene in the heart is consistent with its postulated role in the generation of slow K^+ currents in both muscle and epithelia. Data consistent with a direct role in the formation of the K^+ channel itself was obtained from mutagenesis experiments. Deletion- and point mutations within the carboxy- terminal domain of the protein alter several of the biophysical parameters of the I_{sK} currents expressed in *Xenopus* oocytes, including the voltage dependence of activation, the ionic selectivity, and the kinetics of activation. The changes in each of these properties of the currents, resulting from mutations in the I_{sK} protein, are most readily explained by a model postulating the direct formation of the channel by the I_{sK} protein.

W-Pos134

INTERNAL BLOCK BY QUATERNARY AMMONIUM COMPOUNDS ON INACTIVATION-REMOVED *SHAKER* MUTANT MIMICS THE INTRINSIC FAST INACTIVATION OF THE *SHAKER* WILDTYPE.

Kathleen L. Choi and Gary Yellen. Howard Hughes Med. Inst. and Depts. of Neuroscience and Biophysics, Johns Hopkins Sch. of Med., Baltimore, MD 21205

We have studied the effects of quaternary ammonium compounds on a *Shaker* K^+ channel that has been mutated to remove the normal fast inactivation process (H4:Δ6-46; ShIR). We have found that both 3-phenylpropyl-tetraethylammonium (ppTEA) and tetrapentylammonium (TPe) block at the inner mouth of the channel with high affinity.

The channel blockade by these compound alters the apparent kinetics of K^+ current. The control ShIR current rises rapidly and remains roughly constant for hundreds of milliseconds. In the presence of blockers, the current rises quickly but then falls in a fashion that resembles the normal fast inactivation process. Higher blocker concentrations produce a faster relaxation and a more severe steady state block. The concentrations of ppTEA and TPe required for half-block at steady state are 33 μM and 2 μM, respectively.

With higher concentrations of blockers, the kinetics of the tail current were also altered: 1) the tail current showed a prominent rising phase before the peak, lasting several milliseconds; 2) blockers slowed the channel closing rate. Thus, the blockers do not simply occlude the pore but also interfere with the normal gating process. These observations are similar to those of Clay Armstrong on delayed rectifier K^+ channels. He suggested that the rising phase corresponds to the voltage-dependent exit of blockers, and that the channel closing rate is slowed because channels cannot close when the blocker is still bound to the pore.

We will test whether Armstrong's "foot in the door" model can explain our results and will further examine the properties of blockade at the single channel level.

W-Pos135

EXPRESSION OF A CLONED CARDIAC POTASSIUM CHANNEL IN MOUSE Ltk⁻ CELLS.

Snyders D.J., Roberds S.L., Knoth K.M., Bennett P.B., Tamkun M.M. Vanderbilt University School of Medicine, Nashville, TN

Several cloned mammalian potassium channels have been expressed in *Xenopus* Oocytes; however, processing of these channels may be different in mammalian cells. We therefore expressed a potassium channel cloned from a rat cardiac cDNA library in mammalian tissue culture cells. A CMV promoter driven expression vector was used to generate mouse Ltk⁻ cell lines expressing RK2, a channel identical to the RBK2 channel cloned by others from rat brain. Clonal cell lines were screened for RK2 mRNA expression in this fibroblast derived cell line by Northern blot analysis. Functional expression was assessed using whole cell and patch clamp recording from cells obtained by gentle trypsinization of confluent cultures. GigaΩ seals (5-20GΩ) were obtained with 2-5 MΩ electrodes (filled with 130 KCl, 10 HEPES, 5 ATP, 5 BAPTA, 1 $MgCl_2$). In both control and transfected cells, a small (50-100 pA) 'background' current displaying outward rectification was observed. In approximately half of the transfected cells a time-dependent current of the delayed rectifier type was observed. Activation was steeply voltage dependent with a midpoint near -15 mV. Activation time constants ranged from 50 to 10 msec between -30 and +30 mV. A small degree of inactivation was present for depolarizations beyond +10 mV. The size of the current was variable between cells, ranging from 150 to 1200 pA at +50mV (15-170 pA/pF). In oocyte expressed RK2, we have previously observed similar activation properties, but no definite inactivation. The reasons for this difference and for the variable degree of channel expression in the mouse L-cells remain to be determined.

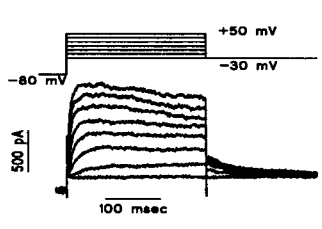

W-Pos136

STRUCTURE-FUNCTION ANALYSIS OF THE DELAYED RECTIFIER K^+ CHANNEL *drk1*: THE FIFTH TRANSMEMBRANE SEGMENT (S5).

A.M.J VanDongen, R.H. Joho and A.M. Brown, (Intro. by A. Yatani) Department of Molecular Physiology and Biophysics, Baylor College of Medicine, One Baylor Plaza, Houston, TX 77030.

Voltage dependent K^+ channels are thought to consist of a core region containing six transmembrane segments (S1-S6) flanked by cytoplasmic domains. The fourth segment (S4) which contains a highly conserved series of positive charges, has been shown to be involved in voltage sensing. The role of the other five segments is unknown. Both S2 and S3, as well as the region linking S5 and S6 have been proposed to form the pore. An important question that has to be addressed is how an outward movement of the sensor (S4) results in an increased probability of opening and which structures are involved in this coupling. In this study we have investigated the functional role of S5, a highly hydrophobic segment containing only a few polar amino acids. The S5 segment is flanked on each side by a glutamate residue, which is strictly conserved in all K^+ channels for which the primary structure is known, and in the first domain of a Na^+ channel of *Drosophila*. We have modified these glutamate residues in *drk1*, a delayed rectifier K^+ channel from rat brain, using site directed mutagenesis. Mutants were expressed in *Xenopus* oocytes and characterized both at the whole cell and single channel level. Changing these glutamates into either aspartate (preserving charge) or glutamine (preserving bulkiness) had very little effect on whole cell activation properties. At the single channel level, however, there was a dramatic effect on the open/close behavior: the mean open times was reduced from 20 msec to in some cases less than 1 msec. There was no effect on first latency. Concomitantly, the steady state open probability was reduced considerably. From these results we would like to propose that the glutamates flanking S5 are involved in stabilizing the open state. (Supported by NIH NS 23877 and NS 28407).

W-Pos137

STRUCTURE-FUNCTION ANALYSIS OF THE DELAYED RECTIFIER K^+ CHANNEL *drk1*: TEMPERATURE SENSITIVITY.
S.A. Fedulova, J.A. Drewe, R.H. Joho, A.M. Brown and A.M.J. VanDongen (Introduced by W. Chiu). Department of Molecular Physiology and Biophysics, Baylor College of Medicine, One Baylor Plaza, Houston, TX 77030.

We have investigated the temperature sensitivity of the delayed rectifier K^+ channel from rat brain encoded by the *drk1* gene. Channels were expressed in *Xenopus* oocytes injected with *drk1* cRNA and voltage clamped. The rate of activation was found to be extremely temperature dependent. We used the Hodgkin and Huxley model to quantitate the effect of temperature on activation kinetics. The time constant of activation as a function of temperature in the range 15 to 25°C is shown in the figure. For *drk1* the time constant changes more than a factor of 10 for a ten degree change in temperature (Q_{10}=10). To study the possible role of phosphorylation we have constructed two C-terminal deletion mutants: ΔC351 which is missing 351 amino acids, but still contains the two putative cAMP-dependent phosphorylation sites and ΔC422 which lacks both sites. As can be seen from the figure, the Q_{10} for ΔC351 is like *drk1*, but the Q_{10} for ΔC422 is around 4. These preliminary results suggest that phosphorylation is involved in the extreme temperature dependence of this channel.

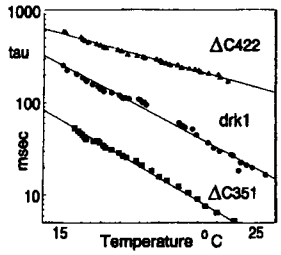

(Supported by NIH NS 23877 and NS 28407).

W-Pos138

ISOLATION OF A PUTATIVE MURINE T LYMPHOCYTE K^+ CHANNEL cDNA AND mRNA EXPRESSION IN STIMULATED CELLS.
B. Freedman*, M. Prystowsky, and C. Deutsch*. Depts. of Physiology* and Pathology and Lab. Medicine., Univ. of Penna., Phila., PA 19104-6085 (Intro. by Bayard Storey).

We have cloned two putative K^+ channel cDNA from an antigen/interleukin 2 (IL2) dependent, non-transformed, murine helper T-lymphocyte clone, L2. We used a mixture of synthetic oligonucleotide primers derived from different K^+ channel sequences to make cDNA from total L2 cellular RNA. The polymerase chain reaction was used to amplify these cDNA. Two clones were isolated. The largest of these clones (MTK1) has been sequenced and shares greater than 90% homology with other K^+ channel sequences. To understand the cellular basis of the IL2-induced increase in whole-cell K^+ conductance in L2 cells (Lee et. al., 1986), we have used MTK1 to probe Northern blots prepared from total L2 cellular RNA at various times after IL2 stimulation. Five mRNA (7.5kb, 4.5kb, 3.7kb, 3.3kb, and 2.4kb) hybridized with MTK1, yet exhibited little IL2 dependent change in steady-state levels throughout the cell cycle. We observed an increase of at least 5-fold in the steady-state levels of three large mRNA (10.5kb, 8.5kb, and 6.0kb) 24 hours after activation of quiescent L2 cells. At 48 hours these cells show a 50-fold increase in ^{3}H-thymidine incorporation. These mRNA return to baseline steady-state levels after 96 hours, when L2 cells no longer divide. The time course and extent of induction of these mRNA are consistent with a model that includes transcriptional regulation as the basis for the increase in whole-cell K^+ conductance induced by IL2. Supported by NIH GM41467, GM36962, GM07170.

W-Pos139

SINGLE CHANNEL K^+ CURRENTS IN PRIMARY HUMAN T LYMPHOCYTES.
S.C. Lee, D. Levy and C. Deutsch. Dept. of Physiology, Univ. of Pennsylvania, Philadelphia, PA 19104-6085.

Several single channel K^+ currents were observed in patch-clamped human T lymphocytes. Using the cell-attached configuration, we could distinguish three types of outward unitary current. The most prevalent type gated with membrane depolarization and reversed direction at ca. -85 mV. Ensemble averages of this conductance gave activation and inactivation parameters similar in magnitude and voltage-dependence to those derived for the voltage-gated K^+ current in whole-cell recording. A second class of voltage-gated conductance gave an ensemble average with an inactivation time-constant 3-5 fold larger than that of the more prevalent channel. The third type was a non-inactivating channel with little or no voltage dependence, characterized by rapid flicker during open-channel bursts, intermittent silent periods, and a reversal potential negative to -80 mV. All three currents are consistent with a K^+ selective unitary conductance of 8-10 pS with normal Ringer's (5 mM K, 2.5 mM Ca) in the cell-attached pipette. These channel types may underlie both the inactivating and non-inactivating current observed during sustained depolarization in whole-cell recording. In whole-cell patch-clamp configuration, we found that both residual unitary currents at 0 mV and voltage-gated non-inactivating macroscopic current were insensitive to charybdotoxin (20 nM) but were abolished by high intracellular TEA or Cs. It remains to be determined if these unitary currents are distinct channels or modifications of a single channel type. Supported by NIH GM 41467.

W-Pos140

CHARYBDOTOXIN AND HIGH EXTRACELLULAR K^+ SPECIFICALLY DECREASE IL2 mRNA STEADY-STATE LEVELS IN STIMULATED HUMAN T LYMPHOCYTES.
B. Freedman, M. Price and C. Deutsch. Dept. of Physiology, Univ. of PA, Phila., PA 19104-6085.

Charybdotoxin (ChTX) is a specific, impermeant and potent blocker of the lymphocyte voltage-gated K^+ channel (Sands et al., 1989; Price et al., 1989). In phytohemagglutinin (PHA) stimulated peripheral blood T-cells, ChTX inhibits elaboration of interleukin 2 (IL2) and proliferation. Exogenous IL2 reverses the inhibition of proliferation (Price et al., 1989). We now show that ChTX (50nM) decreased steady-state levels of IL2 mRNA by ≥80% without any apparent effect upon the constitutive expression of HLA-I mRNA, or c-myc, a mitogen induced gene. ChTX also maximally depolarizes lymphocytes to a potential of -35mV (Grinstein et al., 1990). To test the hypothesis that inhibition of IL2 gene expression and mitogenesis are mediated by ChTX-induced depolarization, we determined the effects of depolarization by extracellular K^+ (K^+_e) on proliferation, IL2 elaboration and IL2 gene expression. Isotonic replacement of extracellular Na^+ with K^+, in serum-free media, inhibits PHA-induced proliferation in a concentration dependent manner, with an IC_{50} of 35mM (calculated E_m = -38mV). At this $[K^+]_e$, steady-state levels of IL2 mRNA were decreased by ≥80% and the amount of secreted IL2 in culture supernatants was decreased by ≥50%. ChTX further inhibited proliferation at $[K^+]_e \leq 35$mM, yet exerted no apparent effect in media containing 35-140mM K^+. Exogenous IL2 increased proliferation at all $[K^+]_e$. These results suggest that ChTX and $[K^+]_e \leq 35$mM inhibit T-lymphocyte mitogenesis by similar mechanisms, while inhibition at $[K^+]_e \geq 35$mM may involve additional pathways. Supported by NIH GM41467 and NIH GM07170.

W-Pos141

ALTERNATIVE SPLICING CONTRIBUTES TO K^+ CHANNEL DIVERSITY IN THE MAMMALIAN CENTRAL NERVOUS SYSTEM Christopher Luneau, Jacinta Williams, Edwin Levitan, John Marshall, Joanne Antanavage, Carlos Oliva, Jeffrey Smith, Kimberly Folander, Richard Swanson, Leonard Kaczmarek, and Susan Buhrow. (Intro. by Charlie Cohen) Dept. of Pharmacology, Yale University School of Medicine, New Haven, CT and Dept. of Pharmacology, Merck Sharp & Dohme Research Laboratories, West Point, PA

Mammalian voltage-gated K^+ channels can be subdivided into several groups on the basis of their sequence homology to each other and to *Drosophila* K^+ channels. The best-characterized mammalian K^+ channel family (the *Shaker*-like family) is comprised of many related genes, apparently intronless, which appear to have arisen from duplication of a primordial gene. In contrast, we demonstrate here that, at least in the mammalian *Shaw* family, genetic diversity can also be generated by alternative splicing of RNA.

A cDNA (K_V4) containing an ORF with homology to the *Drosophila Shaw* gene was isolated from a rat brain cDNA library using another K^+ channel, K_V1, as a probe. In the rat, K_V4 is encoded by an 4.5kb mRNA that increases dramatically in abundance with age from birth to adulthood; the mRNA was found only in brain. Oligonucleotide probes from various regions of K_V4 hybridized to additional, related mRNA species on Northern blots of adult rat RNA, suggesting that it is a member of a multigene family. In fact, K_V4 is identical to a previously-described Shaw channel, NGK2, from amino acid 1 to 501, but thereafter, the proteins diverge completely. The gene encoding the region common to the two proteins is represented only once in the genome as indicated by genomic Southern blots. Comparison of the cDNA with genomic clones encoding the common and unique regions, demonstrates that the point of divergence of the proteins coincides with a splice junction in the gene. The mRNAs for the two proteins are derived from alternative exon usage at that splice junction; in NGK2, the splice junction is read-through into additional coding sequence, and in K_V4, the common exon is spliced to two additional exons downstream to generate the longer K_V4 protein. This alternative splicing generates two proteins that have different consensus sites for phosphorylation by various kinases and, therefore, may be differentially regulated by cellular kinases.

W-Pos142

MOLECULAR CLONING AND DIFFERENTIAL EXPRESSION OF POTASSIUM AND CALCIUM CHANNELS EXPRESSED IN CANINE COLONIC CIRCULAR MUSCLES. John D. Adlish, Kenneth E. Overturf, Padraig Hart, Dawn Duval, Kenton M. Sanders and Burton Horowitz Department of Physiology, University of Nevada School of Medicine, Reno, NV 89557

Gastrointestinal motility has its mechanistic basis in rhythmic electrical events termed slow waves which lead to excitation-contraction coupling. The ionic currents which are characteristic of slow waves include inward Ca^{2+} currents and at least 3 types of voltage-dependent K^+ currents. Utilizing the polymerase chain reaction and oligonucleotide primers which hybridize to DNA sequences within the S5 (sense) and S6 (anti-sense) regions of voltage-gated K^+ channels, we have identified at least 3 distinct amplification products using poly-A^+ RNA isolated from canine colonic circular muscles. DNA sequence analysis suggests that they originate from mRNAs coding for a family of voltage-gated K^+ channels. One of the amplification products, designated b12A, displays 80% homology to the rat brain K^+ channel RCK1. Northern blot hybridization was performed on RNA isolated from canine heart, and colonic longitudinal and circular muscles using this product as a probe. A single band hybridized with a molecular weight of approximately 4.0 kb for RNA derived from all the tissues. RNA was also prepared from dissected tissues representing distinct regions of the colonic circular muscle layer including the submucosal surface, bulk region and the myenteric border, as well as longitudinal muscle. Northern hybridization of these RNA samples with b12A as a probe demonstrates that this K^+ channel is differentially expressed across the circular muscle layer with approximately 3 times the amount of RNA expressed in the bulk and myenteric regions than the submucosal region.

The Ca^{2+} channel $\alpha 1$ subunit expressed in rat brain has been grouped into four distinct classes (Snutch et al., PNAS 87:3391, 1990). Northern blots containing mRNA from regions spanning the cross-section of the colonic circular muscle layer were hybridized utilizing a representative from each of the classes (A - D) as a cDNA probe. The representative from the C class hybridized to RNA from colonic smooth muscle and this Ca^{2+} channel was differentially expressed across the circular muscle layer. There is approximately 2 times the abundance of RNA encoding this channel in the myenteric region than the submucosal region, with a gradient in expression between these two regions. Differential genetic expression of ion channels in circular smooth muscles could contribute, in part, to the heterogeneity in electrical activity in circular muscles throughout the GI tract.

Partially supported by a Program Project Grant from NIDDK, DK41315.

W-Pos143

ALTERED PROPERTIES OF THE MECHANOSENSITIVE ION CHANNEL IN A LIPOPROTEIN MUTANT OF ESCHERICHIA COLI. Kubalski, A.*+, Martinac, B.#, Adler, J.*+ and Kung, C.#, Laboratory of Molecular Biology#, Department of Biochemistry*, and Department of Genetics, University of Wisconsin, Madison, Wisconsin, 53706

We have used the patch-clamp recording to study properties of the mechanosensitive (MS) channel in a deletion mutant (JE5505) of E. coli lacking Braun's lipoprotein (LP). LP is one of the major links between the peptidoglycan (cell wall) and the outer membrane in which the MS channel is located (Buechner et al., BBA 1024:111-121, 1990).

The MS channel of the mutant differs in two ways from the channel of the wild-type strain: (i) pressure sensitivity, which is given by the amount of pressure necessary for an e-fold change in the channel open probability, is reduced in the mutant as compared to its wild-type parent (mutant: 12.7 ± 0.8 mm Hg (n=4), wild-type: 4.7 ± 0.9 mm Hg (n=5)); (ii) amphipathic compounds (chlorpromazine, trinitrophenol) at the concentrations shown to activate the channel reversibly in the wild-type strain (Martinac, Adler and Kung, Nature (in press)), fail to activate the channel in the mutant.

Our data suggest that the presence of LP in the outer membrane may be necessary for proper activation of the MS channel by membrane tension. In addition, LP might be an "endogenous amphipath". Supported by NIH grant DK39121 and by a grant from the Markey Trust.

W-Pos144

MECHANOSENSITIVE CHANNELS AS REPORTERS OF BILAYER EXPANSION: A THEORETICAL MODEL. Markin, V.S.*@ and Martinac, B.#, Institute of Electrochemistry@, Moscow, USSR, Dept. Biochemistry*, Univ. of Minnesota, Twin Cities, St. Paul, MN 55108, Lab. of Molecular Biology#, Univ. of Wisconsin, Madison, WI 53706.

Various amphipathic compounds (e.g. chlorpromazine, trinitrophenol, local anesthetics) have been found to activate the mechanosenstive (MS) ion channel of the bacterium Escherichia coli (Martinac, Adler and Kung, Nature, in press). The results were qualitatively interpreted in terms of bilayer couple hypothesis (Sheetz and Singer, PNAS 71:4457-4461, 1974). Here we have developed a mathematical model which could describe the effects of amphipaths on the MS channel quantitatively.

The free energy available for gating of the MS channel is linearly dependent upon pressure so that channel opening probability Po follows the Boltzmann distribution: $\ln[Po/(1-Po)] = m_0 \gamma + b_0$, where γ is the membrane tension which increases P_o, and m_0 and b_0 are constants. Upon partitioning of amphipaths into the membrane monolayers the model gives the following expression for channel open probability: $\ln[Po/(1-Po)] = m_0 \gamma^{mem} + m_0 E a_0 (|n^{in} - n^{out}|) + b_1$, where E is the elasticity modul of area expansion, n^{in} and n^{out} is the density of an amphipath in the inner and outer monolayer respectively, and a_0 is membrane area occupied by amphipathic molecules. The kinetics of amphipath adsorption to the membrane is accounted for by the expression: $(|n^{in} - n^{out}|) = (|1 - R|) \{K_1 c + [n^{in}(0) - K_1 c] \exp(-t/\lambda)\}$, where K and R are equilibrium constants for amphipath exchange between the bath solution and inner monolayer of the membrane, and between membrane monolayers respectively, c is amphipath concentration in the bath solution, t is time and λ is the time constant.

The model can describe satisfactory previous experimental data on the effects of amphipaths on the MS channel of E. coli. Future experiments will be designed to test the predictions which follow from the model. Supported by NIH grant DK39121 and grant from the Markey Trust to C. Kung and J. Adler, and ONR grant to T. Tsong.

W-Pos145

THE ROLE OF THE STRECH-ACTIVATED CHANNELS OF E.COLI IN OSMOTIC DOWNSHOCK, A. Ghazi, C. Berrier, A. Coulombe, C. Houssin (intro. by M. le Maire). Laboratoire des Biomembranes and Laboratoire de Physiologie Comparée, URA CNRS 1116 et 1121, Université Paris-Sud, 91405 Orsay Cedex, France.

Inner membranes of E.coli bacteria fused into giant liposomes and studied by patch-clamp contain several very large strech-activated (SA) channels (Berrier et al, FEBS Lett. 259: 27- 32, 1989). We found that Gadolinium, which blocks SA channels in Xenopus oocytes (Yang and Sachs, Science, 243: 1068-1071, 1989), inhibits the largest (300, 500, 1000 pS in 0.1 M KCl) E.coli SA channels, at micromolar concentrations. Since direct block should be excluded by the sizes of these channels, this would imply interaction of gadolinium with a strech sensory device, highly conserved during evolution.

It is an old observation that osmotic downshock of bacteria results in an extensive loss of internal ions and metabolites, with no lysis of the cells. Upon shock in cold distilled water, E.coli cells lost all their potassium, and 70-80 % of their internal ATP and of radioactive lactose and glutamate prealably accumulated by active transport. Gadolinium (200 µM) in the shock fluid totally inhibited the loss of ATP, lactose and glutamate and reduced the rate of potassium efflux. Together with the data obtained in patch-clamp, this demonstrates that SA channels control the efflux of osmoticants, thus playing a major role in the response to osmotic shock. Also, these experiments furnish compelling evidences in favor of the (debated) localization of the SA channels in the inner membrane.

W-Pos146

A STRETCH-SENSITIVE K CHANNEL FROM CULTURED APLYSIA MECHANOSENSORY NEURONS. **David H. Vandorpe & Cathy E. Morris, Neuroscience Unit, Loeb Institute, Ottawa Civic Hospital & Biology Department, University of Ottawa, Ottawa K1N 6N5.**

Stretch-activated K channels are readily detectable during single channel recording of snail neurons, but it has not been established what physiological role the channels play. We have therefore made single channel recordings from mechanosensory neurons of the ventro-medial cluster of the pleural ganglion of Aplysia; since these neurons respond to peripheral mechanostimulation by producing action potentials, we would anticipate that their mechanotransduction channels should be non-selective cation channels like those of crayfish mechanosensory neurons. The cell bodies of Aplysia mechanosensory neurons, however, exhibited no such channel activity. Instead, patches characteristically had 1-4 K-selective channels whose open probability increased with membrane stretch (typically, ~40 mmHg suction through the pipette would double the open probability). Under cell-attached conditions with artificial seawater (plus 10 mM tetraethylammonium to block Ca-activated K channels) the channel had a near-linear I/V relation with a conductance of 51 ± 3 pS (n=5; voltage range, 20-100 mV depolarized from rest). It seems likely that this stretch-sensitive Aplysia K channel is related to the ubiquitous stretch-activated K channels of snail neurons (Sigurdson & Morris, 1989, J. Neurosci. 9: 2801), and it is difficult to conceive how it could play a direct role in mechano-excitation.

Funded by NSERC, Canada.

W-Pos147

STRETCH ACTIVATED POTASSIUM CHANNELS IN THE LATERAL WALL OF THE AUDITORY OUTER HAIR CELL Minxu Li, Min Jia, and Kuni H. Iwasa, Biophysics Lab, NINDS, National Institutes of Health, Bethesda, Maryland 20892

It has been established that the stereocilia of hair cells are mechano-receptors. Here we report evidence that the lateral wall of the mammalian auditory outer hair cell is also a mechano-receptor.

With patch clamping method, we found stretch-activated potassium channels with 130 pS unit conductance in the lateral wall region of isolated auditory outer hair cells from the guinea pig. The reversal potential of these channels was determined with excised patches and was about —70 mV. The open probability of these channels were larger when internal Ca ion concentration was higher, when the membrane potential was more depolarized, and when suction applied to the pipette was greater.

In order to determine the physiological importance of these channels, we subjected isolated outer hair cells to osmotic stress. Exposure of these cells to hypo-osmotic media (with the same ionic composition as the bathing medium) applied with a perfusion pipette under whole-cell recording mode resulted in hyperpolarization (up to 10 mV). The reversal potential for the whole-cell current responding to the stress agreed with that of the stretch activated potassium channels we observed with single channel recording. Since the medium in the pipette contained calcium buffer with 5 mM EGTA, this current is attributable to the opening of the stretch activated potassium channels as the direct effect of the stress to the membrane rather than opening of potassium channels mediated by an elevation in the internal free Ca ion.

Since stretch activated potassium channels were observed only in the lateral wall, we can conclude that the lateral wall is the structure sensitive to mechanical stress. Morphological studies revealed a unique structure in the lateral wall of the outer hair cells: a submembranous lattice structure connecting plasma membrane with cisternae system. This structure may be a significant factor in achieving a high efficiency in mechano-electrical transduction. The channels we have observed could be related to another distinctive feature of the outer hair cells, i.e. the production of a largely hyperpolarizing response to sound stimuli, in contrast to other hair cells in which the response is more depolarizing. These channels could also produce a feedback to mechanical stimuli, a physiological role expected of outer hair cells. This is considered to be a basis for the fine tuning mechanism of the mammalian hearing organ.

W-Pos148

PRESSURE AND VOLTAGE DEPENDENCE OF STRETCH-ACTIVATED CHANNELS IN BOVINE AORTIC ENDOTHELELIAL CELLS. *Teryl R. Elam and Jeffry B. Lansman. Department of Pharmacology, University of California; San Francisco, CA 94143.*

Activity of single mechanosensitive channels was recorded from cultured bovine aortic endothelial cells. Applying pressure to the patch electrode reversibly increased channel activity in a manner which was fit by a Boltzman distribution (8 mm Hg/e-fold change in P_o; $P_{1/2}$=34 mm Hg). The single channel current-voltage relationship rectified with a slope conductance of 36 pS for inward currents in isotonic potassium. Divalent cations also carried current through the channel (13 pS in 110 mM $BaCl_2$). Membrane depolarization increased channel open probability and the relationship followed a Boltzman distribution (25.4 mV/e-fold change in P_o; $V_{1/2}$=67mV). Analysis of the duration of open and closed channel lifetimes showed a single open (τ=16 ms; -50mV) and multiple closed states (τ_1=11 ms, τ_2=719 ms; -50mV). Applying pressure or depolarizing the patch increased the open times and decreased the long closed times, which can account for the observed increase in open probability. Another mode of channel gating was observed at negative holding potentials. Inward single channel conductance was 39 pS in isotonic potassium and mean open time was on the order of tens of seconds. It was activated by applying suction, but releasing the pressure did not produce a reversible return to the low pre-suction activity level. Channel activity could be returned to a low level by briefly stepping the patch potential to positive test levels. Inactivation during these steps consisted of discrete channel closings which, when many sweeps were averaged, could be fit by two exponentials with time constants of 88 and 1023 ms. Upon returning to negative holding potentials, activity remained low and could only be increased by applying pressure again.

W-Pos149

A VOLTAGE DEPENDENT STRETCH-ACTIVATED CHANNEL IN CHICK SKELETAL MUSCLE. Masahiro Sokabe and Noboru Hasegawa, Dept. Physiol., Nagoya Univ. Sch. Med., Nagoya 466, Japan

A stretch-activated (SA) channel was firstly discovered in cultured chick skeletal muscle cells (Guharay and Sachs, 1984). In addition to this channel we found a voltage-dependent SA channel with three times the conductance of the former (190 pS at 150mM KCl). The channel appeared to be more permeable to cations than to anions. The permeability sequence (P_K: P_{Na}: P_{Ca}: P_{Cl} = 1: 0.22: 0.43: 0.017) allowed us to classify this channel as a nonselective cation channel like as the original SA channel. Kinetic analyses of single-channel currents indicated one open (O) and two closed (C_1,C_2) states. Analysis based on a linear transition model (C_1-C_2-O), suggested that only the rate constant ($k_{1,2}$) that governs the C_1 to C_2 transition was stretch-sensitive. This rate constant ($k_{1,2}$) increased exponentially with the square of the applied suction; the sensitivity to pressure was somewhat smaller than that of the original SA channel. On the other hand, the forward and backward transitions between C_2 and O were voltage-sensitive. Depolarization increased $k_{2,3}$ and decreased $k_{3,2}$ exponentially; the sensitivity to voltage was several times higher than that of the original SA channel. In contrast to the original SA channel, where the voltage and pressure dependence occur in the same rate constant ($k_{1,2}$ in a C_1-C_2-C_3-O diagram), the voltage sensitivity of the newly found SA channel resides in transition steps distinctive from the pessure sensitive step. As the two kinds of SA channels can often be seen in the same patch, the density and distribution of these channels may be comparable.

W-Pos150

STRETCH-ACTIVATED CHANNELS IN THE PLASMA MEMBRANE OF PLANT MOTOR CELLS Nava Moran. Dept. of Neurobiology, Weizmann Institute, Rehovot Israel.

Water loss from shrinking cells in the plant motor organ (pulvinus) responsible for leaflet movements follows the loss of KCl through depolarization-activated K-channels (K_D) and - perhaps - via Ca-dependent Cl-channels (Cl_{Ca}) in the plasma membrane. In a pursuit for (a) a signal to INITIATE cell shrinking, and (b) anion-efflux pathway to SUSTAIN osmoticum loss and support shrinking, Stretch-Activated (SA) channels were studied in the plasma membrane of pulvinar motor cells of Samanea using the patch- clamp technique. Negative pressure applied to the membrane, in the range of -10 to -30 mm Hg, reversibly increased the open probability of voltage-independent SA channels within the rim of the patch-pipette. Pressure of -50 to -60 mm Hg activated a less readily reversible channel (3 pS channel). Judging by amplitudes, five channel types were discerned (3, 9, 14, 27 and 50 pS). Judging by selectivities, two types of SA channels were observed: (i) with quite appreciable permeability ratio P_{Cl}/P_K: >20 (9 pS and 50 pS channels); (ii) poorly discriminating, with permeability ratios ranging between 7.3 - 2.4 (the 3 pS channel), 4.7-1.7 (the 27 pS channel) and 1-0.75 (14 pS channel). The Cl^--selective SA channels, activated in the inflated cell, should provide both the depolarizing signal to open the K_D channels and the pathway for Cl^- efflux during cell shrinking. In addition, the non-selective SA channels might admit Ca^{2+}, which could then provide the signal for the opening of Cl_{Ca} channels.

W-Pos151

SINGLE-CHANNEL CONDUCTANCE NOISE IN OPEN ALAMETHICIN CHANNELS

Don-on D. Mak, Watt W. Webb, School of Applied and Engineering Physics and Department of Physics*, Cornell University, Ithaca, NY 14853*

Voltage clamp recording at controlled temperatures was used to make high-resolution wide-band measurements of electrical current passing through single alamethicin channels in gigaohm sealed patches of lipid membranes formed from vesicles or by tip-dip through solvent-free lipid monolayers. The current noise spectrum of the channel during its residence time in each of the multiple conductance states was measured systematically. The conductance noise was found to be several orders of magnitude greater than the intrinsic ion shot noise even after subtraction of the bare membrane background noise. The excess noise extends smoothly at nearly constant power spectral density at least between our limits of accurate measurement of 50 Hz and 20 kHz. The current noise of higher conductance states was greater than that of lower conductance states and the measured rms noise was linearly proportional to the mean current levels of each conductance state. We conjecture that this current noise is caused by changes in the cross-sectional area of the channel pore due to conformational fluctuations of the assembly of alamethicin monomers that form the channel and that it may therefore be used to probe the low-frequency cooperative fluctuations of the membrane protein structure. (Work supported by ONR grant N00014-89-J-1656)

W-Pos152

COOPERATIVITY OF ALAMETHICIN INDUCED CONDUCTIVITY DETECTED BY PERFUSION EXPERIMENTS.

I. Vodyanoy and S.M. Bezrukov[1] (Intro. by M. Marron). Office of Naval Research, Arlington, VA 22217 & Dept. of Physiol. and Biophys., Univ. of Calif. Irvine, Irvine, CA 92717; [1]LBM/NIDDK, Natl. Inst. of Health, Bethesda, MD 20892 (on leave from Leningrad Nucl. Phys. Inst., Ac. Sci., Gatchina, 188350, USSR).

A bilayer membrane doped with alamethicin which was added to one solution compartment only was perfused by an antibiotic free electrolyte solution (5 volumes). Both compartments were stirred continuously during the perfusion (lasting about 3min). Both the membrane current noise and membrane conductance were monitored before and after the perfusion.

A nonexponential long-term relaxation of alamethicin induced conductance was observed. The normalized initial relaxation rate correlates with the membrane conductance before perfusion. A higher conductance will correspond to the higher rate.

The perfusion of the membrane at alamethicin concentration corresponding to only a few channels (at about 100 mV membrane potential) does not considerably change induced conductivity. Whereas, at 10 times higher alamethicin concentration perfusion results in two orders of alamethicin conductance magnitude decrease. A spectral analysis of channel current noise shows that either perfusion or following conductance relaxation does not change single-channel properties.

Significant conductivity reduction under higher alamethicin concentrations could be explained by cooperativity of the alamethicin desorption.

W-Pos153

EFFECT OF POLYETHYLENE GLYCOLS ON ALAMETHICIN CHANNELS.

S.M. Bezrukov and I. Vodyanoy[1]. LBM/NIDDK, NIH, Bethesda, MD 20892 (on leave from Leningrad Nucl. Phys. Inst., Ac. Sci., Gatchina, 188350, USSR); [1]Office of Naval Research, Arlington, VA 22217 & Dept. of Physiol. and Biophys., Univ. of Calif. Irvine, Irvine, CA 92717.

Osmotic and viscosity effects by polyethylene glycols (PEG) of various (200-20,000) molecular weights on alamethicin pores reconstituted into a lipid bilayer were studied using single-channel and noise analysis. It was found that an osmotic pressure reduces alamethicin conductivity. Addition of 15% (by weight) of PEG with the molecular weight above 1,500 to the membrane bathing solutions does not significantly change any of the three lowest open channel levels (1,2 and 3 on the graph) of alamethicin conductance. The PEG 200 reduces conductance of these levels as much as that of the bulk solutions. The osmotic effect can not be explained by the PEG inaccessible channel volume influence alone.

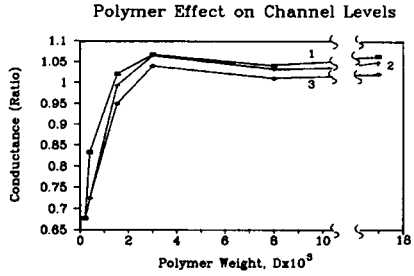

W-Pos154

MEMBRANE TOPOGRAPHICAL ANALYSIS OF *COLE1* GENE PRODUCTS: (I) THE HYDROPHOBIC ANCHOR OF THE COLICIN E1 CHANNEL IS A HELICAL HAIRPIN; (II) THE IMMUNITY PROTEIN.

H. Y. Song[1], F. S. Cohen[2], and W. A. Cramer[1](Intro. by W. L. Pak), [1]Dept. of Biological Sciences, Purdue University, West Lafayette, IN, 47907; [2]Dept. of Physiology, Rush Medical College, Chicago, IL, 60612.

The colicin E1 ion channel domain contains one prominent hydrophobic region near its COOH-terminus that has been assumed to be a membrane anchor. Saturation site-directed mutagenesis of this hydrophobic region, A471-I508, was used to probe whether it spanned the bilayer once or twice. A non-polar amino acid was replaced by a charged residue in twenty-nine mutations made at twenty-six positions. Substitution of the non-polar by a charged amino acid at all positions except those in the center of the hydrophobic domain caused a large decrease in cytotoxicity of the purified mutant colicin E1 protein. This implies that the hydrophobic domain spans the membrane bilayer twice in a helical hairpin loop with the center of this domain, G489-G493, residing in an aqueous or polar phase. Ion selectivity measurements indicate that these mutations do not grossly perturb the structure of the channel and that the hairpin forms part of the channel lining.

The topography of the colicin E1 immunity (*imm*) protein was determined from the pattern of Tn*PhoA* and complementary *lacZ* fusions, and site-directed substitution of charged for non-polar residues. These data imply that the 113 residue *imm* protein folds in the membrane as three *trans*-membrane α-helices, with the NH_2- and COOH-termini on the cytoplasmic and periplasmic sides of the membrane, respectively. The approximate spans of the three helices are N9-S28, I45-F65, and L84-L104. An extrinsic highly charged segment, K66-K74, containing 7 charges in 9 residues, extends into the cytoplasmic domain. The specificity for interaction with (i) the translocation apparatus, and (ii) the colicin E1 ion channel, is thought to reside on the cytoplasmic side in the charged peripheral segment K66-K83 and the 8-residue NH_2 terminal-segment, and/or on the periplasmic side in the extrinsic segments E29-Y41 and the terminal segment G105-N113-COOH [GM-18457 (WAC) and GM-27367 (FSC)].

W-Pos155

VOLTAGE-DEPENDENT GATING OF COLICIN E1 IS ASSOCIATED WITH MEMBRANE TRANSLOCATION OF A SEGMENT OF THE PROTEIN. Charles K. Abrams, Karen S. Jakes, Alan Finkelstein and Stephen L. Slatin. Depts. of Physiology & Biophysics, and Neuroscience, Albert Einstein College of Medicine, Bronx, N.Y. 10461

Colicin E1 is a soluble, bacteriocidal protein that forms steeply voltage-dependent channels in planar lipid bilayers. The channel-forming domain of the 522-amino acid protein is located within the region between residue 345 and the C-terminus. A 35 residue hydrophobic segment very near the C terminus is believed to form 2 α-helices firmly anchored in the membrane, and several lines of evidence have led to the hypothesis that the gating mechanism involves a voltage-driven insertion of another region of the protein into the membrane. Here, using site-directed mutagenesis, we have identified a residue, His440, belonging to this region by showing that the positive charge on this residue is a gating charge that moves a substantial fraction of the electrical distance across the membrane when the channel gates. Specifically, we find that replacing the wild type histidine at position 440 with cysteine decreases the steepness of the voltage dependence of the turn-off rate by an amount consistent with residue 440 moving from the *trans* to the *cis* side of the membrane as part of the gating process. In addition, we have independently confirmed the *trans* location of His 440 in the open channel by carboxymethylating the introduced cysteine and analysing the resulting change in ion selectivity as a function of the *cis* and *trans* pH. The carboxylated mutant is more cation selective than wild type only when the *trans* pH is high enough to deprotonate the new COOH (17 mV difference at *cis* pH 4.1/*trans* pH 5.0, 10:1 KCl gradient). This difference is seen even in the presence of a 100-fold excess of permeant buffer on the *cis* side, presumably because the residue at position 440 does not sense the pH of either the *cis* side or the lumen. These results suggest that the channel is formed from at least 2 pairs of helices, each pair starting and ending on the *cis* side: a hydrophobic pair (473-509), and an amphipathic pair (420-459) that reversibly inserts into the bilayer in response to the transmembrane voltage.

(Supported by NIH grant 29219-12 and NSF grant DMB88-17641)

W-Pos156

CORRELATION OF FLUORESCENCE PARAMETERS OF SINGLE TRYPTOPHAN MUTANTS OF A COLICIN E1 CHANNEL PEPTIDE WITH ITS TRANSLOCATION-COMPETENT STATE.

A.R. Merrill[1] ‡, A.G. Szabo[2], and W.A. Cramer[1]. [1]Dept. of Biol. Sciences, Purdue University, W. Lafayette, IN 47907; [2]Dept. of Biol. Sciences, Natl. Res. Coun., Ottawa, Ont., K1A OR6; ‡ present address, Dept. of Chem. & Biochem., Univ. of Guelph, Guelph, Ont., N1G 2W1.

The thermolytic peptide of colicin E1 can be activated *in vitro* by acidic (< 4.5) pH or detergents. The activation of this channel peptide to its translocation-competent state results in an increased ability of the protein to bind and to form channels in artificial membranes. We have used fluorescence methods to study the conformational changes occurring in the channel peptide in solution at low pH. This 178-residue peptide contains three tryptophan residues, W-424, W-460, and W-495. In order to study the structural and dynamic requirements for activation of the peptide, we have prepared single tryptophan-containing peptides by site-directed mutagenesis. All of these peptides displayed *in vitro* channel activity and cellular cytotoxicity comparable to the wild-type peptide. The steady-state and time-resolved fluorescence results show that tryptophan 424 reports conformational changes which are associated with the translocation-competent state. Acidification of the peptide solution (pH 6 → 3.5) resulted in an increase (c.a. 90%) in the fluorescence quantum yield (ϕ) for W-424, indicating a significant change in the local environment of this tryptophan. Time-resolved measurements revealed that the radiative lifetime (τ_r) of W-424 also changed significantly upon a pH shift. The anisotropy data suggest that local segmental dynamics of the peptide, reported by all three tryptophans, are highly restricted [supported by NIH GM-18457 (WAC), an NSERC Fellowship from the Government of Canada (ARM), and the National Research Council of Canada (AGS)].

W-Pos157

TWO-SIDED PROTONATION OF THE ALPHA TOXIN CHANNEL INFERRED FROM THE EFFECTS OF TRANS-MEMBRANE PH GRADIENTS

J.J. Kasianowicz[a], C.R. Moore[a], J. Zimmerberg[a], C. Pasternak[b], C.L. Bashford[b], and V.A. Parsegian[a]
a) *National Institutes of Health, NIDDK/LBM, Bethesda, MD*
b) *St.George's Hospital Med. School, Div. Bioch. London*

Single channels of *S. aureus* α-toxin were observed after adding the toxin to one side of diphytanoyl PC planar bilayer membranes. The conductance (g ≈ 200 pS, 0.1M KCl, pH 4.5) scales with bulk conductivity which was changed by D_2O or glycerol. Krasilnikov et al. (Gen. Physiol. Biophys. 7:467-473) demonstrated that neutral polymers of PEG with MW < 3K Da are channel permeant. Both results imply that these channels are large water-filled pores. Despite the channel's large apparent diameter, it exhibits pH and ionic strength dependent anion selectivity (Menestrina, J. Membrane Biol. 90:177-190; Krasilnikov & Sabirov, Gen. Physiol. Biophys. 8:213-222). In symmetric solutions, the channel is approximately ohmic for 4 < pH < 6, but exhibits rectification for 6 < pH < 8. The direction of rectification depends only upon the side to which the toxin is introduced. This suggests the toxin inserts vectorially and always in the same orientation with respect to the bilayer membrane (Menestrina, J. Membrane Biol. 90:177-190). Trans-membrane pH gradients also change the I-V curve for 4 ≤ pH ≤ 8. However, the effects depend upon the direction of the gradient. Titrating one side affects the I-V curve for positive voltages, and titrating the other side primarily affects the curve for negative voltages. This is direct evidence for the existence of separately titratable groups on either side of the membrane. These groups appear to modulate the channel's ion selectivity. [Supported in part by grants from the Office of Naval Research (VAP) and the Cell Research Fund (CP).]

W-Pos158

CHEMICAL MODIFICATION OF S.AUREUS α-TOXIN BY DEPC: EFFECTS ON ITS CHANNEL-FORMING PROPERTIES.

C. Pederzolli, L. Cescatti and G. Menestrina
Physics Department, University of Trento, Italy
(Intro. by Daniela Pietrobon)

Staphylococcus aureus α-toxin is a cytolytic exotoxin secreted as a single water-soluble 33 kDa polypeptide with pI 8.5. It causes erythrocyte lysis and lethal damage to nucleated cells. Current evidences indicate that α-toxin oligomerizes on the cell surface forming an hexameric channel responsible for ion leakage.
In consistence we have observed that α-toxin interacts with planar lipid membranes and small unilamellar vesicles by opening ionic channels comprising several toxin monomers. These water-filled pores have an average diameter of 11±1 Å and are rather anion-selective. The selectivity increases at low pH suggesting that it is due to the overall toxin positive charge below pH 8.5.
To investigate the role of the electric charge of this protein on its pore-forming properties we have modified it by treatment with diethylpyro-carbonate (DEPC) which modifies histidyl and lysyl residues removing the positive charge on their amino-group. The extent of histidyl modification can be followed spectrophotometrically and saturates at about three histidines per toxin monomer, i.e. the known histidine content of α-toxin. As expected histidine modification is fully reversible by treatment with hydroxylamine.
We have found that two (out of the three) histidines are essential for its activity on model lipid membranes. Loss of activity is mainly due to defective binding but the oligomerization step is also inhibited. All the activity is restored by hydroxylamine treatment. We think that the two essential histidines of α-toxin are located one in the lipid binding site and one in the site promoting hexamerization. In fact when α-toxin hexamers are assembled onto lipid vesicles two of the histidines become protected from DEPC modification.

W-Pos159

ROFLAMYCOIN CHANNELS IN THE LIPID MEMBRANE.

P. A. Grigorjev, S.M. Bezrukov[1] (Intro. by M.C. Andresen). Inst. Biol. Phys., Ac. Sci., Puschino, 142292, USSR; [1]Leningrad Nucl. Phys. Inst., Ac. Sci., Gatchina, 188350, USSR.

A lipid bilayer membrane with ion channels formed by polyene antibiotic roflamycoin* represents a unique model of ion transport through cell membranes. We have studied the dynamic properties of these channels using spectral analysis of current fluctuations of the bilayer with many channels. It was found that in addition to low-frequency noise of channel switching between open and closed states there is a Lorentzian with much higher characteristic frequency ranging from 100 to 1000 Hz. This result shows that the open channel conductance has two substates with short lifetimes. The frequency of transition between these substates depends on the species of the permeate anion, whereas the conductance of these substates is determined by the cation type and concentration.

It is suggested that penetrating anion controls gating of the channel. The duration of the open state of the gate depends on the strength of the London-Van-der-Waals interactions of the anion with the channel structure in the series I > Br > Cl > F. Within the experimental precision a cation type does not influence gating dynamics.

*P.A. Grigorjev, et al. 1985. BBA. 821:297.

W-Pos160

CADMIUM SELECTIVELY INHIBITS GATING AND TRANSLOCATION IN THE DIPHTHERIA TOXIN CHANNEL. W.-L. Yuan and B.L. Kagan, Department of Psychiatry and Brain Research Institute, UCLA School of Medicine and West Los Angeles Veterans Administration Medical Center, Los Angeles, CA 90024

Diphtheria toxin (DT) is a 2 subunit (A-B) protein (M_r=59,000) capable of killing most eukaryotic cells via ADP-ribosylation of elongation factor 2 by the enzymatic A subunit of DT. The B subunit of DT forms a channel gated by voltage, pH gradients, and inositol phosphates, and it has been suggested that the channel plays a role in translocation of the A subunit across cell membranes. Cadmium (Cd^{++}, 1 mM added to the extracellular or cis side) has been reported to inhibit DT channel formation and to close DT channels in cells and lipid bilayers. We report here that cis Cd^{++} can block DT channel formation in planar lipid bilayers, but can only close a fraction of DT channels up to 30' after addition of DT. After 30' cis Cd^{++} has no effect. Preincubation of DT with Cd^{++} also inhibits channel formation indicating this is not a surface potential effect, but rather a specific effect of Cd^{++} on DT. Cis Cd^{++} also has no effect on channels opened in the presence of a pH gradient. Trans Cd^{++} has no effect on open channels, but strongly inhibits the pH gradient stimulation of DT channel opening. pH Gradients have been shown to be essential for A subunit translocation in vivo. Trans Cd^{++} does not block the stimulation of channel formation by inositol phosphates, indicating that this is a relatively selective inhibition of DT gating. All of these Cd^{++} effects can be reversed by addition of EGTA, but the preincubation effect can only be reversed by trans EGTA, indicating that Cd^{++} does not inhibit DT binding or insertion into the membrane. Zn^{++}, Ca^{++}, and Mg^{++} have no similar effects on DT channels. Taken together, these results suggest that Cd^{++} acts on a selective site on DT to inhibit the A subunit translocation step which results in channel opening.

(Supported by grants from NIMH and the Department of Veterans Affairs).

W-Pos161

ION CHANNEL ACTIVITY IN CULTURED LEPIDEPTORAN CELLS EXPOSED TO Bacillus thuringiensis δ-ENDOTOXIN AND THEIR GATING BY pH. Line Garneau, Luke Masson, Roland Brousseau and Jean-Louis Schwartz*. Biotechnology Research Institute, National Research Council, Montreal, Quebec, and *Institute for Biological Sciences, National Research Council, Ottawa, Ontario, Canada.

We demonstrate, using the patch-clamp technique and Fura 2-microspectrofluorescence, that, when lepideptoran SF-9 cells are exposed to sublethal doses of either native or recombinant CryIC activated toxin from B. thuringiensis, there is, in simplified culture medium at pH 6.3, an immediate, non-toxic rise in Ca^{2+}_i followed by activation of anion selective channels in the plasma membrane. These channels are mainly permeable to chloride and their formation or activation rate is calcium-dependent. Furthermore, identical channels are seen when the cytoplasmic side of the membrane patch is exposed to the toxin, indicating a possible mode of action through toxin internalization. At higher pH, these channels become principally permeable to cations. Therefore, in addition to a dual effect of the toxin on SF-9 cells (i.e. from outside or from inside the cells), this study provides evidence for another dual mode of action of the CryIC δ-endotoxin: at the pH found in the midgut environment (e.g. 9.0), the toxin forms cation selective pores, and at slightly acidic pH, like that found in the optimal culture conditions for SF-9 cells, the toxin forms anion-selective channels. This insecticidal protein , which acts at the plasma membrane level, appears to be a member of the larger class of pH-dependent bacterial toxins, like botulinum, diphtheria and tetanus toxins, that are thought to be involved in channel formation in cytosolic vesicles.

W-Pos162

REGULATION OF BACTERIAL PORIN ACTIVITY BY MEMBRANE-DERIVED OLIGOSACCHARIDES STUDIED WITH PATCH CLAMP. A. H. Delcour*, B. Martinac#, E. P. Kennedy§, J. Adler*, and C. Kung#. *Dept. of Biochemistry and #Lab. of Molecular Biology, University of Wisconsin, Madison, WI, and §Harvard Medical School, Boston, MA.

We have studied the activity of a voltage-dependent channel by use of the patch-clamp technique on liposomes reconstituted with outer membrane of *Escherichia coli* . From the voltage-dependence of the channels, we can assert that the channels are reconstituted right-side out. Properties typical of porins, such as high opening probability, cooperative gating, voltage-dependent closing and ion preference, characterize this channel. However, the channel gating kinetics is dramatically altered in presence of membrane-derived oligosacchrides (MDO's), bacterial-specific polyanions synthesized in the periplasmic space between the cytoplasmic and outer membranes. The MDO's, applied to excised patches at the periplasmic side of the channel (facing the bath solution), increase the frequency of closing, decrease the single-channel conductance and affect the gating cooperativity in a concentration-dependent manner. This effect is more pronounced with more depolarizing voltages and is readily reversible. Low molecular weight charged constituents of MDO (glycerophosphate and succinate) or other anionic oligosaccharides (heparin, dextran sulfate) do not have this effect. The observation that bacterial outer-membrane channels can be regulated by periplasmic compounds in a concentration range physiologically relevant supports the idea of a more dynamic nature of the outer membrane than anticipated. Supported by NIH DK39121.

W-Pos163

PALYTOXIN FORMS ION CHANNELS THROUGH Na,K-ATPase. S.Y. Kim, C.H. Wu, T. Narahashi, and L. Beress. Dept. of Pharmacol., Northwestern University Medical School, Chicago, IL

Palytoxin is a potent marine toxin isolated from coelenterates of the genus Palythoa. It has a wide variety of actions on the mammalian system including depolarization of excitable cells. It has been found to form a new type of ion channel in cardiac cells (Ikeda et al., 1988, Muramatsu et al., 1988). We have found similar channels induced by palytoxin in frog red blood cells and in mouse neuroblastoma cells (N1E-115). We have examined palytoxin-induced single channels in cell-attached and excised patches. These channels had a conductance of about 10 pS and were selective for Na^+ and other small monovalent cations. Current amplitudes changed linearly with changes in membrane potentials. In excised patches with Na^+ as the major cation in the pipette and K^+ as the major cation in the bath solution, channel currents reversed near a membrane potential of 0 mV.

Ouabain and other cardiac glycosides are known to antagonize palytoxin action. Ouabain has been found to compete with radiolabelled palytoxin for specific binding in human erythrocytes (Bottinger et al., 1986). We have found that ouabain inhibits the formation of single channels by palytoxin. These results suggest that the formation of ion channels may be the fundamental action of palytoxin and that these channels are formed through an interaction between palytoxin and Na,K-ATPase.

W-Pos164

VOLTAGE DEPENDENT CHANNEL OF THE INNER MEMBRANE OF E.COLI, A. Coulombe, C. Berrier, C. Houssin, A. Ghazi (intro. by Y. de Kouchkovsky). Laboratoire des Biomembranes and Laboratoire de Physiologie Comparée, URA CNRS 1116 et 1121, Université Paris-Sud, 91405 Orsay Cedex, France.

Inner membranes, isolated from E.coli bacteria, were fused into giant liposomes amenable to patch-clamp recording (Berrier et al. FEBS Lett. 259 : 27-32, 1989). Among the several channels present in this preparation, one was further characterized. The channel has a conductance of 200 pS (in 0.1 M KCl), is slightly cationic (PK/PCl = 4) with the following selectivity order : PK > PCs > PNa > PLi. The channel stays open at negative or low positive holding membrane potential and shows increasing probability of closure with increasing voltage. The channel is rarely observed alone but is rather found in clusters of up to twenty identical elements. Upon application of voltage pulses from a negative holding potential of - 40 mV to increasing positive potentials (40-140 mV) very slow transitions were observed from the open state (o) to an absorbing closed state (i), on which are surimposed rapid flickerings between the open state and a second closed state (c), according to the following minimum scheme $i \rightleftharpoons o \rightleftharpoons c$.Pulses to potentials higher than 140 mV resulted in the complete closure of the channels of a cluster. Slow closures followed monoexponential kinetics with a time constant of 0.5 s at 140 mV and 90 s at 80 mV. Return to negative potentials resulted in complete and rapid reopening of the channels.

W-Pos165

PAF-INDUCED INCREASE IN CYTOSOLIC CALCIUM AND TRANSMEMBRANE CURRENT IN MONOCYTE-DERIVED MACROPHAGES. C. Katnik and D.J. Nelson. The University of Chicago, Dept. of Neurology, Chicago, IL 60637.

Platelet-activating factor (PAF) is synthesized and secreted by macrophages in response to inflammatory stimuli. When exogenously applied to macrophages, PAF induces a rapid rise in cytosolic free calcium ($[Ca_i]$) believed to be an early triggering event in macrophage activation. We investigated PAF-induced Ca^{+2} signalling in monocyte-derived macrophages using the calcium indicator fura-2, combining single cell ratio fluorometry and imaging with whole-cell recording techniques. Application of PAF (2 ng/ml) to adherent macrophages induced transient increases in $[Ca_i]$ with peak changes 5-10 times that of basal levels. $[Ca_i]$ peaked 5 to 30 seconds after PAF stimulation and attained steady-state levels within 10-15 minutes ($[Ca_i]$ did not always return to pre-PAF stimulation levels). Subsequent applications of PAF following repeated washing failed to elicit a second transient. PAF-induced changes in $[Ca_i]$ were biphasic consisting of a rapid phase presumably due to internal release which could be observed in Ca^{+2}-free solutions and a slower phase which was critically dependent upon Ca^{+2} influx and which showed tight temporal correlation with transmembrane current changes. External Cd^{+2} (100 μM) did not block the fluorometric response in all cells. Whole-cell and "perforated-patch" experiments were performed on fura-2 loaded PAF-activated cells. Pipette solutions contained CsCl to block K^+ channel activation. Membrane current was recorded over a range of potentials as voltage ramps (-160 to +80 mV over a 1 sec period at 3 sec intervals) were applied to the cell from a holding potential of V_H = -60 mV. Upon PAF stimulation, outwardly rectifying currents became linear with an average 9.9 fold increase in current magnitude observable at -60 mV (basal currents ranged from -10 to -50 pA and peak currents ranged from -60 to -670 pA, n=7). Increases in current magnitude were observable throughout the voltage range, were reversible, and were correlated with the rising phase and, in some cases, the falling phase of the fluorescence transient. In current clamp experiments, PAF-induced depolarizing shifts in membrane potential (≈30 mV) were roughly equal to shifts in zero-current potential observed in the voltage ramp studies. Thus, Ca^{+2} influx appears to play a central role in the early events triggering macrophage activation. Supported by NIH RO1 GM36823.

W-Pos166

SINGLE CHANNEL RECORDINGS FROM SINGLY-INNERVATED AND MULTIPLY-INNERVATED FIBERS OF EXTRAOCULAR MUSCLE. J. Jacoby, Dept. of Ophthalmology, New York University Medical Center, New York, NY 10016.

Extraocular muscles (EOM) are responsible for a broad repertoire of precise movements, some extremely rapid and transient, as well as others that are slow and tonic. EOMs of mammals are also comprised of several populations of both singly-innervated and multiply-innervated fibers, the latter resembling, in some respects, the tonic fibers of lower vertebrates.

EOMs were dissected from adult rats that had been killed by overdose injection of sodium pentobarbitol. In order to enzymatically eliminate the dense connective tissue sheath that is a characteristic of EOM, intact muscles were incubated for four to four and one half hours in a normal Ca saline containing 3 mg/ml collagenase/dispase (Boehringer-Mannheim) and 1 mg/ml crude collagenase (Sigma). This treatment resulted in fibers which had membranes that were sufficiently smooth to patch, while leaving, in most cases, enough surface structural features to identify endplates of either singly- or multiply-innervated fibers.

For patch-clamp recordings, intact 5-25 um fibers were teased and pipetted into chambers containing either: 1) normal Ca saline, 2) low Ca saline, or 3) a relaxing, low Na saline containing Cs-Aspartate, ATP and EGTA. Recordings were made from cell attached- and isolated-patches. Both outward, and inward voltage-activated channels were observed. In multiply-innervated fibers, depolarization produced inward currents comprised of early very brief openings (especially near small endplates), short bursts and also late, long sustained openings. (Supported by NIH EY06232)

W-Pos167

POTASSIUM AND ANION CURRENTS IN RABBIT OSTEOCLASTS.
M.E.M. Kelly, S.A. Arkett, S.J. Dixon & S.M. Sims. Dept. of Physiology and Div. of Oral Biology, University of Western Ontario, London, Canada.

Ionic currents were studied in freshly isolated rabbit osteoclasts using whole-cell and perforated patch recording. Inwardly rectifying K^+ current (I_K) was present in all cells studied with K^+ as the principal cation in the recording electrode. This current reversed direction close to the estimated equilibrium potential for K^+. In ion substitution experiments, the reversal potential for the inwardly rectifying current, as well as the voltage around which rectification occurred, shifted positive with elevation of $[K^+]_{out}$. When I_K was blocked with Cs^+ in the recording pipette and Ba^{2+} in the bath, we found no evidence for voltage-activated inward currents. In approximately 50% of osteoclasts studied, a non-inactivating outwardly rectifying current was observed. This current persisted when I_K was blocked with internal Cs^+ and TEA^+ and external Ba^{2+}, suggesting that it was not K^+ current. Furthermore, the outward current was reversibly blocked by the anion transport inhibitors 4,4'-diisothiocyanostilbene-2,2'-disulphonic acid (DIDS) and 4-acetamido-4'-isothiocyanostilbene-2,2'-disulphonic acid (SITS) applied to the outside of the cells. The DIDS- and SITS-sensitive current reversed direction close to the predicted equilibrium potential for Cl^-, and the reversal potential shifted as expected for a Cl^- current when internal and external [Cl^-] were altered. We conclude that rabbit osteoclasts exhibit an inwardly rectifying K^+ conductance and an outwardly rectifying anion conductance, which can carry Cl^-. The properties of rabbit osteoclasts described here resemble those previously described for rat osteoclasts, suggesting that these characteristics are important in mammalian osteoclast function and regulation. Osteoclastic bone resorption involves acidification of an extracellular compartment, a process thought to be mediated by an electrogenic H^+-ATPase. Transport of protons (H^+) across the osteoclast membrane therefore requires the appropriate movement of counterions. Both the inwardly rectifying K^+ conductance and the anion conductance reported here provide conductive pathways that may compensate for electrogenic H^+ transport. (Supported by The Arthritis Society and the Medical Research Council of Canada).

W-Pos168

THE ROLE OF CHLORIDE CHANNELS IN CHICKEN GRANULOSA CELLS.
Jean-Louis Schwartz, Paul Morley*, Geoffrey A.R. Mealing, Benjamin K. Tsang* and James F. Whitfield. Institute for Biological Sciences, National Research Council, Ottawa, Ontario, and *Loeb Institute for Medical Research, University of Ottawa, Ontario, Canada.

Previous studies in our laboratory using single channel patch-clamp recording have demonstrated the presence of potassium and calcium channels in chicken granulosa cells. The role of these channels in progesterone secretion induced by luteinizing hormone (LH) is unknown. In other studies using the whole-cell configuration of the patch-clamp technique, we showed that, under voltage-clamp conditions, there is an inward calcium current and a delayed outward potassium current in these cells. We now present evidence of electrical excitability of granulosa cells as recorded in the current-clamp mode, where various types of action potentials, including calcium spikes and long-lasting transients followed by deep hyperpolarizations were observed. We disclose also the existence of maxi-conductance chloride channels in granulosa cells. In secretory studies, we show that chloride ions play a role in LH-induced progesterone secretion. The mechanisms by which secretion is affected and the ionic events underlying the development of the slow action potentials appear to be related to chloride channels. This study provides the first evidence of the existence of chloride channels in ovarian cells.

W-Pos169

CHLORIDE CHANNEL LIGANDS FROM SCORPION VENOM.
J.A.DeBin and G.R. Strichartz, Anesthesia Res. Labs of Brigham & Women's Hospital and the Dept. of Biol. Chem. & Mol. Pharmacology, Harvard Medical School, Boston MA, 02115.

The lack of high affinity ligands has hindered research in the area of non-neurotransmitter activated chloride channels. During our studies on such anion channels (ACs) derived from rat brain growth cones reconstituted into planar lipid bilayers, we discovered that crude or partially purified Leiurus quinquestriatus scorpion venom (LqV) produces a substantial block of small ($\gamma \approx 40$pS) ACs. LqV is also effective against small ACs derived from rat colonic epithelium, but is ineffective against large ACs (120-150 pS) from bovine platelets, indicating some specificity to the action of the scorpion venom. When applied to the "intracellular" surface of an AC, 0.1 mgLqV/ml produces a 2/3 reduction in open probability as a result of discrete blocking events which last up to several tens of seconds, as shown below. The effect of LqV is concentration dependent and reverses upon perfusion of the "intracellular" bath. Preliminary results indicate that the effect also is voltage dependent with mean unblocked times decreasing upon depolarization. Early attempts to purify the active component from crude LqV using liquid chromatography and HPLC indicate it is probably a peptide, with a molecular weight ca. 5 kD. Assuming the active component to be 1% of crude LqV dry weight, a K_I of $\approx$100 nM is obtained.
Single channel currents from a rat colonic epithelium AC reconstituted into a lipid bylayer:

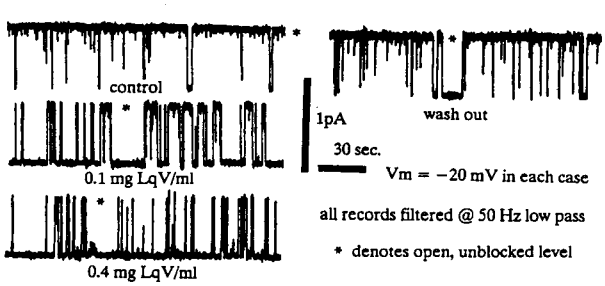

W-Pos170

KINETIC ANALYSIS OF A CHLORIDE CHANNEL WHEN TWO IDENTICAL CHANNELS ARE PRESENT UNDER THE PATCH

FORESTIER C., DISERBO M., NISSOU M.F.*, CROUZY S. and CHAPRON Y.
CENG- DBMS/BMC - BP85X - F38041 GRENOBLE
*INSERM U318 - F38700 LA TRONCHE

We have shown that A431 cells exhibit a high density of non-independent calcium channels (1). These channels are voltage independent and activated by EGF or IP_3. In the same cell-line, chloride channels have recently been discovered. These independent channels present a small conductance (17 pS), and are activated either by voltage or by phosphorylation with PKA. Two channels were almost always seen under the patch and a preliminary analysis showed that a simple CO scheme for each channel could not describe the kinetic data adequately.
Therefore, a linear CCO scheme was chosen and the probability density function of closed and open dwell times was calculated after the correct decomposition of the two-channel three-state scheme into an equivalent one-channel six-state scheme. The four rates necessary to completely define the scheme shown below, were found upon fitting the open and closed dwell-time histograms to sums of exponentials and were confirmed with a spectral analysis. The power spectral density of the signal was best fitted with two lorentzians, with cut-off frequencies Fc_1 = 33 Hz and Fc_2 = 13 Hz, very close to those that where calculated from the rate constants : Fc_1 = 38 Hz and Fc_2 = 13 Hz.

The kinetic scheme with constants in Hertz (sec^{-1}) is:

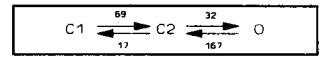

(1) CHAPRON Y. et Al (1989) Biochem. Biophys.Res. Comm., 158, 527-533

W-Pos171

VOLATILE ANESTHESTICS GATE AN ANION PERMEABLE CURRENT WITH ATYPICAL PROPERTIES IN CULTURED RAT HIPPOCAMPAL NEURONS J.Yang and C.F.Zorumski, Depts Anesthesiology & Psychiatry, Washington Univ Sch Med, St.Louis, MO 63110

Volatile anesthetics (VA) have been shown to decrease neuronal excitability by direct action on regenerative membrane activities, synaptic transmission, and resting membrane potential. Previous reports indicate that in both vertebrate and invertebrate central neurons, VA hyperpolarize the cell by activating a specific K^+ conductance. We report that in cultured rat hippocampal neurons, VA gate an anionic current with atypical pharmacological and biophysical properties.

Experiments were conducted on enzymatically dissociated hippocampal neurons isolated from 1 - 2 D old post-natal rats, cultured for 3 - 4 days in vitro. Electrophysiological recordings were obtained with the standard whole cell patch-clamp methods. VA solution, at various concentration diluted from a saturated solution at room temperature, was applied to neurons by pressure ejection from a blunt pipette.

With symmetric Cl^- across the membrane, VA induce a non-desensitizing current with a reversal potential near 0 mV. With increasing Cl^- asymmetry, the IV curve shows outward rectification. However, the rectification is well described by the GHK formulation without assigning channel voltage dependence. Ion substitution experiments show strong Cl^- selectivity with an E_{rev} shift of 50 mV per 10 fold change in Cl^- gradient. The current shows a steep dose dependence with ED_{50} near 0.8 mM for isoflurane. Qualitatively similar responses are seen with applications of halothane and enflurane. The current is not an artifact due to pressure or pH, it persists with no external Ca^{++}, and is not blocked by picrotoxinin (1mM) or strychnine (10uM). A nonspecific anion blocker ,DIDS (1 mM), completely blocks the current. These properties distinguish this I(Cl,An) from the well known barbiturate induced Cl^- current (a $GABA_A$ mimetic current blocked by picrotoxinin), the glycinergic current, or the phorbol ester sensitive voltage-gated Cl current present in these neurons.

Our results document the presence of VA gated current in vertebrate CNS neurons. The outward rectification observed with low internal [Cl^-] makes it likely that under physiologial conditions, VA will selectively depress depolarized neurons with high activity levels, while having less effect on quiescent neurons. Thus selective action of VA in the vertebrate CNS may depend on the functional status, rather than on physical distribution, of VA sensitive channels, as has been proposed for the invertebrate CNS. (Supported in part by FAER-BOC fellowship).

W-Pos172

SINGLE CHANNELS ARE ACTIVATED ALONG WITH NA-CA EXCHANGE IN CARDIAC GIANT EXCISED PATCHES.
Doering, A.E. and Lederer, W.J.
Dept. of Physiology, University of Maryland School of Medicine, Baltimore, MD.

The Na-Ca exchanger is a transport protein co-existing in the sarcolemma with ion channels. We used the giant patch technique (Hilgemann, Nature 344:242, 1990; Pflugers Archiv 415:247, 1989) to study channels activated simultaneously with the Na-Ca exchanger. Adult ventricular cells incubated overnight in 135 KCl develop membrane blebs. A giant patch pipette (10 μm tip) is sealed to a bleb and lifted to excise an inside-out patch. The pipette solution contains (in mM) 140 NaCl, 40 N-methyl glucamine (NMG), 10 TEACl, 20 PIPES, .020 EGTA, 1 $CaCl_2$, .025 ouabain, .0025 D-600, and 1 4-AP. In the bath is 140 NMG, 10 TEACl, 5 ATP, 1 $MgCl_2$, 20 PIPES, 20 BAPTA, and 0.3μM free Ca^{++}. Rapid solution changes are achieved using an oil-gate chamber (Qin and Noma, Am. J. Physiol. 255:H90, 1988). Raising cytoplasmic sodium from 0 to 60mM with V_{hold} = 0mV activated outward Na-Ca exchange current and, in 11 out of 25 patches, single channels (fig. below). The reversal potential of the single channel current indicates that the channel is permeable to sodium and calcium but not NMG or chloride. Channel conductance with bath Na^+ of 80mM is 50pS. Greater concentrations of sodium increase the channel open probability. While the observed channel activity may be due to the direct action of Na^+ on a channel, it may also arise indirectly from the calcium transported across the membrane by the exchanger into a restricted space, possibly created as the membrane patch is pulled into the pipette. Support for this suggestion comes form the observation that directly increasing bath Ca^{++} to 1mM also activated single channels, suggesting that sodium-calcium exchange may open a calcium-activated non-specific cation channel. (cf. Ehara. et.al., J. Physiol. 403:117, 1988).

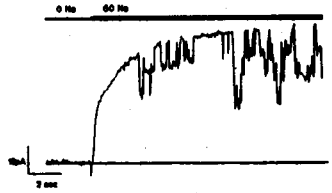

W-Pos173

A NOVEL CALCIUM-PERMEABLE ION CHANNEL OPEN AT RESTING MEMBRANE POTENTIALS IN CEREBELLAR NEURONS FROM *MDX* MICE. Christine M. Haws and Jeffry B. Lansman. Department of Pharmacology, School of Medicine, University of California, San Francisco, CA 94143-0450.

An absence of the cytoskeletal protein, dystrophin, is the primary genetic lesion responsible for human X-linked muscular dystrophy. We have have recently shown (Franco & Lansman, *Nature* 344:670, 1990) that myotubes from the *mdx* mouse, an animal model for the human disease, possess a novel calcium-permeable, mechano-transducing ion channel. Because mammalian brain is the only non-muscle tissue which has been found to possess dystrophin, we asked whether an abnormality in ion channel behavior might be found in neurons from *mdx* mice. Recordings of single channel activity from cell-attached patches on cerebellar granule cells from *mdx* mice with 110 mM $BaCl_2$ in the electrode showed the activity of a novel channel open at holding potentials near rest. The conductance is 8-10 pS in the presence of Ba or Ca. An analysis of the distributions of open and closed times shows there are two closed state and a single open state with a mean open time of ~7 ms. Resting channel open probability was ~8% and was insensitive to membrane potential. Recordings from wild-type neurons was only rarely observed and had a much lower resting open probability (<1%). Although the channel in brain differs from the channel found previously in skeletal muscle - the conductance is smaller in Ba, opening is not sensitive to membrane potential, and the channel does not show obvious mechanical sensitivity - the results suggest that the lack of dystrophin in tissues in which it is normally expressed is associated with the expression or enhanced activity of ion channels that are permeable to Ca. The demonstration of Ca-permeable channel in neurons from *mdx* mice supports the hypothesis that the primary defect associated with the loss of dystrophin is an increase in the Ca permeability of the cell membrane.

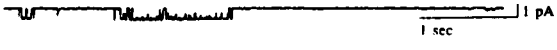

W-Pos174

NONGATED OUTWARD RECTIFYING CATION CONDUCTANCE IN NEUROBLASTOMA CELLS. F.N. Quandt. Multiple Sclerosis Center and Dept. of Physiology, Rush University, Chicago, IL 60612.

Patch clamp techniques were used to measure the current across patches of membranes in N1E-115 neuroblastoma cells grown in tissue culture and differentiated in 2 % DMSO. Depolarizion of the membrane from the holding potential of -50 mV with successive 10 mV voltage steps to +50 mV revealed an outward rectifying membrane current. For example in one excised membrane with NaCl, 3 mM Ca external solution, and Kglutamate, EGTA internal solution the slope conductance was 10 pS for a 10 mV step between -50 to -40 mV, 100 pS for a step from -10 to 0 mV, and 600 pS for a voltage step from +40 to +50 mV. This outward-rectifying conductance was observed in cell-attached, as well as excised membranes. The nonlinear current was not generated by a channel with voltage dependent gating since current jumps associated with channel opening were not observed in response to the steps. The outward rectification was observed when internal K was replaced by Cs, but was reduced when K was replaced by Na using inside-out membranes. The current was almost eliminated when internal K was substituted by N-methylglucamine, indicating that the conductance pathway is selective for cations. Reduction in extracellular Ca from 3 mM to 0 added Ca, or with addition of EDTA increased the conductance, but reduced the extent of outward rectification. This oberservation supports the idea that the rectification may be due to block of a cation conductance at the more negative membrane potentials. Perhaps this component of membrane conductance contributes to the resting potential, even though it appears rather nonselective for various cations. Block by an external divalent would prevent inward Na current at a negative potential, but outward K current could develop if the membrane were to depolarize. Supported by the National Multiple Sclerosis Society.

W-Pos175

KINETICS OF PORE-MEDIATED RELEASE OF MARKER MOLECULES FROM LIPOSOMES OR CELLS

Gerhard Schwarz and Charles H. Robert
Department of Biophysical Chemistry, Biocenter of the University, CH-4056 Basel, Switzerland

We present a general theoretical basis to interpret the efflux of entrapped marker material from cells (including liposomes). This comprises permeation of marker through any kind of pore-like structural defects in the membrane, especially those induced by the action of an external agent. The experimentally observed efflux function is formulated in terms of the rate of pore formation as well as the distribution of pore lifetimes. The detailed time course of the release is derived for a first-order inactivation of a pore. The approach has been applied to experimental data obtained with lipid vesicles added to a solution of a pore forming peptide. That system exhibits a slowing down of the apparent pore formation as also observed in many other analogous cases reported in the literature. To some degree this can be related to a possible distribution of cell sizes. On the other hand, it appears likely that such slowing down is primarily caused by a slow step in the underlying molecular mechanism resulting in a decline of some prepore state. We illustrate this by means of relevant examples.

Supported by grants no. 3.285.85/31.25230.88 from the Swiss National Science Foundation and by the North Atlantic Treaty Organization (fellowship to C.H.R.)

W-Pos176

POISSON ANALYSIS AS A SIMPLE TEST TO SORT KINETIC SCHEMES. S. Ginsburg*†, J. Edry-Schillller† and R. Rahamimoff†. *The Open University, P.O Box 39328, Tel Aviv, Israel, †Physiology Department, Hebrew University-Hadassah Medical School, P.O. Box 1172, Jerusalem, Israel.

Lifetime distributions of intervals such as openings and closures derived from single-channel records, characterize kinetic properties of channels. However, these distributions do not, in themselves, suffice to distinguish among competing kinetic schemes that govern channel gating. Correlations between interval durations (Jackson, Wong, Morris & Lecar, Biophys. J. 42, 109-114, 1983) and adjacent interval analysis (Blatz and Magleby, J. Physiol. 410, 561-585, 1989) enable such distinction. However, these techniques require large numbers of intervals for analysis and may be extremely time consuming.

We suggest a simple and fast method to distinguish among schemes or to sort "families" of kinetic schemes. In this method, the total record is divided into successive traces of equal length and the number of openings (closures, bursts) commencing in each trace is counted. If the probability of opening is either very large or very low, then a Poisson distribution of appearance of openings (closures, bursts) is expected in some schemes and a non-Poisson distribution is expected in others. Thus, for example, if the probability of opening is low, Poisson distributions are expected when the open state does not interrupt the closed states. Therefore, the number of openings per trace for the channel $C_2 \rightleftharpoons C_1 \rightleftharpoons O$ should follow Poisson, while for the channel $C_2 \rightleftharpoons O \rightleftharpoons C_1$ it should not (unless the lifetimes of C_1 and C_2 are similar). Similarly, bursts arising from the schemes $C_3 \rightleftharpoons C_2 \rightleftharpoons C_1 \rightleftharpoons O$ and

$$\begin{array}{l} C_3 \rightleftharpoons C_1 \rightleftharpoons O \\ \quad\updownarrow \\ \quad C_2 \end{array}$$

are expected to appear according to Poisson, while bursts originating from $C_2 \rightleftharpoons C_1 \rightleftharpoons O \rightleftharpoons C_3$ are expected to be distributed differently. Relatively small numbers of intervals are sufficient in order to determine whether the distribution is Poissonian or not. (Supported by GIF, CTR and The Israel Academy of Sciences.)

W-Pos177

TIME-DEPENDENT INCREASE OF CHLORIDE CURRENT IN CANINE ATRIAL CELLS DURING WHOLE CELL PATCH CLAMP EXPERIMENTS.

Steve Sorota, Michael S. Siegal and Brian F. Hoffman. Department of Pharmacology, Columbia University, New York, NY 10032

We studied canine atrial cells under whole cell patch clamp conditions with K^+ currents blocked by Cs^+. Chloride concentrations were 40 and 152 mM for internal and external solutions, respectively. Current-voltage relationships were measured using voltage ramps from +30 to -110 mV over 8 seconds. Under these conditions, 5 of 6 cells showed an increase in conductance over time. The increase in whole cell current became apparent between 5 and 20 minutes after patch rupture. A decrease in seal resistance could not account for this result. The time-dependent whole cell current consistently had a reversal potential near -25 mV and displayed outward rectification. The amplitude of the outward component of this time-dependent current was decreased when extracellular Cl^- was replaced by methanesulfonate. We also observed a beta-adrenoceptor agonist-enhanced current in canine atrial cells. It was undetectable or small initially and increased in amplitude over time with repeated short duration exposure to 10^{-6} M isoproterenol. The time course of the increase in isoproterenol-stimulated whole cell current paralleled the time-dependent changes in whole cell conductance. In three experiments lasting 35 minutes or longer, no time-dependent increase in whole cell current was observed when the pore forming antibiotic, nystatin, was used to gain electrical access to the cell interior. In these experiments, isoproterenol had no detectable effect on chloride conductance. The increase in whole cell current over time does not therefore appear to be related to equilibration of patch electrode monovalent cations or chloride with the cell interior. Under ruptured patch conditions, dialysis into the cell of a factor that stimulates chloride conductance, diffusion from the cell of an inhibitory factor and/or cell swelling induced by bulk flow of fluid from the patch electrode may explain the time-dependent changes observed.

W-Pos178

CHLORIDE INDEPENDENT VOLUME REGULATORY CHANGES IN SPHERICAL AGGREGATES OF CULTURED CHICK HEART CELLS

R. Rasmusson, M. Rigby, M. Lieberman. Dept. of Cell Biology, Div. of Physiology, Duke Univ. Med. Ctr., Durham N.C. 27710.

Osmotically induced volume changes in heart cells were measured optically as changes in diameter relative to that obtained under control conditions. Control solution contained (in mM) NaCl 143, KCl 5.4, CaCl 1.0, NaH_2PO_4 0.8, $MgSO_4$ 0.8, HEPES 5.4, TRIS 4.6 and 5.6 Dextrose; pH 7.4; 290 mOsm. Hypotonic solution contained 36 mM NaCl (90 mOsm). Cl^- free solutions substituted methanesulfonate for Cl^-. Fig. 1 shows that aggregates exposed to hypotonic solution in the presence of Cl^- swell rapidly and then immediately begin to regulate towards original volume (regulatory volume decrease). When hypotonically swollen aggregates returned to control solution they shrank but failed to reattain the initial volume. This behavior has also been confirmed in single cells. In Fig. 2 exposure to Cl^- free solutions produced a shrinkage consistent with Cl^- depletion. When these aggregates were exposed to Cl^- free hypotonic solution we observed a volume regulatory decrease comparable to that observed in Cl^- containing conditions. This suggests that organic as well as inorganic solutes play a role in volume regulation.

Supported in part by NIH grants:HL-07063, HL-17670, HL-27105

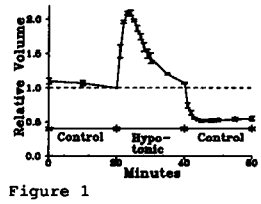

Figure 1

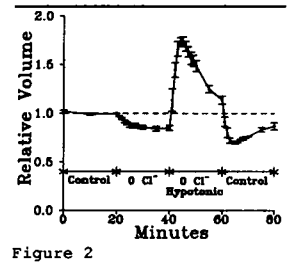

Figure 2

W-Pos179

VOLTAGE-DEPENDENT BLOCKADE OF THE CARDIAC SARCOPLASMIC RETICULUM (SR) K^+ CHANNEL BY Mg^{2+}

Q-Y. Liu and H.C. Strauss (Intro. by Fred Schachat) Departments of Medicine and Pharmacology, Duke University Medical Center, Durham, NC 27710

Cytosolic free Mg^{2+} levels have been reported to increase nearly 3-fold between 10 and 15 min of myocardial ischemia (from ~0.85 mM to ~2.1 mM) (J Biol Chem 264:5622, 1989). The SR K^+ channel has been shown to be an important modulator of Ca^{2+} release from the SR (J Gen Physiol 93:1, 1989). To investigate the potential effect of Mg^{2+} on the SR K^+ channel, the channel was isolated and incorporated into planar lipid bilayers. We found that Mg^{2+} is impermeant, and that its presence in either the *cis* (cytoplasmic) or *trans* (lumenal) side of the channel reduced the K^+ current without detectable flickering. This reduction was voltage-dependent due to the rapid blocking and unblocking of the channel by Mg^{2+}. Blockade by Mg^{2+} is reversible, is competitive with K^+, and can be described by a two-binding-site model, which has been successfully applied to the analysis of blockade of the cardiac SR K^+ channel by Ca^{2+}. In 50 mM K^+, 10 mM histidine, pH 7.2 solution, the zero voltage apparent dissociation constants ($K_b(0)$) were ~10 mM and ~6 mM for *cis* and *trans* Mg^{2+} block, respectively. The fractional electrical distances for the block sites were δ_c~0.14 and δ_t~-0.21 for *cis* and *trans* sites, respectively. $K_b(0)$ values for Mg^{2+} were approximately twice that for Ca^{2+}. As there is believed to be no K^+ or Mg^{2+} gradient across the SR membrane, Mg^{2+} blockade was examined under symmetrical conditions and appeared to be voltage-independent, which is consistent with our model. The increase in cytosolic Mg^{2+} concentration during myocardial ischemia will decrease the conductance of the SR K^+ channel and may contribute to the decrease in contractility during ischemia. Supported by NIH HL-19216.

W-Pos180

A MODEL OF THE ACTION POTENTIAL FROM GUINEA-PIG VENTRICULAR MYOCYTES WITH AN EMPHASIS ON REPOLARIZATION MECHANISMS. Vijay Kowtha and John R. Clay, Lab of Biophysics, NINDS, NIH, Bethesda, MD

We have developed a mathematical model of the action potential (AP) from guinea-pig ventricular myocytes based on voltage clamp measurements in the literature of the underlying ion current components. These include the inward sodium ion current, I_{Na} (L. Ebihara & E. A. Johnson, Biophys. J. 32:779, 1980); the calcium ion current, I_L (T.F. McDonald, et al., Pflugers Arch. 406:437, 1986; A. Shrier & J.R. Clay, Biophys. J. 50:861, 1986); the delayed rectifiers, I_{Ks} and I_{Kr} (H. Matsuura, et al., Pflugers Archiv. 410:596, 1987; M.C. Sanguinetti & N.K. Jurkiewicz, J. Gen. Physiol. 96:195, 1990; Shrier & Clay,1986) and the background potassium ion current, I_{K_1} (Y. Kurachi, J. Physiol. 366:365, 1985). In some simulations we included the background, potassium ion, plateau current, I_p (D.T. Yue & E. Marban, Pflugers Archiv. 413:127, 1988). Repolarization in the model is initiated by I_{Ks}, I_p, and calcium current mediated inactivation of I_L. The latter phase of repolarization (-30 to the resting potential, ~ -90 mV; phase 3 of the AP) is dominated by I_{Kr}. The I_{Ks} component is significantly less than I_{Kr} during phase 3, as is I_{K_1}. The latter component is a major determinant of the resting potential. Sanguinetti & Jurkiewicz (1990) have shown that I_{Kr} is selectively blocked by Class III antiarrhythmic agents. These drugs also prolong the duration of the AP without altering its shape. The duration of our model AP is increased by removal of I_{Kr}, so much so that it effectively does not repolarize to the rest potential. This result suggests that either a significant fraction of I_{Kr} is insensitive to Class III agents, or a current component is missing from the model which contributes to phase 3 repolarization.

W-Pos181

GAP JUNCTIONAL CONDUCTANCE IN VENTRICULAR MYOCYTE PAIRS ISOLATED FROM POSTISCHEMIC RABBIT MYOCARDIUM.
Robert S. Kieval, Joseph F. Spear, E. Neil Moore (Intro. by Samuel Chacko), University of Pennsylvania Veterinary School, Philadelphia, PA.

A new model was developed for studying the effects of myocardial ischemia and reperfusion on gap junctional communication between adult heart cells. Langendorff-perfused rabbit hearts received 30 min of global normothermic ischemia followed by 30 min of reperfusion with Tyrode solution. Following reperfusion, hearts were enzymatically digested for the isolation of postischemic ventricular myocyte pairs. Control hearts were digested 1) immediately upon cannulation, or 2) following 60 min of Tyrode perfusion without ischemia. Gap junctional conductance (g_j) was measured under voltage clamp using whole cell techniques. Postischemic myocytes were morphologically similar and showed action potentials equivalent to myocytes from both control groups. Mean g_j in postischemic myocyte pairs was 0.92 ± 0.29 μS (± SEM, n=14), with 8/14 pairs having g_j < 0.5 μS (median = 0.27). Tyrode-perfused and untreated myocyte pairs were more symmetrically distributed ($\bar{x}$=0.99 ± 0.16, median=0.75, n=7; and $\bar{x}$=1.24 ± 0.25, median=0.82, n=13; respectively). In these groups, the proportion of myocyte pairs having g_j below 0.5 μS was 0/7 and 2/13, respectively. The distribution of g_j in the postischemic group was significantly different from that in both control groups ($p < .02$). The degree of cell coupling in reperfused myocyte pairs was thus heterogeneous, with a significant population of cells having poor gap junctional communication. If present in the intact postischemic heart, such non-uniformity of cell coupling could provide a substrate for the generation and perpetuation of cardiac arrhythmias.
Supported by NIH HL-33593, MSTP GM-07170, SEPA Am Heart Assoc., and the W.W. Smith Charitable Trust.

W-Pos182

WENCKEBACH RHYTHMS AND IONIC CURRENTS IN RABBIT ATRIOVENTRICULAR NODAL CELLS
R Adjemian, MR Guevara and A Shrier, Department of Physiology, McGill University, Montréal, Québec, Canada, H3G 1Y6

Spontaneously active and quiescent single rabbit atrioventricular nodal cells were stimulated with brief-duration current pulses. During periodic stimulation a variety of Wenckebach-like rhythms were found whose primary feature was a beat-to-beat increase in latency from stimulus to action potential upstroke. Reverse Wenckebach and alternating Wenckebach (type B) rhythms were also found. During premature stimulation, increased prematurity was associated with greater latency. In whole cell voltage clamp, we found that the removal of inactivation of an L-type like calcium current (I_{Ca}) occurred over a time period that encompassed the range of action potential restitution. The sodium current (I_{Na}) was absent from most cells. A delayed rectifier current (I_K) was found whose time constant of deactivation varied from tens to hundreds of milliseconds, in the range of the pacemaker potential. Transient outward potassium current (I_{to}, I_A) was seldom seen in nodal cells, but was prominent in virtually all atrial myocytes. In contrast, an inward current, resembling the pacemaker current (I_f), was evident only in nodal cells, but at relatively negative potentials (-90 mV). Thus Wenckebach rhythms in isolated nodal cells involve a beat-to-beat increase in latency which may be related to the kinetics and magnitude of I_{Ca} recovery and I_K deactivation.
Supported by the Cdn heart and Stroke foundation and the MRC Canada.

W-Pos183

THE EFFECTS OF THE K-OPIOID AGONIST U50,488H ON GUINEA PIG VENTRICULAR MYOCYTES.
W.H. duBell and E.G. Lakatta. Gerontology Research Center, Baltimore MD 21224

The effects of the K-opioid agonist U-50 on the electro-mechanical properties of guinea pig ventricular myocytes were examined. Action potential (AP) and voltage clamp (VC) recordings were made with patch-type microelectrodes (1-3 MΩ) in the whole-cell mode. Ca transients (CaT) were indexed as the change in indo-1 fluorescence ratio, and twitch contractions (TC, % resting length) were measured with a photodiode array. All experiments were done at room temperature. Steady state (SS) TC decreased by 78.0% (n = 4) in the presence of U50 (10 μM) and SS CaT decreased by 51.2% (PANEL A for representative ex.). The overshoot and the plateau potential of the SS AP were decreased in U50 (PANEL B). SS Isi (elicited by 500 ms VC pulses from -40 to +10 mV) was decreased by 44% (n = 4) in 10 μM U50 (PANEL C). An outward current (PANEL C, arrows), present upon repolarization from pulses used to elicit Isi, was inhibited by U50. This current was blocked by CsCl, was decreased in the presence of 0.2 mM Cd and had a voltage dependence like that described for the delayed rectifier K current. These results suggest that the decrease in Isi contributes to the decrease in the AP plateau potential and the decrease in CaT.

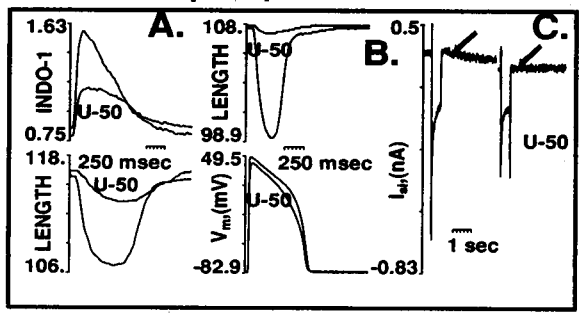

W-Pos184

ELECTROTONIC INFLUENCES ON ACTION POTENTIALS FROM ISOLATED VENTRICULAR CELLS.
Rosemarie C. Tan and Ronald W. Joyner
Department of Pediatrics Emory University, Atlanta, GA

This work combines a theoretical study of electrical interactions between two excitable heart cells, using a variable coupling resistance (R_c), with experimental studies on isolated rabbit ventricular cells coupled with a variable R_c to a passive R-C circuit. The theoretical results show that the response of an isolated cell to an increased frequency of stimulation is strongly altered by the presence of an R_c to another cell. As the R_c is gradually decreased, the stimulated cell becomes able to respond successfully to more rapid stimulation and then, at levels of R_c which allow conduction between the two cells, the coupled pair of cells exhibit arrhythmic interactions not predicted by the intrinsic properties of either cell. The experimental results show that the isolated rabbit ventricular cell is extremely sensitive to even a very small electrical load, with shortening of the action potential duration (APD) by 50% with electrical coupling to a model cell (of similar input resistance and capacitance to the ventricular cell) as high as 1000 Mohms, even though the action potential amplitude and current threshold are very insensitive to the electrical load.

The large effect on the APD of this small coupling current is reasonable. After the initial spike, the cell is depolarized about 100 mV from rest. For a cell with 100 pF capacitance, a charge of Q = CV = $(10^{-10}$ F)(0.1 V) = 10^{-11} Coulombs must exit the cell in order for repolarization to occur. For a normal APD of 200 mSec, the average intrinsic outward current must then be 10^{-11} C / 0.2 Sec = 50 pA. If the coupling current for R_c = 1000 Mohm (about 100 pA) is added to this intrinsic average outward current, then the predicted APD would become 10^{-11} C / 150 pA = 67 mSec, a decrease in APD of more than 50%. The small size of the required current to induce significant APD shortening is also of importance in regards to the effects of potassium channels which are activated at lowered ATP levels. From estimates of 30 pS conductance of these channels in normal $[K^+]_o$, the required current of only 100 pA would require the average opening of only 30-40 of these channels to reduce the APD by 50%, assuming an average plateau potential of 0 mV and a reversal potential for K^+ of -100 mV.

W-Pos185

LONG TERM RECORDING OF VENTRICULAR MYOCYTE ACTION POTENTIALS USING SUCTION PIPETTES WITHOUT "RUN-DOWN". INTRACELLULAR CALCIUM REGULATES TETRODOTOXIN MEDIATED REDUCTION OF ACTION POTENTIAL DURATION. M. Craig McKay and Kai S. Lee. Cardiovascular Diseases Research, The Upjohn Company. Kalamazoo, MI 49001.

Associated with the use of suction pipettes (whole-cell) is the widely reported phenomenon of Ca^{++} current "run-down" which restricts the life-time of voltage-clamp recordings. Almost unreported in the literature is the analogous problem of making stable long-term current-clamp recordings using suction pipettes. The longevity of a recording is apparently related to the composition of the pipette filling solution. Using a filling solution of the following composition: in mM; K^+Glu,115;KCl,5;$CaCl_2$,1;EGTA,10;MOPS,10; Glucose,20; Mg^{++}-ATP,5;Na+Creatine phosphate,5;pH7.2, we can record stable action potentials (35°C) for several hours from acutely dissociated ventricular myocytes using low resistance pipettes (0.5-1Mohm). Voltage-clamp recordings made before and after action potential recordings (constant stimulation 1Hz) lasting 1-2 hrs. confirm no diminution of peak inward Ca^{++} current (Vh=-40mV, 10mV step depolarization to +70mV). Typical suction pipette recordings of action potentials gives Vmax measurements of 500-700 V/s and total amplitude measurements are typically 130-140 mV, accompanied by a long lasting plateau phase. It is well known that, in cardiac tissue, the action potential duration (APD) of Purkinje fibers is the most sensitive to TTX. Similar sensitivity has not been shown in ventricular cells. Using suction pipettes to record action potentials we find that when intracellular Ca^{++} is buffered to 10^{-6}M, TTX (10^{-9}M to 10^{-6}M) induces a dose-dependent decrease (10% to 44%) in APD. Vmax is unaffected at doses of TTX < $5*10^{-7}$M. The effect of TTX on APD is independent of the fast inward Na^+ channel (or Na^+ window current) since depolarizing resting membrane potential to -45mV (elevated external K^+) does not abolish the effect. When EGTA is omitted from the pipette filling solution APD remains unchanged by doses of TTX < $5*10^{-6}$M, but when intracellular Ca^{++} is lowered (continuous internal perfusion) by addition of EGTA to the internal perfusate, APD is decreased. The extreme sensitivity of ventricular myocytes to low doses of TTX suggests that there is a high affinity receptor independent of the low affinity TTX receptor of the fast sodium channel. Our observations may be the first electrophysiological evidence for the "second" TTX sensitive receptor in heart cell membranes that has been reported in the biochemical literature.

W-Pos186

EFFECTS OF Na^+ and Ca^{2+} CONCENTRATION IN CARDIOPLEGIC SOLUTIONS ON THE INTRACELLULAR Ca^{2+} ACTIVITY OF CARDIAC MUSCLE CELLS. So Ra PARK, Myung Jin KIM, Duck Sun AHN, Chang Kook SUH*. Department of Physiology, Yonsei University College of Medicine, Seoul and* Inha University College of Medicine, Inchon, Korea.

High K^+ cardioplegic solution can rapidly arrest the heart during cardiac surgical procedure. To avoid intracellular Ca^{2+} overload, low Ca^{2+}-and/or Ca^{2+} antagonists-containing cardioplegic solutions are being used. However, the removal of Ca^{2+} from the cardioplegic solutions could cause the danger of inducing a calcium paradox during reperfusion. Since intracellular Ca^{2+} activities are coupled to Na^+ activities via Na^+-Ca^{2+} exchange, an increase in intracellular Na^+ activities during the cardioplegia could cause an abrupt Ca^{2+} influx during the reperfusion of normal solution. To study the effects of Na^+ and Ca^{2+} concentrations in cardioplegic solutions on intracellular Ca^{2+} activities during the cardioplegia and subsequent recovery period, the membrane potential and intracellular Na^+ and Ca^{2+} activities of guinea pig ventricular papillary were measured with following results.

1. A cardioplegia with low Ca^{2+} solution significantly decreased the overshoot and duration of the first action potential after cardioplegia, but the changes in action potential configuration were minimized after a cardioplegia with Ca^{2+} concentration adjusted according to Na^+-Ca^{2+} exchange mechanism. 2. Intracellular Na^+ activity was kept high with low Ca^{2+} cardioplegic solution. 3. Intracellular Na^+ and Ca^{2+} activities were continuously decreased during the cardioplegia with Ca^{2+} concentration calculated according to Na^+-Ca^{2+} exchange mechanism. 4. The rate of increase in intracellular Ca^{2+} activity with reperfusion of Tyrode solution was dependent upon intracellular Na^+ activity during cardioplegia, in a way that the higher intracellular Na^+ activity was, the faster intracellular Ca^{2+} activity increased. From these results, it was suggested that Na^+-Ca^{2+} exchange mechanism may play an important role in regulation of intracellular Ca^{2+} activity during the recovery after cardioplegia.

W-Pos187

COMPUTER MODEL OF CONDUCTION BETWEEN CELLS WITH HIGH INTERCELLULAR COUPLING RESISTANCE BASED ON DATA FROM ISOLATED VENTRICULAR MYOCYTES. Charles Nordin, Albert Einstein College of Medicine, Bronx, New York.

Ventricular arrhythmias frequently originate in damaged regions of the syncytium, where anatomical connections between cells are disrupted. Since Ca2+ overload causes increase in gap junctional resistance (rj), interactions between cells with sparse anatomical connections and high rj may be crucial to the genesis of arrhythmias. To analyze these interactions, a model was constructed of 5-10 guinea pig myocytes connected by gap junctions with variable resistance. The model of the myocyte is based on more than 80 experimental measurements and reproduces both normal and oscillatory responses. Preliminary simulations with the syncytial model have been used to analyze cell-to-cell conduction of the action potential in regions with high rj. The model demonstrates that conduction in such regions is not decremental, but all-or-none. In cells with two gap junctions and normal transmembrane currents, conduction fails with a critical rj of 90 Mohms. The value of rj at which conduction fails is primarily a function of 1) magnitude of the threshold outward current needed to elicit action potentials; 2) magnitude of the action potential; 3) duration of the action potential and height of the plateau. With subcritical but elevated rj, conduction is slowed up to 45 msec between each cell. Na+ channel conductance (ina) has minimal effect on the magnitude of rj at which conduction fails but increases delay between cells. A 50% reduction in ina slows conduction about 10% with rj=80 Mohms. If rj is near 90 Mohms, one way block develops with propagation 1) from cells with high rj to cells connected by low rj, and 2) from cells with 2 gap junctions to cells with 3 or more gap junctions. The model should be useful to determine properties of myocardial syncytia that cause arrhythmias due to slow propagation.

W-Pos188

NEONATAL HEART RATE VARIABILITY INCREASES DURING SUCCESSFUL EXTRACORPOREAL MEMBRANE OXYGENATION THERAPY. J. Randall Moorman, M. Pamela Griffin. University of Virginia Health Sciences Center, Charlottesville, VA

To test the hypothesis that health is characterized by greater heart rate variability (HRV) than illness, we measured time and frequency domain parameters of HRV in 7 critically ill neonates who underwent extracorporeal membrane oxygenation (ECMO) therapy for refractory respiratory failure. Six recovered in 5-10 days; one had a fatal intracranial hemorrhage; all had only sinus rhythm. The EKG was highpass filtered (10 Hz), recorded on videotape or digitized online (2.5 msec/point) for 5-10 days, and artefact-free lists of 16,000 RR intervals were used to calculate coefficient of variation (CV) and proportion of the power spectrum from 0.02-0.1 Hz (power), two heart rate-independent parameters in the time and frequency domains, respectively. The power spectrum was constructed from Fourier transformation of the time series of RR intervals, and cycles per beat were converted to equivalent Hz. Qualitatively, time series of RR intervals became "noisier" as the infants recovered. Slow trends in heart rate were observable at all stages. CV for a sliding window of 1,000 beats rose from <1% to 4-10% during therapy but was not specific, as CV was sometimes >4% during severe illness. In the six survivors, power was (%, mean ± SD) 5.3 ± 1.4 at the outset, 9.9 ± 3.9 at 24 hrs, and 20.2 ± 8.4 at the end of ECMO ($p<0.01$, one-way analysis of variance). In the one infant who died, power was 7.7% at the outset and 6.3% at the end of ECMO. We conclude that neonatal HRV increases during recovery from severe illness. (Supported by the Kempner Foundation, University of Texas Medical Branch, Galveston, TX)

W-Pos189

SEA ANEMONE TOXIN INDUCES EARLY AFTER-DEPOLARIZATIONS IN CARDIAC MYOCYTES

Mohamed Boutjdir, Mark Restivo, Yansheng Wei, Nabil El-Sherif. SUNY Health Science and VA Medical Centers, Brooklyn, New York

Early afterdepolarizations (EADs) are among mechanisms proposed to cause polymorphic ventricular tachyarrhythmia known as torsades de pointes. Sea anemone toxin, (ATXII), which has been reported to delay Na inactivation and to induce plateau level oscillations, provides a model to study the formation of EADs in adult rat ventricular myocytes. Action potential and membrane currents were studied using the whole-cell current clamp and voltage clamp techniques, respectively. ATXII prolonged the duration of the action potential and induced EADs without significant change in the resting potential and action potential amplitude. The prolongation of the action potential and the development of EADs were cycle length dependent. The effects of ATXII were reversible upon washout. Ca channel blockers (Verapamil 10^{-5}M, Cobalt 2 mM) and a sarcoplasmic reticulum (SR) modulator (ryanodine 10^{-6}M) did not antagonize ATXII effects on the action potential. However, Na channel blockers (Tetrodotoxin $3x10^{-7}$M, lidocaine $4x10^{-7}$M) and rapid stimulation consistently shortened the prolonged action potential and suppressed EADs. In presence of ATXII and under voltage clamp conditions, a slowly decaying inward current followed the transient inward current during depolarizing pulses. These results suggest that, in rat ventricular myocytes, ATXII-induced EADs are not dependent on transsarcolemmal Ca entry nor cyclic release of Ca from SR. ATXII-induced action potential prolongation and EADs are likely due to slowly inactivating modified Na channels.

W-Pos190

EGTA PROTECTS CARDIOCYTE ACTION POTENTIALS AND ION CHANNELS FROM THE EFFECTS OF H_2O_2.

P.L. Barrington and Ke Zhang, Department of Pharmacology, Northwestern University, Chicago, IL 60611.

Exposure of cardiocytes to H_2O_2 results in a reproducible 3 stage sequence of changes in the cellular action potential (Barrington, et al., 1988). This suggests that H_2O_2 may selectively modifying one or more of the ionic currents which contribute to the action potential. Action potentials were recorded from enzymatically isolated feline cardiocytes using high resistance microelectrodes (35-50 MΩ) filled with 3 M KCl or low resistance patch pipettes (0.8-2.0 MΩ) filled with a physiological solution either with or without EGTA. Whole-cell voltage-clamp techniques were used to determine if H_2O_2 altered the sodium (I_{Na}), calcium (I_{Ca}) or potassium (inward rectifier, I_{K1} and transient outward, I_{to}) currents. Each current was isolated by varying the holding potential and by addition of appropriate channel blockers to intracellular and extracellular solutions. The intracellular solutions for I_{Ca}, I_{K1} and I_{to} included 5 mM EGTA which should prevent large fluctuations of $[Ca^{2+}]_i$. Current-voltage relationships for each current were compared to time controls recorded from separate cells. Superfusion of 100 μM H_2O_2 for 20 minutes caused increased action potential amplitude and duration of cells monitored with high resistance electrodes or low resistance pipettes without EGTA. These effects were greatly attenuated if EGTA was present in the pipette solution. The effects of H_2O_2 on I_{Na}, I_{Ca}, I_{K1} or I_{to} were minimal when EGTA was present in pipette solutions. These results suggest that H_2O_2 does not alter the cellular action potential by direct modification of membrane channel proteins or adjacent lipids. The results do not exclude possible modulation of channel function, i.e. by alteration of $[Ca^{2+}]_i$ or of calcium-dependent second messenger systems.

W-Pos191

STUDIES ON REENTRANT ARRHYTHMIAS AND ECTOPIC BEATS IN EXCITABLE TISSUES BY BIFURCATION ANALYSES.

Teresa Ree Chay* and Young Seek Lee**, *Department of Biological Sciences, University of Pittsburgh, Pennsylvania 15260 and **Department of Biochemistry, Hanyang University, Seoul, Korea

To elucidate the mechanisms that underlie the development of reentry and ectopic beats in cardiac arrhythmias, we have formulated a model which is simple enough to be mathematically tractable, yet captures the nonlinear features of cardiac excitation and conduction. In this model, single cells are connected in a circular fashion by gap conductances. Each cell carries two types of currents: A passive outward current and an inward "excitable" current, whose activation gate is responsible for the upstroke of activation potential and inactivation gate is responsible for the plateau potential. Contrary to the common understanding that a premature stimulus of the right magnitude with the right timing is a prime factor for inducing circus movement, our bifurcation analysis revealed that a special geometry of excitable tissue is a prime requirement for the existence of a rotor. Our analysis also revealed the existence of four distinct multi-stable phases: (1) bistability between a rotor and a quiescent state, (2) bistability between an ectopic beat and a quiescent state, (3) bistability between a rotor and an ectopic beat, and (4) three stable states coexisting among a quiescent state, a rotor, and an ectopic beat. Brief current pulses exert interesting effects on these four regions: In region 1, an impulse can initiate reentrant arrhythmia from a quiescent tissue. In region 2, an impulse can send an ectopic tissue to permant depolarization. In region 3, impulses can convert reentrant arrhythmia to ectopic beats and then switch back to reentry. Depending on the frequency and strength of impulses, in region 4 the tissue can switch back and forth among quiescence, circus movement, and ectopic beat. Since our two-variable model is not quite realistic (other than it captures a qualitative feature of action potential), we also included a more realistic Beeler-Reuter cardiac cell model in our analysis and obtained essentially the same results. From the behavioral similarities of these different models, we can conclude that reentrant and ectopic arrhythmias are intrinsic properties associate with such an excitable tissue and external impulses can convert one mode of arrhythmias to another.

W-Pos192

PROPERTIES OF ARRHYTHMOGENIC TRANSIENT INWARD CURRENTS INDUCED BY REOXYGENATION OF ISOLATED CARDIOCYTES

K. Benndorf, M. Friedrich, C. Biskup, Hj. Hirche (Intro. by S. Moreland) Institut für Vegetative Physiologie, Universität Köln, Robert-Koch-Str. 39, 5000 Köln 41, FRG.

Ionic currents were recorded in isolated guinea pig cardiocytes by a patch clamp technique in the whole-cell configuration while the extracellular solution was switched between normoxic and anoxic ($pO_2 < 0.1$ torr) substrate-free Tyrode. Exposure to anoxia generated a large time-independent K current. One minute after the K current became maximal, the cells were reoxygenated and the K current disappeared. Within the following 10 seconds, transient inward currents (TIs) developed to maximum amplitude and then vanished after at most 140 sec. TIs were evaluated between -90 and +80 mV (holding potential (V_h) -45 mV, pulse duration 350 ms, frequency 1 Hz). The amplitude of the TIs at the holding potential (TI_{-45}) was proportional to the amplitude and duration of the preceding depolarizing test pulse. The current-voltage relationship peaked between -30 mV and -10 mV and approximated zero at the most positive potentials. No reversal of TI was found up to +80 mV. Using double pulse protocols (prepulse potential +40 mV), TIs were found to be enhanced at potentials negative to -30 mV and were also present in the range of the normal resting potential of ventricular heart cells. The interval between the peaks of the first two successive TIs_{-45} (t_{Int}) was 237 ± 35 ms (mean±SD, n=27). t_{Int} increased by 5.2 ± 0.5% (mean±SD) for every 100 pA decrease in TI_{-45}. The increase in t_{Int} with smaller TI_{-45} was generated by a deceleration of the activation time course of TI_{-45} . A noise analysis of TI_{-45} showed that if one assumes that nonspecific ionic channels are responsible for generation of TIs, then the unitary current can not exceed 16.5 fA. The arrhythmogenic potency of reoxygenation-induced TIs was shown under current clamp conditions.

Conclusion: Our findings may be best explained by the hypothesis that reoxygenation-induced TIs are triggered by a cyclic release of Ca from the sarcoplasmic reticulum under conditions of Ca overload and are mediated by the Na-Ca exchanger. Reoxygenation-induced TI may play a predominant role in the generation of reperfusion arrhythmias in the whole heart.

W-Pos193

EFFECTS OF HYDROGEN PEROXIDE ON EXCITATION AND CONTRACTION IN ISOLATED VENTRICULAR MYOCYTES.

M. Horackova and A. Beresewicz, Dept. of Physiology and Biophysics, Medical School, Dalhousie University, Halifax, N.S., Canada, B3H 4H7.

The development of H_2O_2-induced changes in membrane potentials, membrane currents and corresponding contractile activity (shortenings) were studied in rat and guinea-pig ventricular myocytes using the suction-pipette whole-cell clamp method. The effects of 30 μM H_2O_2 are described in three phases: (1) prolongation of action potential duration (APD) accompanied by increased contractility. With a prolonged exposure, the increased APD was accompanied by early afterdepolarizations (EADs), delayed afterdepolarizations (DADs) and aftercontractions. The changes in APD and the EADs were fully and permanently abolished by TTX but not by nifedipine, while the DADs and aftercontractions were abolished by ryanodine. These changes preceded phase (2), which was characterized by APD shortening, a decrease in contractility, membrane depolarization, single or multiple extrasystoles, or steady spontaneous activity; this phase could not be prevented by any of the above pharmacological interventions and resulted in a final phase (3) characterized by full depolarization and inexcitability. All the above changes were prevented by intracellular application of deferoxamine, indicating that OH^- generated intracellularly in the presence of Fe^{3+} induces the observed changes. The examination of membrane currents indicated that the increased APD may be due to an increase in the TTX-sensitive Na^+ current as well as to the decreased delayed current, while L-type Ca^{2+} channels appear to be unaffected.

Supported by grant from MRC Canada (MT-4128).

W-Pos194

LONG TERM EFFECTS OF FREE RADICALS ON AUTOMATICITY OF CULTURED RAT HEART CELLS: DEVELOPMENT OF REFRACTORINESS FOLLOWING SINGLE EXPOSURE TO FREE RADICALS.

S. Rohr and H. Isliker (Introduced by Annemarie Weber). Dept. of Physiology, U. of Penn. School of Medicine, Phila., PA 19104-6085.

Oxidant stress may play a significant role in reperfusion induced cellular injury and arrhythmias (Manning & Hearse *J. Mol. Cell. Cardiol.* 16:497-518, 1984). We examined the timecourse of the effect of free radicals on automaticity of cultured rat heart cells up to several days using a longterm beat rate monitoring system (Rohr *Eur. J. Physiol.* 416: 201-206, 1990) and xanthine/xanthine oxidase (X/XO) as a free radical producing system.

The addition of X/XO (but neither alone) resulted, after an initial delay without any appreciable beat rate changes (0.5 to 1 hr), in a bell-shaped transient positive chrontropic response lasting up to 10 hrs. Peak beat rates were dependent on the concentration of X/XO used and maximal effects (100 % increase) were seen in the presence of 50 µg/ml X and 5 mU/ml XO. This concentration was not accompanied by any morphological signs of cellular injury, while doubling the concentration of X/XO resulted in partially granulated and detached cells. Different interventions pointed to OH^- radicals as the active principle: (i) a similar transient beat rate increase could also be elicited by H_2O_2 (40 µM); (ii) catalase (2 µg/ml) or deferoxamine (1 mM) completely abolished the effect and (iii) superoxide dismutase (50 µg/ml) was ineffective.

Reexposure of cell cultures to X/XO within 24 hrs failed to elicit any beat rate change even after extensive washing of the cells. However, 30 % of the cultures were again responsive 4 days after the primary exposure and 100 % 12 days thereafter. When the normal medium exchange frequency (exchange every other day) was increased, the refractory period could be abbreviated. The transfer of medium bathing X/XO exposed cells to non-exposed cells did not prevent the latter from being stimulated by X/XO. This suggests that the refractoriness was an intrinsic cellular property. It remains speculative whether refractoriness was due to the induction of antioxidative mechanisms within the cells or whether the primary free radical attack resulted in the disappearance of cellular compounds which were responsible for the positive chronotropic response and which had to be resynthesized before the same reaction could be elicited again.

W-Pos195

pH_i-INDUCED CHANGES IN VENTRICULAR MYOCYTE LENGTH.

Kenneth W. Spitzer and John H.B. Bridge. Nora Eccles Harrison CVRTI, University of Utah, Salt Lake City, UT 84112

We examined the effect of intracellular pH (pH_i) on cell length in resting adult ventricular myocytes (guinea pig, cat) held at 37°C (pH_o 7.40). pH_i was measured with SNARF-1 following 10 min of AM (13µM) loading and 30-50 min of perfusion in indicator-free solution containing (mM): NaCl 126, dextrose 11.0, KCl 4.4, $MgCl_2$ 1.0, $CaCl_2$ 2.7, Hepes 24.0, NaOH 13.0. pH_i was determined from the ratio of fluorescence emission (640nm/580nm) during continuous excitation at 515nm. Cell length was monitored with a video motion detector. The intracellular alkalosis elicited by exposure to 10mM NH_4Cl caused a reversible decrease in cell length (Fig. left panel). In this guinea pig myocyte there was a nonlinear relationship between the alkaline contracture and pH_i which also displayed hysteresis (right panel). Equilibration in solution containing 2mM EGTA and no added calcium did not affect the pH_i changes elicited by NH_4Cl and only slightly decreased the alkaline contracture. Application of 15mM diacetyl monoxime during the alkaline contracture caused relaxation without changing pH_i. Internal dialysis of cells with a suction pipette (2-3MΩ resistance) containing no added Ca and 14mM EGTA (pH 7.1), with Ca_o = 2.7mM, completely inhibited twitches but did not prevent the alkaline contracture. These results suggest that while changes in myofilament Ca sensitivity may partially explain the response of resting cells to increased pH_i, other factors are involved, perhaps a pH_i-induced change in myofilament surface charge (Elliott, G.F. et al, in "Electrical Double Layers in Biology", 277-285, 1985).

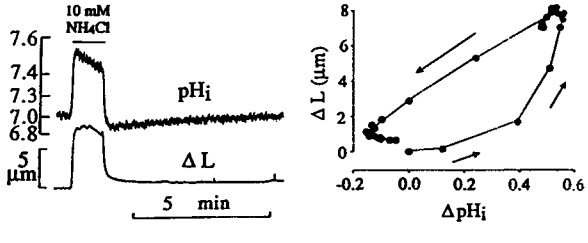

W-Pos196

DIFFERENCES IN THE POSITIVE INOTROPIC EFFECT RESULTING FROM THE STIMULATION OF α_1-ADRENERGIC AND MUSCARINIC RECEPTORS IN LEFT AND RIGHT GUINEA PIG PAPILLARY MUSCLES.

JORGE ARREOLA, ROBERT T. DIRKSEN, G. PATRICIA PEREZ C., AND SHEY SHING SHEU. Department of Pharmacology, University of Rochester School of Medicine and Dentistry, Rochester NY 14642.

The effects of α_1-adrenergic and muscarinic receptor stimulation on action potential and tension were studied. Differences between left and right papillary muscles were found. In right side papillary muscles, α_1-adrenergic receptor stimulation with 300 µM methoxamine (MTX) maximally decreased the action potential duration (APD) (-8.1 ± 0.5%) and produced a positive inotropic effect (PIE) (90.8 ± 28.6%). In contrast, MTX (300 µM) did not produce a PIE (-20.2 ± 8.8%), but still decreased the APD (-8.7 ± 0.4%) in left side papillary muscles. These effects were all blocked by the α_1-adrenoceptor antagonist, prazosin (1-3 µM). Stimulation of muscarinic receptors from both left and right side papillary muscles with 300 µM carbachol (CA) produced a shortening in the APD (left: -4.76 ± 0.33%, right: -5.6 ± 0.63%) and a PIE (left: 46 ± 7%, right: 60 ± 10%). Both effects were blocked by 1 µM atropine. Experiments in right side papillary muscles showed that 300 µM MTX and 300 µM CA produced additive effects on the action potential and tension. Furthermore, the direct protein kinase C activator, phorbol 12,13-dibutyrate (PDBU) (1 µM), also decreased the APD in a manner which was additive to both MTX and CA. However, PDBU reversed the PIE produced by both CA and MTX.

The different effects produced by α_1-adrenoceptor activation seen in right and left papillary muscles suggests differences between the receptor-activated events ocurring in the two sides of the heart. The mechanism(s) for the increase in tension caused by CA and MTX may not be dependent of the activation of PKC or on the shortening of the APD. Different or localized precursor pools of second messenger systems may be involved in the CA and MTX effects on APD and tension.

J.A. is a fellow from AHA (88-120F).

W-VCR2

MECHANICAL STIMULATION OF CARDIAC MYOCYTES INCREASES INTRACELLULAR CALCIUM. W.J. Sigurdson and F. Sachs. Department of Biophysics, SUNY at Buffalo 14214.

We have examined the transduction of mechanical stimuli in chick cardiac myocytes by monitoring changes in intracellular Ca^{2+} concentration. Cultured chick embryonic heart cells were loaded with 4 μM FLUO-3 AM, a Ca^{2+} indicator fluorescent dye (Molecular Probes) and examined with a Zeiss Axiovert equipped with fluorescein optics, a Video Scope image intensifier and Dage CCD camera. Real-time imaging of FLUO-3 fluorescence revealed low resting levels of intracellular Ca^{2+} in non-contracting cells and cyclic fluctuations of Ca^{2+} in synchrony with cellular contraction. When cells were prodded with a fire-polished patch pipette, a wave of fluorescence increase was seen to originate from the site of stimulation and spread throughout the cell. This could be repeated 2-3 times, until the cells became over-loaded (intracellular storage-sites became fluorescent) or the dye was bleached. The "degree" of prodding, although not quantified, was comparable to that used when attempting to form a patch for single-channel recording. Prodding or pulling on one cell could indirectly induce fluorescence increases in attached cells. When bath Ca^{2+} was removed, small increases in fluorescence were observed only after severe mechanical abuse of the cell. These observations are consistent with the activation of mechano-sensitive (MS), Ca^{2+} -permeable ion channels known to be present in these cells. To test this, we added 20 μM Gd^{3+} (a known blocker this channel) to the normal bath saline. Gd^{3+} did not abolish intrinsic rhythmic Ca^{2+} fluctuations, but did block the mechanically induced Ca^{2+} increase. In normal saline we occasionally saw bright spots of fluorescence near the pipette during prodding, indicating possible locations of individual MS channels. Our ability to detect normal physiological changes in intracellular Ca^{2+} shows that qualitatively, the mechanically induced increases in Ca^{2+} are due to realistic ie., physiological increases in membrane tension. MS channels could act as the transducers of this tension which becomes translated into a Ca^{2+} influx which in turn stimulates Ca^{2+}-induced Ca^{2+} release. The ease at which these changes could be produced and the apparent ubiquity of MS channels may have implications on cell-attached single-channel recording where the intracellular Ca^{2+} is assumed to be at resting levels. Quantification of Ca^{2+} changes correlated with MS channel conductance will allow estimates of the number of activated channels.

W-Pos197

INVESTIGATION OF ASYMMETRIC PERTURBATIONS OF NI(II)-OCTAETHYLPORPHYRIN IN SOLUTION BY RESONANCE RAMAN SPECTROSCOPY.

R. Schweitzer-Stenner, U. Bobinger and W. Dreybrodt
Institute of Experimental Physics, University of Bremen, W-2800 Bremen 33, Germany

It is increasingly appreciated that an in depth understanding of the mechanism determining heme-protein interactions requires a detailed knowledge about the influence of side chains on the symmetry properties of metalloporphyrins. Earlier Raman studies have shown that even in Ni(II)-octaethylporhyrin (NIOEP) the symmetry of the porphyrin macrocycle can be lowered due to specific steric arrangements of the ethyl-side chains (1). In order to explore their influence on the vibronic patterns of the NIOEP-molecule we have measured the depolarization ratio dispersion and resonance excitation profiles of the Raman lines of twelve NIOEP-modes, i.e. ν_3, ν_4, ν_5 (A_1 in D_4), ν_{10}, ν_{11}, ν_{13} (B_1), ν_{29} (B_2), ν_{19}, ν_{20}, ν_{21}, ν_{22} (A_2) and a $\nu(C_1C_2)$ - ethyl mode. The data cover the resonance region of the Q- and Q_v-bands and the preresonance region between Q_v- and B-band. A selfconsistent analysis of the DPDs and REPs was carried out by explicit consideration of their multimode contributions to the polarizability tensor of each mode (2). The thus derived vibronic coupling parameters show that the A_2, B_1 and B_2 modes are affected by B_2 and A_2-distortions. The symmetric A_1-modes investigated are less distorted than the asymmetric and antisymmetric modes and are exclusively affected by B_2-perturbations. In contrast to what has been found for porphyrins in a protein matrix B_1-distortions are comparatively small(3). These results suggest that the symmetry lowering distortions affect the C_β-atoms of the pyrroles rather than the central part of the macrocycle.

1) R.G. Alden, B.A. Crawford, R.Doolen, M.R. Ondrias and J.A. Shelnutt, J.Am.Chem.Soc. 111,2070,1989
2) R.Schweitzer-Stenner, U. Bobinger and W. Dreybrodt, J. Raman Spectrosc., in press (1990)
3) R.Schweitzer-Stenner, Quart.Rev.Biophys.,22,381,1989

W-Pos198

VIBRATIONAL ANALYSIS OF HYDROPORPHYRINS

D. F. Bocian and Alexander D. Procyk

Vibrational analysis of several hydroporphyrins have been performed by using the Wilson FG matrix formalism. The observed infrared and Raman frequencies of the normal isotope and meso-deuteriated analogues were used to refine the force fields. Collectively, these force fields provide a detailed description of the normal modes of vibration of reduced pyrrole macrocycles.

W-Pos199

FT-IR MICROSCOPY AND RESONANCE RAMAN SPECTROSCOPY OF HEME A AND ITS Ni^{2+}- AND Cu^{2+}-MODEL COMPOUNDS

Jose A. Centeno, Department of Environmental and Toxicologic Pathology, Division of Environmental Toxicology, Armed Forces Institute of Pathology, Washington, DC 20306-6000

Infrared microscopy in conjunction with resonance Raman (RR) spectroscopy have been applied to study the effects of porphyrin-center metal-ion substitution in heme a and its model compounds, and to obtain information on those vibrational modes with contributions from the formyl and vinyl peripheral substituents. The C-H stretching motions of heme a at 2930 and 2858 cm^{-1}, respectively, are highly insensitive to metal-ion substitution. Likewise, the deformation modes of the terminal methyl groups at 1463 and 1380 cm^{-1} do not change upon metal-substitution. Metal-ion infrared sensitive bands were observed at 1606, 1410, 1263, 1176, 914, and 738 cm^{-1}. The Raman spectrum of 2,6-dipentyl-4-vinyl-8-formyl-Ni^{2+} porphyrin display metal-ion sensitive vibrations at 1123, 1241, 1306, 1381, 1519, 1602, and 1665 cm^{-1}. Although most of these lines can be assigned to core-size vibrations, some of them appear to have contributions from formyl and vinyl vibrations as demonstrated by substitution of ^{18}O at the $-CH^{16}O$ position of the formyl group. Low-frequency lines at 419 and 461 cm^{-1} in the RR spectrum of Ni^{2+}-porphyrin a are assigned to pyrrole-ring in-plane deformation modes with contribution from formyl- and vinyl-substituents, respectively. The selective enhancement of these modes in the RR and infrared spectra of Ni^{2+}-porphyrin and Ni^{2+}-porphyrin a are attributed to the decrease in porphyrin core-size upon Ni^{2+} substitution.

W-Pos200

CYTOCHROME *c* OXIDASE (aa_3-TYPE) OF *RHODOBACTER SPHAEROIDES* IS SIMILIAR TO THE MITOCHONDRIAL ENZYME BUT CONTAINS A UNIQUE LOCAL ENVIRONMENT FOR CYTOCHROME *a*

J.P. Hosler, M.M.J. Tecklenburg, M. Atamian, A. Revzin, S. Ferguson-Miller and G.T. Babcock, Departments of Biochemistry and Chemistry, Michigan State University, E. Lansing, MI 48824.

Much of the information required to elucidate the mechanism by which cytochrome *c* oxidase transfers electrons and pumps protons may come from studies of bacterial systems because the prokaryotic enzymes are simpler in structure (2-3 subunits) and genetic engineering is possible. We have purified the aa_3-type oxidase of *Rhodobacter sphaeroides* from aerobically grown cells as a three subunit enzyme (apparent molecular weights of 45, 37 and 23 kD) by solubilizing purified cytoplasmic membranes with lauryl maltoside, followed by anion exchange chromatography. Structural homology to the mitochondrial enzyme is indicated by specific labeling of the third subunit with ^{14}C-DCCD and reaction of subunit II with antisera to yeast oxidase. The oxidase shows unusually high activity (V_{max} > 2000 sec^{-1}) and good respiratory control following reconstitution into phospholipid vesicles. The steady state kinetics of O_2 uptake activity show a biphasic dependence on cytochrome *c* concentration, indicating a mechanism of interaction with its substrate similar to that of the mammalian oxidase. Resonance Raman spectra of *Rhodobacter* oxidase closely resemble those of the mitochondrial enzyme, including the signals attributed to the formyl group of cytochrome *a*. The EPR spectrum is similar to beef heart oxidase in the g = 2.0 region, suggesting a comparable Cu_A binding site; however the low-spin heme signals at g = 2.83, 2.31 and 1.62 are shifted from the signals assigned to cytochrome *a* of beef heart cytochrome *c* oxidase. Previous studies of cytochrome *a* models (Babcock *et. al.* in Cytochrome Oxidase, King *et. al.*, eds., p. 105, Elsevier, Amsterdam, 1979) show that this difference may arise from the deprotonation of one of the histidine ligands of cytochrome *a* in the bacterial enzyme.

W-Pos201

THE EFFECTS OF PHMB-MODIFICATION AND HEAT-TREATMENT ON THE Cu_A REDUCTION POTENTIAL OF CYTOCHROME C OXIDASE

Zhuyin Li, Randy W. Larsen, Lian Ping Pan and Sunney I. Chan
A. A. Noyes Laboratory of Chemical Physics, California Institute of Technology, Pasadena, CA 91125

Cytochrome c oxidase catalyses the terminal electron transfer in the mitochondrial respiratory chain from ferrocytochrome c to molecular oxygen. In addition, it is an electrogenic proton pump capable of translocating vectorially up to four protons from the matrix of the inner mitochondrial membrane to the cytosol for every dioxygen molecule reduced.The two "low-potential" metal centers of oxidase have been considered to be the most plausible candidates for the site of redox-linked proton pumping. Recently, several experiments on Cu_A modified oxidase from this laboratory seem to implicate Cu_A as the site of redox linkage. In this paper, we look more closely into the question of how the pHMB-modification and heat-treatment affect the dioxygen activity and the proton pumping behaviour of the enzyme. The reduction potential of the Cu_A site of both pHMB-modified and heat-treated oxidase have been measured under different conditions, the titration data have been fixed to a single interaction model. The results indicated that Cu_A reduction potential has been decreased to 100 mV upon pHMB-modification while heat-treatment increased the Cu_A reduction potential to about 295 mV. In addition, the interactions between Cu_A and the remains metal centers are purturbed upon Cu_A modification. This data supports the assignment of Cu_A as the redox linked proton pump in cytochrome oxidase.

W-Pos202

THE NATURE OF Cu_X IN CYTOCHROME C OXIDASE

L. P. Pan, Z. Li, R. W. Larsen, and S. I. Chan
A. A. Noyes Laboratory of Chemical Physics, 127-72, California Institute of Technology, Pasadena, California 91125

We report here extensive and accurate analyses of the Cu, Fe, Zn and Mg contents in bovine heart cytochrome c oxidase by direct current plasma atomic emission spectrometry. The precision of an individual measurement is within ± 5%. The analyses confirm a stoichiometry of 5Cu/4Fe/2Zn/2Mg per dimer. The results of the present study also confirm that Cu_x, Zn and Mg ions are intrinsic components of the enzyme. Although the enzyme exhibits high affinity for exogenous Cu and Zn as well, those can be readily removed from the enzyme by dialyzing against 40 mM EDTA. Seven enzyme preparations treated by various methods are also analyzed to investigate the nature of Cu_x. It is shown that Cu_x is removable by either monomerization of the enzyme or subunit III depletion. This result suggests that Cu_x is associated with subunit III and that it plays a structural role in enzyme dimerization. EPR measurements indicate that Cu_x is heterogeneous and mostly reduced. In addition, we find Cu_x has no effect on the spectroscopic properties and electron transfer activity of the enzyme. Supported by NIH GM22432.

W-Pos203

STRUCTURE AND REACTIVITY OF HEME a RECONSTITUTED MYOGLOBIN AND HEME a RECONSTITUTED HORSERADISH PEROXIDASE

R. W. Larsen[1], D. J. Nunez[2], J. Mcleod[1], M. R. Ondrias[2], and S. I. Chan[1],[1]A. A. Noyes Laboratory of Chemical Physics, California Institute of Technology, Pasadena, Ca., 91125, Dept. of Chemistry,[2]University of New Mexico, Albuquerque, NM, 87113.

The data to be presented in this study focuses on the role of heme active structure (ie. porphyrin structure and local protein environment) on the catalytic function of aa3-type terminal oxidases. Because these native enzymes are complex membrane bound proteins, detailed analysis of the functional properties of the heme active sites has been elusive. The structural aspects of heme a which may be relevant to the catalytic function of these enzymes has been examined indirectly by reconstituting heme a into different protein matrices. Specifically, the structure and reactivity of two heme a reconstituted proteins have been investigated. Optical absorption studies indicate that addition of 1 equivalent of heme a to either apomyoglobin (apoMb) or apohorseradish peroxidase (apoHRP) produces 1:1 high affinity protein-porphyrin complexes. The heme a apoMb complex displays optical and resonance Raman signals characteristic of a distribution of high- and low-spin heme chromophores in both the oxidized and reduced forms. Interestingly, the low temperature EPR sprectra of this complex display only high-spin heme resonances. The optical and vibrational properties of the heme a:apoHRP complex also displays both high- and low-spin heme signals in both oxidized and reduced forms. The ratio of the high-spin to low-spin signals is, however, higher in this complex, relative to that of the heme a:apoMb complex. In addition, the heme a:apoHRP complex displays catalytic activity toward peroxide, although at a reduced rate relative to native HRP. These results will be discussed in relation to the environment and reactivity of heme a in aa3-type terminal oxidases.

W-Pos204

ULTRAFAST AND NOT-SO-FAST DYNAMICS OF CYTOCHROME OXIDASE.

P.O. Stoutland[1], J.-C. Lambry[2], K.A. Peterson[1], K.A. Bagley[1], R.B. Dyer[1], J.-L. Martin[2], and W.H. Woodruff[1], [1]Los Alamos National Laboratory, Los Alamos, NM, and [2]Ecole Polytechnique-ENTA, Palaiseau, France.

Subpicosecond electronic spectroscopy has been used to study the photoexcitation and subsequent reactivity of resting, reduced unliganded, and reduced-CO cytochrome oxidase. In both reduced derivatives the results are consistent with the formation of an excited state of cytochrome a which decays in 3-5 ps. We tentatively assign the product of this excited state decay to a 5-coordinate ground state which subsequently rebinds the photodissociated axial imidazole with a halflife of ca. 20 ps. In the unliganded reduced enzyme cytochrome a_3 does not appear to contribute significantly to the observed absorption transients. In the CO derivative, however, bleaching of the cytochrome a_3-CO absorbance occurs in <150 fs and persists until CO rebinds on the millisecond timescale. After photodissociation of CO, the cytochrome a_3 α-band exhibits a blue shift with a halflife ca. 10 ps. Time-resolved infrared, resonance Raman, and MCD suggest that the binding of photo-dissociated CO to Cu_B (in ca. 1 ps) triggers transfer of an endogenous ligand from Cu_B to Fe_{a3} (in ca. 10 ps). This ligand appears to bind on the distal side of cytochrome a_3 , displace the proximal histidine imidazole, and remain bound to Fe_{a3} for the lifetime of the Cu_B-CO complex (ca. 1 μs). This is an additional aspect of the previously proposed (Dyer, R.B., Einarsdóttir, Ó., Killough, P. M., López-Garriga, J.J., and Woodruff, W.H. (1989) J. Am. Chem. Soc. 111, 7657-7659) "ligand shuttle" activity of the Cu_B/Fe_{a3} pair. We speculate as to the identity of the transferred ligand and the functional role of the ligand shuttle.

W-Pos205

TIME RESOLVED RESONANCE RAMAN STUDIES ON A PHOTOLABILE INTERMEDIATE FORMED AFTER PHOTODISSOCIATION OF CARBON MONOXIDE FROM REDUCED CO-CYTOCHROME C OXIDASE.

K.A. Bagley[a], R. B. Dyer[b], and W. H. Woodruff[a], [a]INC-4 and [b]CLS-4, Los Alamos National Laboratory, Los Alamos, NM 87545.

In recent work we have suggested that following photodissociation of CO from reduced CO-cytochrome *c* oxidase, a photolabile intermediate is formed within 10 ps which persists for 1μs.[1] Using low probe power densities we have obtained the resonance Raman spectra at a number of times following the photodissociation of CO. We note that the resonance Raman spectra obtained 200 ns after photodissociation using a low power density probe (10μJ/pulse) is different than that obtained with a relatively high power density (2.0mJ/pulse) thus confirming the photolability of the species. Furthermore, the resonance Raman spectrum taken 200 ns after CO photodissociation, using low power density, is different than the resonance Raman spectrum taken with low power density 10 μs after photodissociation. The resonance Raman spectra taken together with recent time resolved magnetic circular dichroism data[1] suggest that the intermediate formed 200 ns after CO photodissociation is a 5-coordinate high spin species, in which binding of an endogenous ligand to the distal side of heme a_3 has forced the breaking of the proximal imadozole bond to a_3.

[1]Woodruff, W.H., Ó. Einarsdóttir, R.B. Dyer, K.A. Bagley, G. Palmer, S.J. Atherton, R.A. Goldbeck, T.D. Dawes, and D.S. Kliger (1990) PNAS, in press.

W-Pos206

ULTRAFAST LIGAND DYNAMICS IN CARBONMONOXY CYTOCHROME *c* OXIDASE. DIRECT EVIDENCE FROM TIME-RESOLVED INFRARED SPECTROSCOPY.

R. Brian Dyer,† Kristen A. Peterson,† Page O. Stoutland‡ and William H. Woodruff,‡ †CLS-4 and ‡INC-4, MS-J567, Los Alamos National Laboratory, Los Alamos, NM 87545.

The dynamics of the photodissociation of CO from cytochrome *c* oxidase (CcO) and of subsequent reactions have been probed directly using ultrafast time-resolved infrared spectroscopy (TRIRS). Picosecond TRIR transients were obtained in pump-probe experiments at a fixed infrared probe wavelength. The time resolution was accomplished by optical delay between the visible pump pulse (595 nm, 2 ps) and the tunable infrared probe pulse (~5 μm, 2 ps). We have observed a subpicosecond bleaching of the 1963 cm^{-1} absorption of CO bound to cytochrome a_3 of CcO, which we attribute to the photodissociation of CO. This result is consistent with transient UV-vis measurements which suggest that the photodissociation of CO occurs in less than 50 fs (Lambry, J.-C., Stoutland, P. O., Woodruff, W. H., Martin, J. L., unpublished results). No recovery of the bleach is observed out to 100 ps, indicating that the barrier to geminate recombination must form rapidly. We propose that the transfer of CO to Cu_B triggers the formation of a long lived (microseconds) barrier, the binding of a distal ligand to the heme. The rate of transfer of CO from Fe_{a3} to Cu_B was measured directly by monitoring the peak of the transient Cu_B-CO absorption at 2061 cm^{-1}. The magnitude of the signal observed indicates complete formation of the Cu_B-CO complex on this timescale. The risetime of this transient was best fit with a convolution of a 1 to 2 ps exponential with the experimentally determined instrument response function. A significant fraction of the rise-time of the Cu_B-CO transient is the time necessary to form the new stationary spectrum (~600 fs, assuming a homogeneous linewidth of 8 cm^{-1} for the Cu_B-CO absorption). Consequently, in about 1 ps the CO must move between 2 and 5 Å and then bind to the Cu_B. This remarkable rate of CO transfer from Fe_{a3} to Cu_B provides unique insight into the structure of CcO. The metal centers and surrounding protein appear to be designed to facilitate ligand transfer from Fe_{a3} to Cu_B. This feature of the protein may have some significance to the role of Cu_B as a ligand "shuttle" to Fe_{a3} in the functional dynamics of the protein.

W-Pos207

INTERMEDIATES FORMED IN THE REACTION OF CYTOCHROME *C* OXIDASE WITH OXYGEN

Sanghwa Han, Yuan-chin Ching, and Denis L. Rousseau
AT&T Bell Laboratories, Murray Hill, NJ 07974

The reaction of cytrochrome *c* oxidase with oxygen has been studied over a wide time range by resonance Raman spectroscopy. The progression of the intermediates formed in the reaction was followed from a few microseconds to several milliseconds by monitoring the oxygen isotope sensitive lines in the resonance Raman spectrum. At the earliest time, a line at 568 cm^{-1} was detected, which we assign as the Fe-O_2 stretching mode of the primary intermediate. At later time, an intermediate with an oxygen isotope sensitive mode at 786 cm^{-1} was formed and finally, an intermediate was formed with a mode at 450 cm^{-1}. We assign the intermediate with a mode at 786 cm^{-1} as a ferryl species and that at 450 cm^{-1} as a hydroxy species. Hydrogen isotope studies demonstrate that the ferryl oxygen atom is hydrogen bonded. By monitoring the high frequency region of the resonance Raman spectrum, the rate of oxidation of cytochrome *a* may be followed thereby allowing for the determination of the rate at which electrons are transfered to the bi-nuclear oxygen binding site. We find that this oxidation of cytochrome *a* occurs very rapidly. With the firm identification of the intermediates reported here and the determination of the rate of electron tranfer to the bi-nuclear site, the dominant structures at nearly all of the O_2 reduction levels are now known and the catalytic pathway may be postulated with some certainty.

W-Pos208

NANOSECOND TIME-RESOLVED MAGNETIC CIRCULAR DICHROISM SPECTROSCOPY OF PHOTOLYZED CYTOCHROME *C* OXIDASE-CO

Robert A. Goldbeck,[1] Ólöf Einarsdóttir,[1] Timothy D. Dawes,[1] William H. Woodruff,[2] and David S. Kliger[1]

[1]*Department of Chemistry and Biochemistry, University of California at Santa Cruz, Santa Cruz, CA 95064.*
[2]*Isotope and Structural Chemistry Group (INC-4), Los Alamos National Laboratory, Los Alamos, NM 87545.*

Time-resolved magnetic circular dichroism (TRMCD) and natural circular dichroism (TRCD) are measured on a nanosecond timescale following the photolysis of the CO complex of cytochrome *c* oxidase (CcO-CO). TRMCD is a sensitive probe of the heme iron spin state following ligand photodissociation. Heme spin state is closely correlated with the extent of heme axial ligation; ferrous heme A is low spin when hexacoordinate, high spin when pentacoordinate. We find that the iron promptly changes from low spin to high spin, as expected for simple photodissociation of CO from the heme. However, evidence from other time-resolved spectroscopies suggests that unusual coordination occurs at the (cytochrome a_3) iron and at a nearby copper (Cu_B) after photolysis. We present a model of CcO-CO photolysis which is consistent with all of the spectroscopic results, including TRMCD. A novel feature of this model is a "shuttling" of ligands between Fe_{a3} and Cu_B. This ligand shuttle may play a role in the physiological function of the protein as a redox-driven proton pump.

W-Pos209

THE MECHANISM OF O_2 REDUCTION BY CYTOCHROME OXIDASE. TIME-RESOLVED RESONANCE RAMAN DETECTION OF TRANSIENT INTERMEDIATES. C. Varotsis and G. T. Babcock, Department of Chemistry, Michigan State University, East Lansing MI 48824

Cytochrome oxidase, also known as cytochrome aa_3, the terminal enzyme of the mitochondrial respiratory chain, catalyzes the oxidation of reduced cytochrome *c* by molecular oxygen. In the work reported here, we used flash photolysis of carbon monoxy cytochrome oxidase subsequent to its rapid mixing with oxygenated buffer to initiate the reduction of O_2 by the enzyme. In the Raman spectrum recorded at 10μs subsequent to CO photolysis, a mode is observed at 571 cm^{-1} that shifts to 546 cm^{-1} when the experiment is repeated with $^{18}O_2$. The appearance of this mode is dependent upon the laser intensity used and disappears at higher-incident energies. The 571 cm^{-1} $\nu(Fe\text{-}O_2)$ frequency in the fully reduced enzyme/O_2 adduct is essentially identical to the 572 cm^{-1} frequency we measured for this mode during the reduction of O_2 by the mixed-valence enzyme, which indicates that the O_2-bound cytochrome a_3 is independent of the redox state of the cytochrome a/Cu_A pair. In the spectrum recorded at 800μs in the reaction of the fully reduced enzyme with O_2, a mode is observed at 790 cm^{-1} that shifts to 755 cm^{-1} when the experiment is repeated with $^{18}O_2$. The frequency of this vibration and the magnitude of the $^{18}O_2$ isotopic frequency shift allow us to assign the 790 cm^{-1} mode to the Fe^{IV}=O stretching vibration of the low-spin oxygen adduct that forms in the reaction of the fully reduced cytochrome oxidase. The appearance of this mode is not affected when D_2O is used as a solvent. This suggests that the ferryl-oxo intermediate is not hydrogen bonded at 800μs in the reaction. In this presentation, we will summarize the time-resolved spectra of the intermediates in the cytochrome oxidase/oxygen reaction and the insights they provide into the mechanism of dioxygen reduction.

W-Pos210

AROMATIC DONOR BINDING TO MAMMALIAN PEROXIDASE ENZYMES. M. Ikeda-Saito, K. S. Booth, W. S. Caughey, S. Kimura, and H. Hori. Case Western Reserve Univ. Cleveland, OH. 44016, Colorado State Univ. Fort Collins, CO. 80523, NCI, NIH, Bethesda, MD 20892, and Osaka Univ. Toyonaka, Osaka 560 Japan

Salicylhydroxamic and benzohydroxamic acids (SHA & BHA) were found to bind to the resting state of myeloperoxidase to inhibit ligand binding to the heme iron. An ionizable group on the enzyme with pK_a = 4 affects salicylhydroxamic acid binding; binding occurs when this group is not protonated. The binding of the heme iron ligands, (e.g. cyanide, nitrite, and chloride) is probably controlled by the same ionizable group, the distal histidine residue. The equilibrium dissociation constant of the SHA-myeloperoxidase complex is about 2 x 10^{-6} M and the association rate constant is 7.4 x 10^6 $M^{-1}sec^{-1}$. SHA serves as a donor to the higher oxidation state of myeloperoxidase and thereby inhibits guaiacol oxidation. SHA was also found to bind to intestinal peroxidase and lactoperoxidase. SHA binding to all three mammalian peroxidase enzymes was about three orders of magnitude stronger than BHA binding. SHA and BHA complexes showed low temperature EPR spectra as the mixture of low spin and high spin states, whereas phenol complexes showed high spin EPR spectra. We conclude that the SHA and BHA bind in the distal heme cavity of these peroxidase enzymes and interacts with the heme ligand binding site.

Supported in part by NIH GM39492, RR05695 and HL15890.

W-Pos211

PROTON NMR STUDIES OF YEAST CYTOCHROME c PEROXIDASE AND ITS CROSSLINKED COMPLEX WITH YEAST ISO-1 FERRICYTOCHROME c James D. Satterlee[1], Susan J. Moench[1] and James E. Erman Departments of Chemistry, Washington State University[1], Pullman, WA 99164-4630 and Northern Illinois University, DeKalb, IL 60158

Cytochrome c peroxidase (CcP) is a 34 kD protein that catalyzes the hydrogen peroxide oxidation of ferrocytochrome c. This process involves two particularly interesting aspects. 1) Stabilization of a ferryl-heme moiety in the oxidized intermediates of CcP is implied in the catalysis. 2) Complex formation between CcP and cytochromes c is part of the electron transfer (oxidation) process. In order to elucidate features of the CcP structure that facilitate these processes we present results from high resolution 2D NMR spectroscopy and covalent crosslinking studies.

Proton NMR assignments of heme pocket, exchangeable and catalytically relevant amino acid protons have been done using 1D and 2D nuclear Overhauser effects for cyanide-ligated CcP. Complete resonance assignments have been achieved for His-175 and His-52, both members of the H-bonding network that facilitates catalysis. In addition proton assignments have been made for protons of Trp-51, Arg-48, Leu-232, Thr-180, Ala-174 and Ala-176.

This work also reveals that there is a pronounced species specificity to the formation of 1:1 molecular redox complexes between CcP and various cytochromes c. In particular, our work reveals that it is possible to trap multiple 1:1 complexes of yeast iso-1 cytochrome c crosslinked to CcP. These results are the first validation of predictions from Brownian Dynamics simulations that molecular redox complexes should involve multiple encounter complexes. The complexes of physiologically accurate yeast proteins are significantly distinct from those formed with other species of ferricytochromes c and indicate that subtle interfacial recognition effects are the discriminators. In particular, formation of the complex of yeast proteins is significantly driven by the hydrophobic effect, in contrast to the complexes of CcP with either horse or tuna ferricytochromes c, where electrostatic effects play a more prominent role in complex formation.

W-Pos212

THE PH-DEPENDENCE STUDIES ON THE FORMATION AND PHOTOLABILITY OF LOW SPIN HEME IRON OF NATIVE CYTOCHROME C PEROXIDASE(II) IN ALKALINE PH *Jianling Wang, & Mark R. Ondrias* **Department of Chemistry, University of New Mexico, Albuquerque, NM 87131.** The ferrous form of native cytochrome c peroxidase (CCP) undergoes a reversible transition when titrated over a pH range of 6.0 to 9.7. This transition produces a conversion from a penta-coordinate high-spin to a hexa-coordinate low-spin heme active site and is clearly apparent in the heme optical absorption spectra. Here we report the characterization using resonance Raman spectroscopy of this transition and its effect upon the local heme environment. ν_3, an excellent coordinate and spin-state marker, was employed to track the transformation of the spin states. Its behavior confirms the presence of photolabile low spin heme iron at alkaline pH solution. The formation of hexa-coordinate low spin heme is interpreted as the binding of His-52 in the distal site after the cleavage of the tensive H-bonded network in the proximal site of CCP(II) hemepocket at alkaline pH. Transient resonance Raman experiments demonstrate that the hexa-coordinate low-spin species can be photolyzed, producing a species similar to the low-pH (high-spin) form of CCP(II). Moreover, the extent of photolysis is quite pH dependent. The circular dichroism investigations of CCP(II) in the far-UV region exhibits different CD spectra for the peroxidase present in pH 8.5 and 9.7, indicating the occurance of at least two protein structural species for CCP(II) in pH higher than 8.5. (Supported by the NIH GM33330)

W-Pos213

THE IMPORTANCE OF A CONSERVED LYSINE TO THE STABILITIES OF CYTOCHROMES C.

Michael Caffrey, Paul Gooley, Neil MacKenzie and Michael Cusanovich, Department of Biochemistry, University of Arizona, Tucson, AZ 85721

Lysine 12 of Rhodobacter capsulatus cytochrome c_2 (the equivalent of lysine 13 of horse cytochrome c) has been replaced by aspartate. With respect to the wild type cytochrome c_2, K12D exhibits no spectral differences in the UV/VIS, however, K12D exhibits a small ionic strength dependent effect on the midpoint redox potential. Gdn-HCl denaturation of K12D indicates that this charge substitution has decreased cytochrome c_2 stability by 1.0 kcal/mol. Two-dimensional NMR analyses of reduced K12D reveal spectral perturbations which are limited to residues in the amino and carboxy terminal alpha helices. Together, these results suggest that lysine 12 of R. capsulatus cytochrome c_2 (or its equivalent in other species of cytochromes c) plays an important role in cytochrome c stability.

This work was supported by USPHS GM 21277.

W-Pos214

RESONANCE RAMAN CHARACTERIZATION OF THE MULTI-HEME SITES OF DESULFOVIBRIO VULGARIS (HILDENBOROUGH) CYTOCHROME C_3.

M. C. Schneebeck [1], J. D. Hobbs [1], J. H. Hazzard [2], R. G. Bartsch [2], M. A. Cusanovich [2] and M. R. Ondrias [1].
1. University of New Mexico, Department of Chemistry, Albuquerque, NM 87131.
2. University of Arizona, Department of Biochemistry, Tucson, AZ 85721.

The cytochromes c_3 are periplasmic, multiheme proteins isolated from the species *Desulfovibrio*, a strictly anaerobic sulfate reducing bacterium. They generally consist of four C-type hemes, having bis-histidine axial ligation and low oxidation-reduction potentials, within a single protein subunit (molecular mass ~13kDa). The redox potentials of the four heme have been shown to cooperative and span an approximate 100mV range.

In this study, we present resonance Raman spectra for the fully oxidized, partially reduced and fully reduced species, as well as, a CO bound form of the enzyme. Preliminary result indicate that the fully oxidized form is photoreducible at moderate UV laser powers. We also observe splitting in at least one heme vibrational mode, ν_{11}, which may suggest structural inhomogeneity among the heme sites. In the CO ligated species we have made an initial observation of $\nu_{Fe\text{-}CO}$ (496cm^{-1}). These observations will be discussed within the context of general structure-function relationship of C-type cytochromes. This work supported by the NIH (GM3300 to MRO) , the Office of Naval Research (Contract No. N00014-90-J1226 to JHH, MAC) and the Howard Hughes Medical Institute Predoctoral Fellowship (to MCS).

W-Pos215

RESONANCE RAMAN SPECTROSCOPY AND MOLECULAR MECHANICS INVESTIGATION OF N-PHENYL-PROTOPORPHYRIN IX ISOMERS.

P. Y.-F. Hsu, M. R. Ondrias, J. A. Shelnutt, Sandia National Laboratories and University of New Mexico, Albuquerque, NM 87185; B. A. Swanson, P. R. Ortiz de Montellano, University of California, San Francisco, CA 94143

The reaction of N-phenylhydrazine with hemoglobin results in N-phenyl-protoporphyrin formation, hemoglobin denaturation, Heinz body formation, and erythrocyte lysis. The reaction with cytochrome P_{450} results in suicide inactivation of the enzyme and formation of N-phenyl-protoporphyrins. The reaction also provides a means of mapping the location of the substrate binding cavity relative to the porphyrin macrocycle by identifying which of eight N-phenyl isomers are obtained in the reaction. To aid in these investigations, we have initiated a resonance Raman spectroscopic study of the N-phenyl-protoporphyrin isomers.

The Soret resonance Raman spectra of an isomer of Zn(II) N-phenyl-protoporphyrin IX dimethylester (ZnN-ϕ-ProtoP) and Zn(II) protoporphyrin IX dimethylester (ZnProtoP) were obtained in methanol solution using a dual-channel Raman spectrometer. The isomer investigated is the third one that elutes during reverse-phase HPLC and has been assigned as the isomer with the phenyl attached to the nitrogen of ring C. For the ZnN-ϕ-ProtoP isomer, a photochemical reaction was observed during data collection of three 20-minute scans of the spectrum in the region between 1300 and 1700 cm^{-1}. By the third scan, the Raman and uv-visible absorption spectra are almost identical to that of ZnProtoP, suggesting photochemical lysis of the phenyl group. The spectrum of authentic ZnN-ϕ-ProtoP, obtained in the first scan, shows an oxidation-state marker line ν_4 at 1376 cm^{-1}. ZnProtoP and photolysed ZnN-ϕ-ProtoP have a lower ν_4 at 1368 cm^{-1}. Core-size marker lines at 1482, 1568, and 1590 cm^{-1} are the same within 1 cm^{-1} for ZnN-ϕ-ProtoP and ZnProtoP. Another Raman line at 1614 cm^{-1} for ZnN-ϕ-ProtoP upshifts to 1621 cm^{-1} upon photolysis, the same location for the line of ZnProtoP. The assignment of the latter mode is a problem because of overlapping modes due to porphyrin macrocycle and vinyl substituents.

Molecular energy-optimization calculations have been carried out for the N-phenyl isomers of Fe(III)ProtoP chloride. The calculations reproduce generally the reported X-ray structures of N-alkyl-porphyrins and show small structural variations between the different isomers.

Supported by U. S. DOE Contract DE-AC04-76DP00789 (JAS), Minority Biomedical Research Support Program (PYFH), and NIH GM25515 (PROM).

W-Pos216

MODELS OF NON-PLANAR BIOLOGICAL CHROMOPHORES: NICKEL(II) OCTA-ALKYL-TETRAPHENYLPORPHYRINS.

L. D. Sparks, M. S. Park, M. R. Ondrias, J. A. Shelnutt, Sandia National Laboratories and University of New Mexico, Albuquerque, NM 87185; C. J. Medforth, M. D. Berber, K. M. Smith, University of California, Davis, CA 95616; K. M. Barkigia, Brookhaven National Laboratories, Upton, Long Island, NY 11973.

The importance of non-planar macrocycle conformations in the biochemical function of tetrapyrroles has recently been recognized. Functional significance has been attributed to non-planar macrocycles for vitamin B_{12} of B_{12}-dependent enzymes, chromophores of photosynthetic reaction centers, and Ni cofactor F_{430} of methylreductase. For F_{430} and B_{12}, the degree of planarity modulates the axial ligand affinity of the metal. Further, a study of Ni-reconstituted hemoglobin has shown that the protein can affect porphyrin planarity. To elucidate the importance of non-planar tetrapyrroles in proteins, spectroscopic methods for detecting and quantifying planarity are needed. Consequently, a series of Ni(II) porphyrins with varying planarity resulting from steric congestion of the peripheral substituents were investigated using UV-visible absorption spectroscopy, dual-channel resonance Raman spectroscopy, and X-ray crystallography. The series includes three octa-*alkyl*-tetraphenylporphyrins (OATPP, *A* = methyl, ethyl, propyl), three tetra-*cycloalkenyl*-tetraphenylporphyrins (TC_nTPP, *n*=5(pentenyl), 6(hexenyl), 7(heptenyl)), dodecaphenylporphyrin (DPP), OEP, and TPP. Molecular mechanics calculations predict that the calculated structures will differ in the degree of planarity: (1) NiOEP, NiTPP and $NiTC_5TPP$ are nearly planar, (2) NiOETPP, NiOPTPP, NiOMTPP, and $NiTC_nTPP$ (n=6,7) exhibit varying degrees of ruffling in which the pyrrole rings are alternately tilted above and below the mean plane. The accuracy of the calculated structures has been verified by X-ray crystal structures of several of the ruffled Ni porphyrins, including NiOPTPP which is predicted to be the most non-planar. The structure-sensitive Raman lines decrease in frequency for the series as the porphyrin ring becomes more ruffled. Correlations with porphyrin core size and $C_\alpha NC_\alpha$ angle for the series are found, but the slope of the linear relationship is positive, while the conventional core size-frequency relationship has a negative slope. The linear relationships with $C_\alpha NC_\alpha$ angle for the Ni porphyrin series and the porphyrins used for the conventional core size correlation have the similar slopes, indicating that the $C_\alpha NC_\alpha$ angle may be the factor that determines the frequency of the Raman lines. For NiDPP, we have detected the presence of multiple conformers in solution. INDO molecular orbital calculations for the series will also be presented.

U.S. DOE Contract DE-AC04-76DP00789(JAS), NSF Grant CHE-86-19034(KMS), U.S. DOE Contract DE-AC02-76CH00016(J.Fajer); Assoc. Western Univ.(LDS).

W-Pos217

CP/MAS SOLID STATE ^{13}C NMR SPECTROSCOPY OF BACTERIORHODOPSIN: ANALYSIS OF SECONDARY STRUCTURE.

S.L. Helgerson[1], S.L. Siemsen[1], E.A. Adams[1], R.D. Renthal[2], and E.A. Dratz[1]
[1]Chemistry Department, Montana State University, Bozeman, MT, and [2]Department of Chemistry, University of Texas, San Antonio, TX.

The secondary structure of bacteriorhodopsin has previously been studied by CD, FT-IR, and solid state powder spectra NMR. There is disagreement as to the secondary structure of the protein, particularly in the transmembrane regions. Transmembrane structures of 100% alpha(I)-helical, 60% alpha(II)-helical/40% beta-sheet, or a combination of 100% alpha(I)+alpha(II)-helical have been proposed. CP/MAS solid state NMR can be used to address this problem. Model compound studies have shown that the 13C resonance of the carbonyl backbone carbon in amino acid homopolymers is 176+/-1 ppm for helical residues and 171+/-1.5 ppm in non-helical structures [1].

The primary sequence of bR has 36 LEU, 21 VAL and 7 LYS residues. Proposed folding models place 90-95% of the LEU in transmembrane helices. For the VAL, 65-80% of the residues are in transmembrane helices and 20-35% in surface loops. For the LYS, 70% of the residues are in transmembrane helices and 30% in surface loops. We have prepared isotopically enriched purple membrane from H. halobium grown on synthetic media containing [13C-1]-LEU (50% sp.act.), [13C-1]-VAL (100% sp.act.), or [13C-1]-LYS (100% sp.act.). Amino acid analysis of the purified pm gave enrichments of 55% for LEU, 110% for VAL, or 90% for LYS with the label appearing only in the enriched residues.

CP/MAS NMR spectra were obtained from wet pm pellets at 4°C using a 13C frequency of 50MHz and spinning speeds of 3-3.5 kHz. The carbonyl resonance region was analyzed by fitting with multiple Lorentzian bands. The results show that 85% LEU (178, 176.5, 175 ppm), 75% VAL (178, 175 ppm), and 80% LYS (177.5, 175.5 ppm) are in helical structures. The range of resonance values may indicate residues in varying helical forms. Also, isotopic-shifts of 13C carbonyl vibrational frequencies were measured by FT-IR for comparison with the NMR results. The net helical contents measured for these residues is in close agreement with the near-atomic resolution structure of bacteriorhodopsin [2]. (Supported by NIH 1 R01 EY06913 and ONR N0014-87-K-0278.)

[1] H.R. Kricheldorf and D. Muller (1983) Macromolecules 16: 615-623.
[2] R. Henderson et al. (1990) J. Mol. Biol. 213: 899-929.

W-Pos218

SCANNING TUNNELING MICROSCOPY OF UNCOATED *E. COLI* RNA POLYMERASE

Rebecca W. Keller, Carlos Bustamante and David G. Bear*
Department of Chemistry and *Department of Cell Biology
University of New Mexico, Albuquerque, NM 87131

Scanning Tunneling Microscopy (STM) images of *E.scherichia coli* RNA polymerase have been obtained. The protein was fixed to a gold substrate using an electrodeposition method. The molecules were either crystallized in a two dimensional array or randomly deposited onto the substrate depending upon the depostion voltage and times used. We found this method to be very reliable and were able to vary the deposition parameters to find optimal conditions for high resolution images.
The molecules appear to be mostly spherical in the crystalline arrangement with a diameter of around 150Å and a height of around 80Å. No intramolecular detail can be seen. When the molecules are randomly deposited, higher resolution can be obtained and some molecules appear jaw shaped with a diameter of 155Å. Also in some images a cleft can be seen on one of the legs of the jaw which may be a site for DNA binding. A model is also presented based on these observations, TEM, STEM, cross-linking and immuno-electron microscopy data showing prosposed postitioning of the five subunits of the the protein togetether with a DNA binding site.

W-Pos219

STRUCTURAL STUDIES OF LECTIN-CARBOHYDRATE INTERACTIONS

Wen Cheng[1], Terence Russell[1], Fred Brewer[2] and Lee Makowski[1]
[1]Dept. of Physics, Boston University, Boston, MA 02215
[2]Dept. of Molecular Pharmacology, Albert Einstein College of Medicine, Bronx, NY 10461

The structure of an assembly made up of LTL-A (isolectin A from Lotus tetragonolobus) cross-linked by a complex carbohydrate is being studied using a combination of electron microscopy, x-ray diffraction and molecular model building. Molecular model building has utilized the known molecular structure of ConA, based on the high degree of homology between LTL-A and ConA. A detailed description of the interactions and the binding properties of such lectin-carbohydrate complexes can lead to an understanding of the activity of the complex carbohydrates and lectins and provide direct insight into the molecular recognition properties of both classes of molecules.
Electron micrographs of negatively stained samples of the precipitate were used to determine approximate dimensions and potential symmetries of the unit cell. This information was combined with the x-ray diffraction data from pellets of the precipitates. Initial modelling suggested that the cross-linked precipitate has two-sided plane group symmetry C222 with lattice dimensions 76.1Åx121.8Å. This symmetry can only be approximate, however, since it places the sugar on a two-fold axis, and the sugar does not have strict two-fold symmetry. This asymmetry can be observed in filtered EM images of the LTL-A lattice. We are constructing a molecular model of the complex based on x-ray diffraction and electron microscopy and the known molecular structure of the highly homologous ConA. This structural model indicates that there are extensive protein-protein interactions stabilizing the cross link. This self-complementarity may be of significance for molecular recognition mediated by this class of lectins.

W-Pos220

PHYSIOCHEMICAL CHARACTERIZATION OF RECOMBINANT APOLIPOPROTEIN (a). Martin Phillips, Audra Lembertas, Richard Lawn* and Verne Schumaker. Molecular Biology Institute, Department of Chemistry and Biochemistry, UCLA, Los Angeles 90024 and *Division of Cardiovascular Medicine, Stanford University, CA 94305-5246.

Recombinant apolipoprotein(a) [r-apo(a)] is secreted in a mammalian expression system as a heavily glycosylated protein of approximately 320 kD which contains 17 type IV kringles as well as the type V kringle and protease-like domain of human apo(a). In the electron microscope r-apo(a) appears as an elongated, flexible string of domains with a contour length of about 800 Å. The $s^{0}_{20,w}$ of r-apo(a) is 9.3S, consistent with an elongated structure with a frictional ratio of about 1.8. Saturation of the weak lysine binding sites in the kringles by 50mM 6-amino hexanoic acid does not alter the sedimentation coefficient of r-apo(a).

Lipoprotein(a) [Lp(a)] is a highly atherogenic complex consisting of a low density lipoprotein [LDL] linked by a disulfide bond to apo(a). When r-apo(a) is mixed with human LDL, a 13.7S Lp(a)-like complex forms spontaneously. 50mM 6-amino hexanoic acid now causes the r-apo(a) to dissociate from the LDL.

W-Pos221

AVIAN MYELOBLASTOSIS VIRUS REVERSE TRANSCRIPTASE: EFFECT OF GLYCEROL ON THE HYDRODYNAMIC PROPERTIES. Thy-Hou Lin+, Tom Quinn+, Mary Walsh*, Duane Grandgenett+ and James C. Lee . +Institute for Molecular Virology, St. Louis University, St. Louis, MO. 63104, *Biophysics Institute, Boston University, Boston, MA. 02118, Dept. of Human Biological Chemistry & Genetics, The University of Texas Medical Branch, Galveston, TX. 77550.

Reverse transcriptase has been the subject of intensive investigation but little is known about the physical properties of the enzyme. The basic hydrodynamic properties of avian myeloblastosis virus reverse transcriptase in solution were measured by both sedimentation velocity and equilibrium measurements in two buffer systems. In a 0.3 M potassium phosphate buffer system (pH 7.8), the enzyme sedimented as a homogeneous particle with a sedimentation coefficient of (7.1 ± 0.3) S with a weight-average molecular weight, M_w, of (1.52 ± 0.05) x 10^5. Since the enzyme consists of an α and β subunit of equal molar ratio with M_w of 6.3 x 10^4, and 9.4 x 10^4, respectively, it was concluded that the enzyme exists as an $\alpha\beta$ heterodimer in this buffer system. In a Tris buffer system (pH 7.9), containing 0.46 M NaCl and 4% glycerol, the native enzyme also sedimented as a homogeneous particle with apparent sedimentation coefficient of (10.1 ± 0.5) S, without considering the effect of glycerol on solvent-protein interaction. Based on the results of Gekko and Timasheff [Biochem. 20, 4667, 1981] and the polarity of the enzyme, it was estimated that there is a significant solvent-protein interaction even at 4% glycerol leading to a value of -0.06 g/g in the preferential solvent interaction parameter. When the solvent effect was taken into consideration, the value for $S^\circ_{20,w}$ increased from 10.1 to 11.9 S, implying that the native enzyme dimerizes in the presence of 4% glycerol. The combined results of gel filtration and sedimentation velocity showed that the dimerization of the enzyme to form $(\alpha\beta)_2$ is favored at 20°C and assumes an $\alpha\beta$ form at 4°C. The secondary structure of the reverse transcriptase was measured by circular dichroism.

W-Pos222

VISUALIZATION OF BOVINE ALPHA-CRYSTALLIN BY ROTARY-SHADOWED STEREOMICROSCOPY

A.K. Kenworthy, T.N. Oliver, and A.D. Magid, Dept of Cell Biology, Duke University Medical Center, Durham, N.C. 27710.

Alpha-crystallin is the principal structural protein of mammalian lenses. It forms from the assembly of 20 kDa subunits. Initially, its native molecular weight is about 900 kDa (LMW) but with age it transforms to an aggregated high-molecular weight (HMW) form with a broad size distribution. We are interested in understanding the structural pathway that this ageing process follows. Until now, the only electronmicroscopic data on alpha-crystallin structure were available from negatively-stained material. The rotary shadowing technique can provide three-dimensional views of the surface topography of proteins and so might help clarify how the HMW alpha-crystallin forms. Alpha-crystallin was obtained by size-exclusion chromatography on Sepharose 6B of bovine lens (18–24 month-old steers) extracts from the nuclear (inner 50% wet weight) and cortical (outer 50%) regions. The extraction and column buffer comprised 50 mM NaCl, 50 mM Tris, 1 mM EDTA, and 5 mM azide, pH 7.6. Procedures were conducted at room temperature. The older, nuclear fraction was highly enriched in HMW alpha-crystallin, while the relatively younger, cortical region contained almost only LMW alpha-crystallin. Three classes of alpha-crystallin, HMW (nucleus) and LMW material from cortex and nucleus, were obtained by pooling appropriate column fractions. The purity of the fractions were confirmed by SDS-PAGE. Samples were glycerol-sprayed onto mica and low-angle rotary-shadowed replicas of platinum/carbon were produced. Calibrated stereopair electronmicroscopic images were recorded at ±10 degrees goniometer tilt on a Philips 420. Preliminary results for LMW alpha-crystallin show highly spherical particles with diameters similar to those reported for negatively stained alpha-crystallin (16-18 nm). Some chain-like aggregates of two to four particles are present. In the HMW alpha-crystallin fractions, irregular aggregates of LMW alpha-crystallin with diameters up to 180 nm are apparent. Stereoscopy both enhances the globular appearance of the LMW alpha-crystallin particles as well as dramatically revealing the globular LMW domains within the HMW aggregates, clearly showing their 3-D arrangement. We are currently using this technique to compare LMW particles from cortex and nucleus in an attempt to visualize the pathway of HMW alpha-crystallin formation in the nucleus with ageing. Partial support from NIH grant GM27278 to T.J. McIntosh and the use of lab facilities of H.P. Erickson are gratefully acknowledged.

W-Pos223

VISCOELASTICITY OF MUCIN GLYCOPROTEIN SOLUTIONS AND GELS C. M. McCullagh, A. M. Jamieson, and J. Blackwell

Mucin glycoproteins are the primary viscoelastic component of mucus secretions. The viscoelastic properties of ovine submaxillary mucin (OSM) and human tracheobronchial mucin (HTBM) are studied in a dissociative solvent as a function of molecular weight and concentration in order to correlate molecular structure with physical properties. OSM has simple disaccharide side chains whereas the oligosaccharides of HTBM are longer, branched and sulfated.

The dynamic storage and loss moduli, $G'(\omega)$ and $G''(\omega)$, and complex viscosity, $\eta^*(\omega)$, were obtained by dynamic frequency sweeps between 0.1-100 rad/s. Lower molecular weight fractions of OSM show predominantly dissipative behavior, $G'(\omega) < G''(\omega)$, throughout this frequency range and the complex viscosities are Newtonian. The highest molecular weight fraction shows shear thinning behavior above 10 rad/s and enhanced elasticity at high frequencies, $G'(\omega) > G''(\omega)$, typical of an entanglement network. At comparable degrees of molecular interpenetration, HTBM forms weak viscoelastic gels, $G'(\omega) \approx G''(\omega)$, which may be due to oligosaccharide interdigitation. The complex viscosity exhibits a power law dependence on frequency. Thus, mucins with longer side chains exhibit better gel-forming capability, larger elastic moduli, and viscosities that are more shear sensitive than mucins with shorter side chains at comparable molecular weight and concentration. Rheological behavior of mucins is discussed in terms of polymer solution theories and gelation theory.

W-Pos224

DYNAMIC LIGHT SCATTERING INVESTIGATIONS OF HUMAN ERYTHROCYTE SPECTRIN

Donna M. Budzynski*, Cynthia C. LaBrake+, L. W.-M. Fung+ and Albert S. Benight*. Departments of Chemistry, University of Illinois at Chicago* and Loyola University of Chicago+, Chicago, Illinois.

We have performed dynamic light scattering (DLS) measurements of spectrin from human erythrocytes in 100 mM NaCl, 25 mM Tris, pH=7.6. Measurements were made as a function of K^2, the square of the scattering vector, from 2 x 10^{10} cm^{-2} to 20 x 10^{10} cm^{-2}, over the temperature range from 23 to 41 °C. Analysis of DLS data reveals the presence of two predominant components over the entire range of K^2. At small K^2 ($\leq$ 4 x 10^{10} cm^{-2}) these components have diffusion coefficients = 20 x 10^{-8} cm^2/s and 7 x 10^{-8} cm^2/s that are attributed to a population of dimers and tetramers of spectrin, respectively. The relative population shifts from tetramers to dimers with increasing temperature. At $K^2 \geq$ 11 x 10^{10} cm^{-2} the diffusion coefficient of the faster component increases by a factor of two to 40 x 10^{-8} cm^2/s while the slower component diffusion coefficient increases to 14 x 10^{-8} cm^2/s, a value that is the average of the fast and slow values observed at lower K^2. At high K^2 the relative populations of the components are independent of temperature (after viscosity correction). These results at high K^2 are consistent with the assignment of the slow component to an unresolvable mixture of dimer and tetramer species that are resolved at low K^2. The fast component is tentatively assigned to internal motions of the spectrin molecules. If this assignment is correct, then the internal motions of spectrin are independent of temperature (after viscosity correction) and indistinguishable in dimer and tetramer molecules.
(Supported by NIH)

W-Pos225

SOLUTION SCATTERING STUDIES OF T7 RNA POLYMERASE AND ITS COMPLEX WITH T7 LYSOZYME.

Kevin R. MacKenzie*, David Jeruzalmi*, Mikio Kataoka#, and John M. Flanagan*. (Introduced by Robert M. Macnab)

*Department of Molecular Biophysics & Biochemistry, Yale University. #Physics Department, Tohoku University, Sendai, Japan.

T7 RNA polymerase is a 98 kDa protein that transcribes phage genes in a regulated fashion during the T7 bacteriophage lifecycle. While transcription initiation at the 17 bp promoter requires no additional initiation factors, the product of a second phage gene, T7 lysozyme, has been shown to inhibit transcription by interacting with the RNA polymerase. We have undertaken solution scattering studies in this system to obtain low-resolution structural data that might complement (or be correlated with) biochemical results obtained by other groups.

We have used small angle X-ray scattering to characterize T7 RNA polymerase under near-physiological buffer conditions. Using both our rotating anode source (at Yale) and the SAXS station at the Photon Factory (Tsukuba, Japan), we have obtained measurements of the radius of gyration (Rg) and the molecular weight of the protein, and have calculated length distribution functions (P(r) curves) from the scattering data collected. These results demonstrate that the polymerase is an oblong molecule with a maximum dimension of approximately 115 Å. Extended scattering curves indicate that the polymerase is composed of at least two distinct domains. Both the inner and extended regions of the curve are altered when sample temperature is varied in ranges that are known to affect polymerase activity (25 - 37 C); possible functional implications of this will be discussed.

To establish the stoichiometry of the T7 lysozyme - polymerase interaction, we have collected data for titration series of polymerase and lysozyme. From the biphasic increase in forward scatter intensity with increasing proportions of lysozyme we have determined that the ratio in the complex is 1:1. Interestingly, the extended scattering curves for the purified complex differ significantly from those of the polymerase alone: there is no evidence for multiple domains in the complex, and no variation with temperature. Models consistent with the experimental results will be discussed.

W-Pos226

SPECTROSCOPIC CHARACTERIZATION OF Cu(I) AND Ag(I) COMPLEXES OF THE DNA-BINDING DOMAIN OF YEAST ACE1 TRANSCRIPTION FACTOR

Jose R. Casas-Finet, Stella Hu*, Dean Hamer*, and Richard L. Karpel. Dept. of Chemistry and Biochemistry, University of Maryland Baltimore County, Baltimore, MD 21228, and *Laboratory of Biochemistry, National Cancer Institute, National Institutes of Health, Bethesda, MD 20892

A polypeptide containing residues 1-122 of ACE1, termed ACE1(122*), contains a metal-dependent DNA-binding domain rich in cysteines and basic amino acids. ACE1(122*) binding to its specific DNA recognition site, UASCL, occurs upon reconstitution with Cu(I) or Ag(I), but not Zn(II). Binding is inhibited by the monovalent ion chelators CN^- or diethyldithiocarbamate (DDC), but not by the divalent ion chelator EDTA. Cu- or Ag-ACE1(122*) show charge-transfer and metal-centered UV absorption bands which are abolished by CN^-, DDC or metal displacement by H^+. Cu(I)- and Ag(I)-ACE1(122*) exhibit identical fluorescence lifetimes of 1.7 ns (50%) and 4.3 ns (50%) from its single Tyr residue, whose emission is quenched by UASCL but not by double-stranded calf thymus DNA. Binding affinity is reduced upon increasing the ionic strength, indicating the involvement of basic residues from ACE1(122*). Only Cu(I)-ACE(122*) exhibits a room-temperature orange luminescence (λ_{max} = 619 nm) with lifetime components of 46 ns and >2 us, typical of Cu-cysteinyl thiolate clusters. This luminescence emission was inhibited by metal chelators or upon oxidation of ACE1(122*) Cys residues by aerobic incubation, and was specifically quenched by *ca.* 20% upon binding to UASCL. The CD spectra of Cu(I)- and Ag(I)-ACE(122*) is devoid of long-range α-helical or β-sheet structure, and is perturbed upon metal complexation by CN^-. Ag(I) binding stabilizes ACE1(122*) against GuHCl denaturation, relative to the apoprotein form. In support of these results, point mutagenesis of the ACE1 amino-terminal domain shows that Cu(I) and UASCL binding requires the integrity of 11 out of its 12 Cys residues. Our results provide evidence that Cu(I) or Ag(I) binding to Cys residues of ACE1 folds its amino-terminal domain into a conformation that results in an active DNA-binding protein that can recognize its specific target DNA sequence, and thus activate transcription.

W-Pos227

DISTRIBUTION OF TRYPTOPHAN-LUMAZINE DISTANCES IN PHOTOBACTERIUM PHOSPHOREUM LUMAZINE PROTEIN MEASURED BY FREQUENCY-DOMAIN FLUORESCENCE ENERGY TRANSFER.

H. Malak, J.R. Lakowicz, University of Maryland School of Medicine, Department of Biological Chemistry and Center for Fluorescence Spectroscopy, Baltimore, MD 21201, and J. Lee, University of Georgia, Department of Biochemistry, Athens, GA 30302.

We used fluorescence resonance energy transfer (FRET) to examine the distribution of distances between two sites in the lumazine protein. The donor (D) was the single tryptophan residue and the acceptor (A) was 6,7-dimethyl-8-(1'-D-ribityl) lumazine, which is a ligand in this protein. The Förster distance for this D-A pair is 19.3 Å. A distribution of D-A distances results in a distribution of donor decay times, and/or acceptor decay times, which were resolved by using frequency-domain fluorometry.

The lumazine protein distance distributions recovered by observing the donor decay times are hw = 13.4 Å and R_{av} = 19.3 Å, those recovered by observing the acceptor decays are hw = 15.9 Å and R_{av} = 20.9 Å, and those recovered from global analysis of donor and acceptor decays are hw = 13.5 Å and R_{av} = 19.3 Å. These results were obtained by assuming, that the orientation factor (κ^2) of D-A pair is 2/3. The widths of the distance distributions were found to be relatively wide, which confirmed previous observation of an extremely mobile tryptophan residue in lumazine protein (Visser et al., *Eur. Biophys. J.*, 17:75-85, 1990). This may indicate that the tryptophan is in an unstructured region of the protein.

W-Pos228

STRUCTURAL STUDIES OF ADENINE NUCLEOTIDE TRANSLOCASE. Peter J. Tummino and Ari Gafni (Intro. by G. Omann), Institute of Gerontology, The University of Michigan, 300 N. Ingalls, Ann Arbor, MI 48109-2007.

Adenine nucleotide translocase (ANT), located in the inner mitochondrial membrane, transports ADP from the cytosol to the mitochondrial matrix coupled to transport of ATP from the matrix to the cytosol in a 1:1 ratio. ANT, a dimer of M.W. 60,000, exists in two conformations in the membrane. One conformation has an ADP binding site facing the cytosol and binds the high-affinity irreversible inhibitor carboxyatractyloside (CAT), while the other conformation has an ATP binding site facing the matrix and is reversibly inhibited by bongkrekic acid. Palmitoyl-CoA also specifically interacts with either conformation of ANT and inhibits translocation.

The fluorescence decay of tryptophans in purified solubilized ANT has been measured and fits well to three components. There is a significant increase in one component of the decay upon addition of the inhibitor CAT, which does not absorb in the UV or visible range. The increase plateaus sharply upon addition of CAT in a 1:1 ratio with ANT dimer. Also, addition of the fluorescent nucleotide analog trinitrophenyl-ATP quenches a different component of the ANT decay with an approximate binding constant of 12 uM. This quenching is not observed upon addition of ATP. These changes in time-resolved ANT fluorescence have been used to test for possible overlap between the palmitoyl-CoA, CAT, and adenine nucleotide binding sites.

In order to study the spatial relationship between the ANT dimers, protein samples were labelled specifically with fluorescein-5-maleimide and eosin-5-maleimide in a 1:1 chromophore/ANT dimer ratio and then purifed and solubilized. Mixing of fluorescein-ANT with eosin-ANT results in quenching of fluorescein emission and an increase in eosin emission. This energy transfer is specifically due to the ANT, since preincubation with the inhibitor CAT inhibits the effect, and is probably due to monomer mixing that yields fluorescein,eosin-labelled ANT dimers. Energy transfer studies with this donor/acceptor pair enable the determination of changes in the relative distance between ANT monomers upon addition of different substrates, inhibitors or denaturing agents, and with varying temperature.

W-Pos229

FLUORESCENCE POLARIZATION FOR DETERMINING THE ASSOCIATIONS OF TRANSGLUTAMINASES WITH A GELATIN-BINDING 42K FRAGMENT OF HUMAN FIBRONECTIN. J.T. Radek*, K.C. Ingham** and L. Lorand*. Department of Biochemistry, Molecular Biology and Cell Biology, Northwestern University, Evanston, IL 60208* and Biochemistry Laboratory, American Red Cross, Rockville, MD 20855**

Human fibronectin (HFN), a large glycoprotein found in plasma, was shown to selectively bind transglutaminases from human erythrocyte (HETG) and guinea pig liver (GPLTG) in an approximately 1:2 stoichiometry even in the absence of Ca^{2+} (Turner and Lorand, *Biochemistry* 28, 628, 1989). HFN may down-regulate the activities of transglutaminases and may also act as a possible clearing system for such enzymes if they were to be discharged into the plasma from disrupted erythrocytes and other cells. The interaction was localized to near the gelatin-binding region of HFN. We have now employed fluorescence polarization techniques to further analyze the interaction between a smaller 42K gelatin-binding fragment of HFN (Forastieri and Ingham, *J. Biol. Chem.* 260, 10546, 1985) and either of the two enzymes. Mixing of the fluorescein-labeled 42K fragment of HFN ($42K^F$) with these enzymes resulted in a significant increase in fluorescence anisotropy. However, an approximately six-fold higher affinity constant was obtained for the interaction of HETG with $42K^F$/HFN than for the GPLTG:$42K^F$/HFN complexation. It was further shown that unlabeled 42K could compete against binding of $42K^F$ and could also displace its fluorescein-labeled counterpart from either of the two enzymes. By contrast, the fluorescein-labeled N-terminal 30K fragment, obtained by proteolysis of 42K, showed no ability to bind to either enzyme. Aided by a USPHS Career Award (HL-03512 to L.L.) and by grants from the National Institutes of Health (HL-02212 and DK-25412 to L.L. and HL-21791 to K.C.I.).

W-Pos230

LUMINESCENCE AND LIGAND BINDING STUDIES WITH TRP APOREPRESSOR FROM E. COLI. Maurice R. Eftink, Dana Hu, Department of Chemistry, University of Mississippi, University, MS 38677, and Camillo A. Ghiron, University of Missouri, Columbia, MO 65201.

Trp aporepressor is a homo-dimeric protein (with two intrinsic trp residues per subunit), which upon association with the corepressor, L-tryptophan, binds to the trp operator and blocks the transcription of the related operon. Time-resolved fluorescence studies with the aporepressor show the decay to be a bi-exponential, with the longer lived component having much greater accessibility to the collisional quencher, iodide. Indole acrylic acid binds very tightly ($K_d \sim 2 \times 10^{-6}$M) and quenches essentially all of the intrinsic fluorescence of the protein, probably by resonance energy transfer. Acryloyl tryptamine binding ($K_d \sim 5 \times 10^{-6}$M) quenches about 33% of the protein's fluorescence. Since the latter ligand possesses an acrylamide moiety, this quenching may be due to electron transfer from the trp residues to the bound ligand. For both of the above ligands, hyperbolic binding curves are seen, indicating an absence of cooperation between subunits. The binding of a number of other trp analogs will be reported, including a study of the conformationally constrained, L-3-carboxy-1,2,3,4-tetrahydro-2-carboline, which is found to bind to the protein with a K_d of 5×10^{-4}M, a value that is 15 fold higher than that for L-trp.

Additional luminescence studies show that the phosphorescence of the two intrinsic trp residues of the protein can be resolved at low temperature. Selective perturbation by the heavy atom "quencher" iodide allows distinction between the more and less solvent exposed trp components and a connection with the fluorescence quenching results. This research was supported by NSF grant DMB 88-06113.

W-Pos231

TIME RESOLVED FLUORESCENCE DECAY MEASUREMENTS OF MYOGLOBIN SINGLE CRYSTALS. A. G. Szabo, K. J. Willis and D. T. Krajcarski. Division of Biological Sciences, National Research Council, Ottawa, Ont. Canada, K1A OR6.

Picosecond time-resolved fluorescence measurements on single crystals are described. Fluorescence spectroscopy is used to probe long range (20 A) intramolecular interactions, between tryptophyl residues and heme, in the solution and crystalline states of myoglobin. The fluorescence of single crystals of sperm whale myoglobin decays with double exponential kinetics (τ_1 = 15 ps, τ_2 = 70 ps), while that of crystals of yellow fin tuna myoglobin obeys single exponential kinetics, (τ = 24 ps). These data are shown to be consistent with a protein structure, at atomic resolution, that is independent of sample state.

W-Pos232

RAMAN SPECTROSCOPY STUDIES OF BULL PROTAMINE AND THE BULL PROTAMINE-DNA COMPLEX. N.V. Hud[1,2], F.P. Milanovich[1] and R. Balhorn[1], [1] Lawrence Livermore National Laboratory, Livermore, CA 94550 and the [2]University of California, Davis, CA 95616.

Protamine, the small protein responsible for the packing of DNA in sperm cells, is the subject of structural investigations in our laboratory. Previous studies have shown that the amino- and carboxy-terminal ends of protamine in bull sperm chromatin are folded inward toward the center of the molecule and locked in place by disulfide crosslinks. The conformation of this protein and the nature of its binding to DNA are currently being studied as a model for other mammalian protamines.

We have performed Raman spectroscopy studies of bull protamine and synthetic peptides corresponding to its amino- and carboxy-terminal domains in solution, before and after folding. Data obtained from the amide I and amide III regions of these spectra and computer modeling studies on the IRIS computer using the modeling and energy minimization programs QUANTA and CHARMm suggest that the amino-terminal domain of this protamine molecule contains a beta turn involving residues his9-ser-gly-ser12 and a short region of antiparallel beta sheet. Analyses of the 830 and 850cm-1 lines indicate that the single tyrosine residue in the amino-terminal domain of the molecule remains exposed to solvent in both the unfolded and folded states. Raman spectra of the native bull protamine-DNA complex have also been acquired. These spectra indicate that protamine binding to DNA in sperm chromatin changes the conformation of DNA from B to a more "C-like" form. Using these data, we have generated a refined model for the secondary structure of bull protamine. This work has been supported under the auspices of the U.S. Department of Energy under contract number W-7405-ENG-48.

W-Pos233

TIME-RESOLVED INFRARED STUDIES OF PROTEIN RELAXATION. B.S. Gerstman, Dept. of Physics, Florida International Univ., M.H. Hong, E. Shyamsunder, R.H. Austin, Dept. of Physics, Princeton Univ., S.S. Chan, Dept. of Chemistry, Rutgers Univ.-- Transient infrared absorbance changes of photolyzed carbon monoxide are used to probe internal dynamics in myoglobin over the time range 50 nanoseconds to 10 microseconds and the temperature range 100K to 240K. The absorbance of the photolyzed carbon monoxide above the glass transition of the glycerol/water solvent disappears long before the CO escapes from the protein, indicating substantial structural relaxation in the protein, and a heterogeneous, polar protein interior.

We have computed the fraction of "relaxed" CO molecules, which are invisible to infrared spectroscopy, as a function of time and temperature. Comparison of the temperature dependent kinetics to both stretched exponential relaxation curves and modified forms of the Arrhenius equation will be presented as a test of theories of relaxation in complex systems. We will also compare our results to the sub-picosecond data of Hochstrasser and his colleagues and Rothberg and his colleagues.

W-Pos234

THE SECONDARY STRUCTURE OF TWO RECOMBINANT GROWTH FACTORS AS EXAMINED BY FTIR, T. Arakawa, S.J. Prestrelski, W.C. Kenney and D.M. Byler*, Amgen Inc., Thousand Oaks, CA 91320 and *Philadelphia College of Textiles and Science, Philadelphia, PA 19144

The secondary structure of two recombinant human growth factors, platelet derived growth factor (PDGF) and the basic fibroblast growth factor (bFGF), has been quantitatively examined by using Fourier transform infrared spectroscopy. These studies, carried out in D_2O focus on the conformation-sensitive amide I region. Resolution-enhancement techniques, including Fourier self-deconvolution and derivative spectroscopy, were combined with band fitting to quantitate the spectral information from the broad, overlapped amide I band. The results indicate that both proteins are rich in β structures. The remainder of the PDGF exists largely as irregular or disordered conformations with a small portion of α-helix and reverse turns. By contrast, the bFGF is much richer in reverse turn structures and contains a lesser portion of irregularly folded or disordered structures. Based on information from CD and X-ray crystallography, components in the 1650-1659 cm^{-1} region of bFGF, which are traditionally assigned to α-helices, are tentatively assigned to loop structures.

W-Pos235

FT-IR AND EXAFS OF HUMAN B_{12} BINDING PROTEINS
Frisbie, S.M., and Chance, M.R., Dept. of Chemistry, Georgetown University, Washington, D.C., 20057

It was possible to isolate three cobalamin binding proteins from human serum that have concentrations in the range of approximately 10^{-12} to 10^{-6} M: Cobalophilin, transcobalamin II, and intrinsic factor. These proteins are involved in the protection and/or transport of cobalamin compounds in vivo. The binding of cobalamins to these proteins provides a model system for B_{12}/enzyme interactions. To understand the mechanisms of B_{12} binding, cobalophilin, transcobalamin II, and intrinsic factor were purified from human serum via affinity chromatography using vitamin-B_{12} agarose beads. Elution of proteins from the agarose beads was accomplished via successive washes with increasing concentrations of guanidine HCl. The proteins were thus isolated in a denatured apoprotein state. According to this purification procedure cobalophilin, which has the lowest B_{12} binding affinity is eluted first from the agarose beads. Transcobalamin II is eluted next, having an intermediate K_{ss}, and lastly intrinsic factor. Due to the similar K_{ss} values, a mixture of proteins is obtained, that can be separated further by a sizing column or selective ammonium sulfate precipitation.

After purification, the three binding proteins were each split into two fractions. The first protein fraction was reconstituted with aquocobalamin and the second fraction was reconstituted with cyanocobalamin. This was possible due to the isolation of the proteins in the absence of cobalamin. Several EXAFS and IR samples were prepared by concentration over an Amicon YM10 membrane to ca. 1 mM. For each EXAFS sample 200 μl was needed, and for each IR sample ca. 50 μl was needed. EXAFS scans were conducted at the National Synchrotron Light Source (BNL). We report on the structural changes in cobalamins when these proteins bind, and the implications for B_{12}/protein binding mechanisms in general.

This research is supported by the CSRS, U.S. Department of Agriculture grant #90-37200-5357 of the Program in Human Nutrition.

W-Pos236

THE INFLUENCE OF METAL IONS ON THE CONFORMATION OF α-LACTALBUMIN AS PROBED BY FTIR, S.J. Prestrelski, D.M. Byler and M.P. Thompson. USDA, ARS, Eastern Regional Research Center, Philadelphia, PA 19118

We have examined the influence of monovalent and divalent cations on the secondary structure of bovine α-lactalbumin (α-LA) using FTIR spectroscopy. Our studies show that upon dissolution, α-LA undergoes a small but significant, time-dependent conformational change, regardless of the ions present. Additionally, these studies provide the first quantitative measure of the conformational change which accompanies calcium binding. Removal of Ca^{2+} from holo α-LA results in local unfolding of the Ca^{2+}-binding loop; the spectra indicate that approximately 16% of the backbone chain changes from a rigid coordination complex to an unordered loop. We also examined the effects of binding of several other metal ions. Binding of Mn^{2+}, while inducing a small but significant conformational change upon binding, does not induce the α-LA backbone conformation to change to that of the holo (Ca^{2+}-bound) form as characterized by FTIR. Similar changes to those induced by Mn^{2+} are observed upon binding of Na+, and Na+ does not stabilize the holo form, even at very high concentrations (0.2 M). Binding of Zn^{2+} to the apo (Ca^{2+}-free) form of α-LA does not result in significant backbone conformational changes, suggesting a rigid Zn^{2+} binding site. Further, binding of Zn^{2+} to holo α-LA does not induce a reversion to an apo-like backbone conformation as has been suggested by previous studies.

W-Pos237

FT-IR ANALYSIS OF RECOMBINANT DNA-DERIVED PROTEINS: IS THE ASSIGNMENT OF ∝-HELICAL UNEQUIVOCAL? A.Friedrich, C.Wilder, G.Daumy, R.Potts & M.Francoeur, Pfizer Inc.,Groton,CT: Fourier transform infrared (FT-IR) spectroscopy has been extensively used to estimate protein secondary structure. The growing IR data base of this analytical technology has improved and enhanced the ability to make predictions on the correlation between secondary structure and bioactivity. To this end, we have analyzed by FT-IR the mature forms of recombinant DNA-derived murine interleukin-1α (rmIL-1α) and β (rmIL-1β). These are interesting proteins in that they only share 30% sequence homology, yet bind the same receptors and display the same wide range of biological activities. Our FT-IR studies showed that rmIL-1α and rmIL-1β were predominantly composed of β-type structure, but exhibited a significant IR absorption band around 1656 cm^{-1} which is typically assigned to α-helical structures. However, CD data failed to confirm the existence of helix structure in these proteins and the IR band was totally absent in human recombinant DNA-derived IL-1α. Further, X-ray and NMR studies reported in the literature on human IL-1's show no evidence for helices although the murine and human forms share greater than 80% homology. Therefore, the presence of a band in the IR region from 1650 to 1659 cm^{-1} for the murine forms of IL-1 must be interpreted with caution and should be attributed to secondary structures other than α-helices.

W-Pos238

PROTEIN CONFORMATION AND CHROMOPHORE ORIENTATION IN BACTERIAL REACTION CENTER STUDIED BY POLARIZED FTIR AND LIGHT-INDUCED DIFFERENCE SPECTROSCOPY.

E. Nabedryk, J. Breton & D.L. Thibodeau.
DBCM, CEN Saclay, 91191 Gif-sur-Yvette Cedex, France.

FTIR spectroscopy has been used to investigate the protein secondary structure of *Rb. sphaeroides* and *Rp. viridis* reaction centers (RC) and the degree of orientation of vibrational modes of pigments and aminoacid groups which are affected by the charge separation in photosynthetic primary reactions. FTIR absorption spectra of RC films were analysed for the amide I band : qualitatively using second derivative and Fourier self-deconvolution, and quantitatively by band-fitting procedures. The figure shows the analysis of the amide I band of *Rb. sphaeroides* RC with its fitted components. The component at 1657 cm^{-1}, characteristic of α-helical structure, corresponds to 52 ± 3% of the integrated area of the amide I band. This result agrees well with the α-helical content deduced from UV CD (51%) and X-ray data (51%). The same analysis for *Rp. viridis* RC yields a 43% α-helix content. Molecular changes in the vibrational modes of the RC cofactors and surrounding aminoacid residues after photo-oxidation of the primary electron donor P (a dimer of bacteriochlorophyll) and photoreduction of the primary quinone acceptor (Q_A) have been monitored by light-induced polarized FTIR difference spectroscopy. The FTIR dichroism changes observed in the 1800–1200 cm^{-1} spectral region are interpreted *i)* in terms of orientation and possible changes of orientation after $P^+Q_A^-$ formation, in particular, of the vibrational transitions of the 10a ester and 9 keto carbonyls of P, and *ii)* together with X-ray diffraction data for which the structural relationship between the protein and the cofactors is well-defined in the relaxed state of RC.

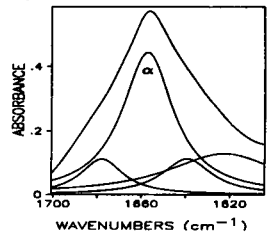

W-Pos239

Solution-phase Fourier-Transform Infrared Spectroscopic Studies on Synthetic Collagen Analogs. Anne George and Arthur Veis, Northwestern University, Chicago, IL 60611.

A prominent feature of the collagen triple helix region is the frequent occurrence of the sequences Gly Pro Pro and Gly Pro OHPro. Within these sequences inter-chain H-bonding and pyrrolidine ring stacking interactions both play a role in triple helix stabilization. The solution spectra of poly-L-proline, poly-L-hydroxyproline, (Pro Pro Gly)$_{10}$ [PPG], and (Pro OHPro Gly)$_{10}$ [PHG], as well as poly-Gly, in H_2O and D_2O have been obtained by FTIRS using a nine-pass reflectance cell. Spectra were collected at temperatures ranging from 4°C to 55°C. The shape of the amide II band in D_2O, and the pyrrolidine ring specific complex C-N vibrations at 1450-1460 cm^{-1} were the most prominent conformation dependent features of the spectra. The amide I regions of [PHG] and [PPG] in H_2O were typical of collagen but the [PHG] had a higher melting temperature than the [PPG]. The complex band in the range from 1468 to 1455 cm^{-1} could be deconvolved into bands differentiating between the amide II deuterated H-bond and C-N vibrations. These data and other subtle shifts in band frequencies with increasing temperature suggest that interactions of the pyrrolidine rings have a more important role in triple helix structure stabilization than the hydrogen bonding interactions. Supported by NIH Grant AR-13921.